Universidad de Granada
Departamento de farmacología

Evaluation of hepatic activity of immunomodulatory compounds and GSK3 inhibitors

José Pérez del Palacio
Doctoral Thesis
February 2017

A thesis

submitted in fulfillment

of the requirements for the degree

of

Doctor

with international mention

at the

University of Granada

by

José Pérez del Palacio

February 2017, Granada, Spain

Declaración

El doctorando José Pérez del Palacio y los directores de la tesis Francisca Vicente Pérez y Julio Gálvez Peralta, garantizamos al firmar esta tesis doctoral, que el trabajo ha sido realizado por el doctorando bajo la dirección de los directores de la tesis y hasta donde nuestro conocimiento alcanza, en la realización del trabajo, se han respetado los derechos de otros autores a ser citados, cuando se han utilizado sus resultados o publicaciones.

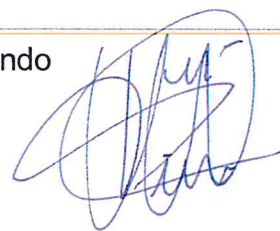Granada 1 de marzo 2017

Director/es de la Tesis   Doctorando

Fdo: Francisca Vicente Pérez

Fdo: Julio Gálvez Peralta

A Mercedes y a mis hermanas

"Nada de lo humano me es ajeno"

Publio Terencio Afro

AGRADECIMIENTOS

en la transferencia del conocimiento relativo a los modelos in vitro para la evaluación de la actividad inmunomoduladora.

A la doctora Ana Martínez Gil del Instituto de química médica –CSIC por la desinteresada cesión de sus compuestos inhibidores de GSK3.

A todos mis compañeros del departamento de farmacología y farmacognosia de la Universidad de Atenas que durante mi estancia me ayudaron a profundizar en mis conocimientos de espectrometría de masas.

Fernando Peláez, director del desaparecido Centro de Investigación Básica de España (CIBE) por ser el precursor de todo este trabajo.

A mi familia por su gran compresión y paciencia.

Y en definitiva a todos aquellos que me han apoyado y ayudado en este largo proceso que ha supuesto la elaboración de esta tesis doctoral.

Table of contents

ABBREVIATIONS

A

ADMET: Absorption, distribution, metabolism, and excretion - toxicity

AMMC: 3-[2-(N,N-diethyl-N-methylamino)ethyl]-7-methoxy-4-methylcoumarin

APCI: Atmospheric pressure chemical ionization

AZT: Azithromycin

B

BFC: 7-Benzyloxy-4-(trifluoromethyl) coumarin and (AMMC)

C

Caco-2: Heterogeneous human epithelial colorectal adenocarcinoma cell line

CID: Collision induced dissociation

Clint: Intrinsic clearance

CLT: Clarithromycin

cLogP: Calculated logP values

COX-1: Ciclooxigenasa 1

COX-2: Ciclooxigenasa 2

CSN: Central nervous system

CSIVM-CYPI: Conventional separate in vitro model for CYP-inhibition evaluation

CSIVM-KS: Conventional separate in vitro model for KS evaluation

CYP2C9: Cytochrome P450 isoform 2C9

CYP3A4: Cytochrome P450 isoform 3A4

CYP450: cytochrome P450

D

DDI: Drug-drug interactions

DMSO: Dimethyl sulfoxide

E

ERY: Erythromacyn

ESI: Electrospray ionization

F

FMO: Flavin-containing monooxygenase

G

GSK3: Glycogen synthase kinase 3

GUI: Graphical user interface GUI

H

HTS: High-throughput screening

HLM: human liver microsomes

HR: High resolution

hrCYP450: human recombinant cytochrome P450

HRMS: High resolution mass spectrometry

I

IL-1β: Interleukin-1β

IL-2: Interleukin-2

IL-4: Interleukin-4

IL-5: Interleukin-5

IL-6: Interleukin-6

IL-8: Interleukin-8

IL-10: Interleukin-10

IL-12: Interleukin-12

iNOS: Inducible nitric oxide synthase

IQM-CSIC: Instituto de química médica-Consejo superior de investigaciones científicas

K

Kinact: Rate of enzyme inactivation for time dependent inhibitors

KI: Inhibition constant for time dependent inhibitors

KS: Kinetic solubility

L

LC-HRMS: Liquid chromatography coupled to high resolution mass spectrometry

LC-MS: Liquid chromatography coupled to mass spectrometry

LLE: Liquid-liquid extraction

LPS: Lipopolysaccharide

M

MBIs: Mechanism-based inhibitors

MFC: 7-methoxy-4-trifluoromethylcoumarin

MS: Mass spectrometry

MS/MS: Tandem mass spectrometry

N

N.A.: Not Applicable

NADPH: Reduced nicotinamide adenine dinucleotide phosphate

NDD: Neurodegenerative diseases

NF-κβ: Nuclear factor kappa-light-chain-enhancer of activated B cells

NIVA-CYPI-KS: Novel in vitro approach to simultaneously assess CYP450 inhibition and KS solubility

NMR: Nuclear magnetic resonance

NOS: Nitric-oxide synthase

NO: Nitric oxide

P

Q

QTOF: Quadrupole time of flight

R

RAW 264.7: Macrophage cell line; Abelson murine leukemia virus transformed

RI: Reversible inhibition

RXT: Roxythromycin

S

SAR: Structure–activity relationship

STDVE: Standard deviation

SPE: Solid phase extraction

T

T1/2: Half-life

TDI: Time dependant inhibition

Th1: T helper 1 linfocites

Th2: T helper 2 linfocites

TIC Total ion chromatogram

IFNγ: Interferon gamma

TNFα: Tumor necrosis factor alpha

U

UGT: Uridine diphosphate glucuronosyltransferase

X

XIC: Extracted ion chromatogram

1 SUMMARY

Nitric-oxide synthase (NOS), the enzyme responsible for mammalian nitric oxide (NO) generation, and cytochrome P450 (CYP450), the main enzymes involved in drug metabolism, share striking similarities. First and foremost, both are heme-thiolate proteins, which employ the same prosthetic group to perform similar chemistry. Moreover, they share the same diflavoprotein reductase as redox partner. Therefore, it makes sense that cytochrome P450 drug-mediated biotransformations might play an important role in the pharmacological modulation of NOS. In this work, we have undertaken an integrated *in vitro* assessment of the hepatic metabolism and NO modulation of previously described dual inhibitors (imidazoles and macrolides) of these enzymes, in order assess the involvement of CYP450 activities in the production of NO. From the experience acquired during this aim, we developed a validated high-throughput screening (HTS) approach in 96-well plate format for the assessment and discovery of molecules with anti-inflammatory/immunomodulatory activity. The *in vitro* models were based on the quantitation of nitrite levels in lipopolysaccharide (LPS) stimulated RAW 264.7 murine macrophages and interleukin-8 (IL-8) in Caco-2 cells stimulated with interleukin 1β (IL-1β)

. In order to validate this new methodology, we used this platform in a pilot project to screen a subset of 5,976 non-cytotoxic crude microbial extracts from the MEDINA microbial natural product collection. As a result, we isolated a previously described molecule with potential activity against inflammation in the central nervous system (CSN). It is widely accepted that CSN inflammation conditions play a significant role in the progression of chronic neurodegenerative diseases such as Alzheimer's disease and Parkinson's disease, neurotropic viral infections, stroke, paraneoplastic disorders, traumatic brain injury and multiple sclerosis. Therefore, it seems reasonable to propose that the use of anti-inflammatory drugs might

diminish the cumulative effects of inflammation. Indeed, some epidemiological studies suggest that the sustained use of anti-inflammatory drugs may prevent or delay the progression of neurodegenerative diseases. However, the anti-inflammatory drugs and biologics used clinically have the disadvantage of causing side effects and the high cost of treatment. Alternatively, natural products offer great potential for the identification and development of bioactive lead compounds into drugs for treating inflammatory diseases with an improved safety profile. To our knowledge, this is the first report on a high-throughput screening (HTS) of microbial natural product extracts for the discovery of immunomodulators.

When assessing enzyme inhibition as is the case of the present work, aqueous solubility of test compounds is a key factor to be considered. This is really a hot topic within drug discovery research that has been explored in this work with the double objective of investigating how solubility is involved in the CYP450 and NOS interactions and in the other hand for improving the methodologies of drug metabolism evaluation at MEDINA drug discovery setting. Therefore, in a first approach we investigated role that compound aqueous kinetic solubility (KS) may play in this lack of correlation observed between different in vitro models for assessment of CYP450 inhibition. In terms of metabolism, drug-drug interactions mediated through CYP450 inhibition are a significant safety concern, and therefore the effect of new candidate drugs should be screened early on CYP450 activity. This is a common practice in drug discovery to screen new chemical entities in order to predict future drug-drug interactions. For this purpose, there are two main assay strategies, one based on human recombinant cytochrome P450 (hrCYP) enzymes and fluorescent detection, and the other one based on human liver microsomes (HLM) and liquid chromatography coupled to mass spectrometry (LC-MS). Many authors have reported a poor correlation between both technologies, giving rise to concerns about the usefulness of fluorometric methods for predicting these drug-drug

interactions. To investigate the effect of aqueous solubility in CYP450 inhibition we used a set of drug discovery compounds within a project for the discovery of glycogen synthase kinase 3 (GSK3) Inhibitors along with well-known inhibitors of main isoforms of CYP450. As a result, we found that drug discovery compounds with unacceptable KS tended to yield higher IC_{50} values in in vitro models based on HLM, whereas compounds with KS values higher than 50 µM showed very similar IC_{50} values in both *in vitro* models. Our results show that the KS assay is a useful tool to identify those discovery compounds that may require further investigation in order to avoid overlooking future drug-drug interactions. From these findings we conclude that the integration of solubility and activity (enzyme inhibition) of the tested products was of critical importance to achieve a rational ranking of drug candidate compounds. In the initial stages of drug discovery, when physicochemical properties such as aqueous solubility have not yet been optimized, there might be a large number of candidate compounds showing artificially low CYP450 inhibition, causing potential drug-drug interaction toxicity to be overlooked. For these reasons, within this work we set a new objective in order to develop and validate a novel in vitro approach to simultaneously assess CYP450 inhibition and KS solubility (NIVA-CYPI-KS). This new methodology is based on fluorogenic CYP450 activities and KS measurements for compound solubility and it provides a significant improvement in the use of resources and a better understanding of CYP450 inhibition data. We have used this approach, among others, to investigate the hepatic metabolism of imidazole derivatives and macrolides in the context of immunomodulation.

2   INTRODUCTION

2.1   Exploring the role of CYP450 mediated drug metabolism in the pharmacological modulation of nitric oxide production

2.1.1   Characteristics, similarities and differences of CYP450 & NOS

Broadly speaking, NOS belongs to the CYP450 family since the label "cytochrome P450" has come to encompass a huge and far-ranging group of closely related enzymes containing a thiolate-ligated heme. Although structurally different, they have a mechanistic resemblance since NOS converts L-arginine to L-citrulline and NO through a P450-like process and complementarily, CYP450 was also seen to transform N-hydroxy-L-arginine into NO and citrulline (Figure 1).
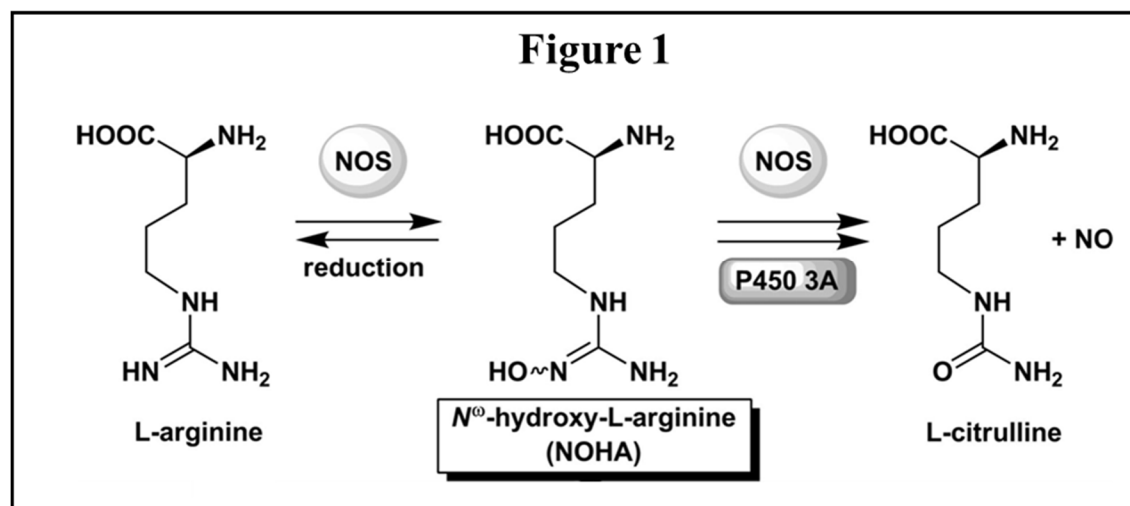
Figure 1. Overview of NOS and CYP450 metabolism and its influence on NO biosynthesis. NOS catalyze the oxidation of L-arginine to L-citrulline and NO via the intermediate NOHA ($N\omega$-hydroxy-L-arginine). However, there are also evidence that cytochromes P450 are able to catalyze the second step of the reaction performed by NO-synthases (eq.l), the oxidation of NOHA by NADPH and 02 with formation of citrulline and NO [1].

Thus, the first step in NO biosynthesis appears to have some precedents in P450 chemistry [2].

Perhaps the most striking among the similarities between CYP450 and NOS is the fact that

both the NOS oxygenase domain and mammalian CYP450 utilize the same electron donor as a redox partner [3] (Figure 2).
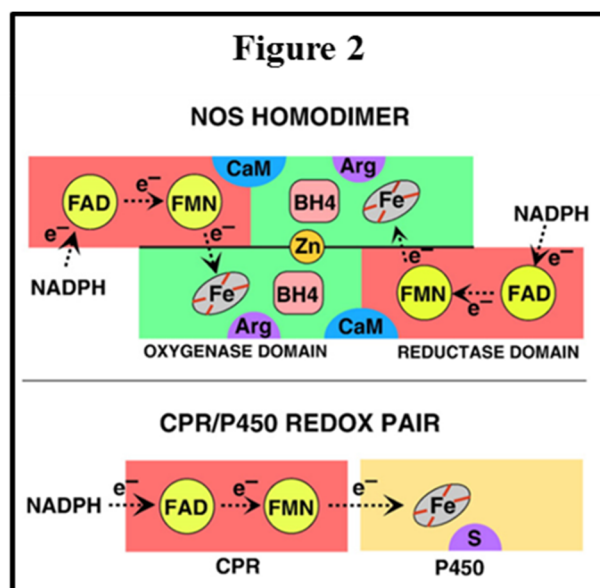
Figure 2. Schematic presentation of the NOS homodimer including all cofactors and the electron transfer pathway. NOS is only active as a homodimer, because electron transfer can only occur from the reductase domain of one subunit to the oxygenase domain of the second subunit. cytochrome P450 reductase (CPR) share~60% sequence homology. This remarkable example of convergent evolution suggests that specific properties of CPR predestine it as a mediator between NADPH and the type of monoxygenase represented by P450 and NOS. For comparison, the CYP450/P450 reductase redox pair is shown in a similar fashion. Note the presence of calmodulin, BH4, and Zn^{2+} as additional cofactors in NOS. The color-coding of the figure illustrates the lack of structural homology, apart from the heme, between the NOS oxygenase domain and CYP450[2].

Given the extensive similarity between NOS and CYP450, and the vast repertoire of drug P450-catalyzed biotransformations [4–6], it is worth assessing the role that CYP450 might play in the development of drug immunomodulation. It makes sense to consider that molecules showing ability to inhibit NOS activity might be especially prone to interacting with the CYP450 family. The CYP450 enzyme system is the main metabolic systems that evolved to enable organisms to deal with lipid-soluble environmental chemicals. In recent time, the importance of the system in metabolizing drugs has been recognized. The CYP450 system performs this function by oxidizing, hydrolyzing or reducing the chemicals. This enables

another group of enzymes, conjugation enzymes, to attach polar groups to make the metabolites water soluble so that they can be excreted in the urine [7]. Drug metabolism might result in the production of both inactive and active metabolites. In fact, active metabolites may be more potent than the parent compound. Thus, although metabolism is ultimately a process of detoxification, it produces intermediate products that may have clinically useful activity or be associated with toxicity, or both [8]. Therefore, the biological effectiveness and the potential toxicity of NOS inhibitors might be strongly influenced by their CYP450 metabolism (Figure 3).
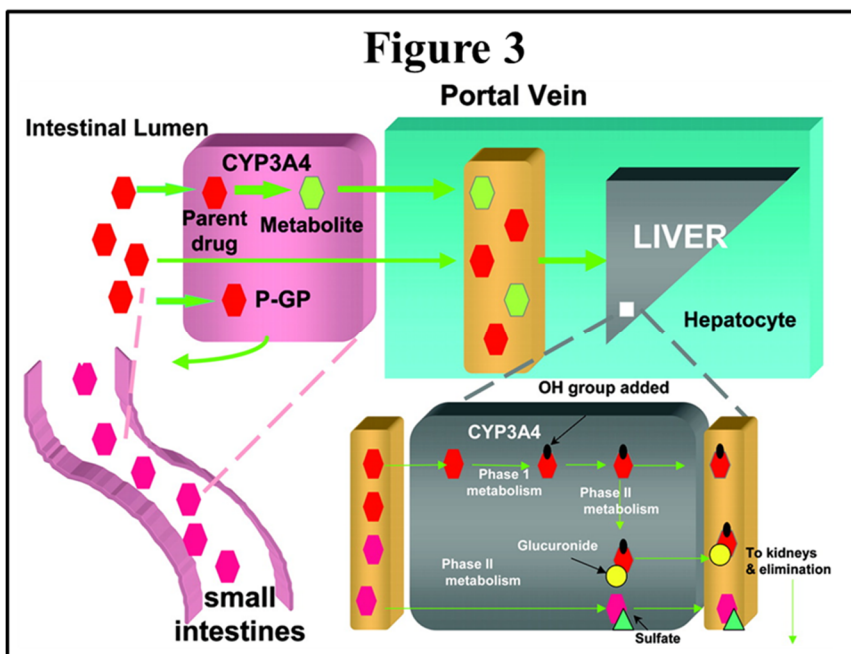
Figure 3. Drug metabolism. During absorption, drugs are metabolized by intestinal cytochrome P450. P-gp assists by pumping drug back into intestinal lumen. Drugs that evade intestinal metabolism enter portal blood and are subject to further biotransformation by hepatic cytochrome P450. Most drugs undergo phase I metabolism in which metabolites may be further conjugated or are directly eliminated by kidney. Small group of drugs may undergo phase II metabolism with no prior biotransformation [9].

Due to the association between the inappropriate release of NO and the pathogenesis of a number of disease states, the NOS isoforms (mainly the inducible isoform, iNOS) have become

attractive targets in drug design for various pathological states, especially neurodegenerative

disorders, inflammation and pain [10].

Among the different compounds able to prevent the biological activity of NOS, we can find

the antifungal imidazole related family, which is also recognized for strongly inhibiting the

enzymatic activity of several CYP450 isoforms [11]. This inhibition of NOS involves a

putative binding of the imidazole nitrogene to the heme iron, reducing the maximal velocity of

citrulline formation [12]. Not surprisingly, in other mechanistic studies for evaluation of

CYP3A4 inhibition by imidazole derivatives, heme coordination by the imidazole functional

group was observed (Figure.4) [13].
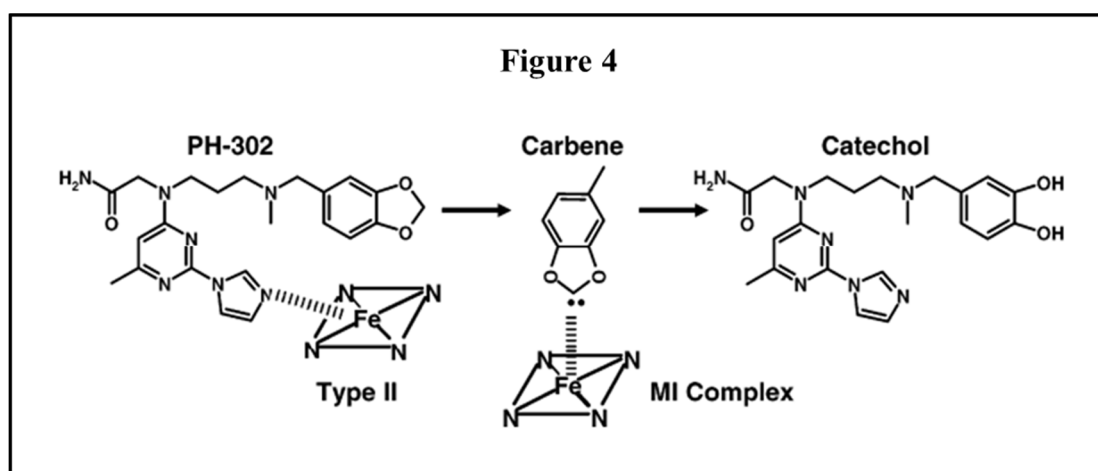
Figure 4. Metabolism of PH-302 by P450 3A4 to its Catechol Metabolite, with the Carbene Intermediate Proposed to Coordinate with the Heme of P450 3A4 and Cause Time-Dependent Inhibition Given the prevalence of nitrogen containing heteroaromatic compounds used in drug scaffolds, nitrogen coordination to the heme-iron of CYP450 enzymes can play a major role in the binding affinity, the potential for drug/drug interactions, the half-life of a potential drug, and the ability of a drug to alter the metabolism of toxins. Tracy and coworkers, have provided evidence that type II interactions (heme coordination) with CYP2C9 reveal minor binding modes, indicative of only weak interactions. Wienkers and coworkers [14] have shown that PH-302, while giving a type II spectra also bound to the CYP3A4 in an alternate orientation that led to metabolism at a site distant from the imidazole that coordinated to the iron. Interestingly, this compound inhibits inducible nitric oxide synthase (iNOS) by coordinating to the heme, and preventing dimerization [15]. PH-302 is a pyrimidineimidazole that potently and selectively inhibits iNOS, Because of the mechanism by which PH-302 inhibits the iNOS enzyme (heme coordination), it seemed likely that the inhibition of the heme containing CYP450 super family of drug-metabolizing enzymes was a potential liability. Time-dependent inhibition of CYPP450 3A4 by PH-302 was also observed because of metabolite-inhibitory (MI) complex formation via metabolism of the methylenedioxyphenyl group.

Analogously, macrolide antibiotics have long been recognized to exert immunomodulatory and anti-inflammatory actions, via inactivation of NO production [16, 17]. In turn, some macrolide antibiotics have also been found to form stable metabolic intermediate complexes with the iron (II) present in the heme group of CYP450, after being metabolized (Figure 5) [18, 19].

It has been extensively reported that expression of biotransforming enzymes in immortalized cell lines is much lower on average than that observed in primary cells from liver, lung, blood and skin [20].
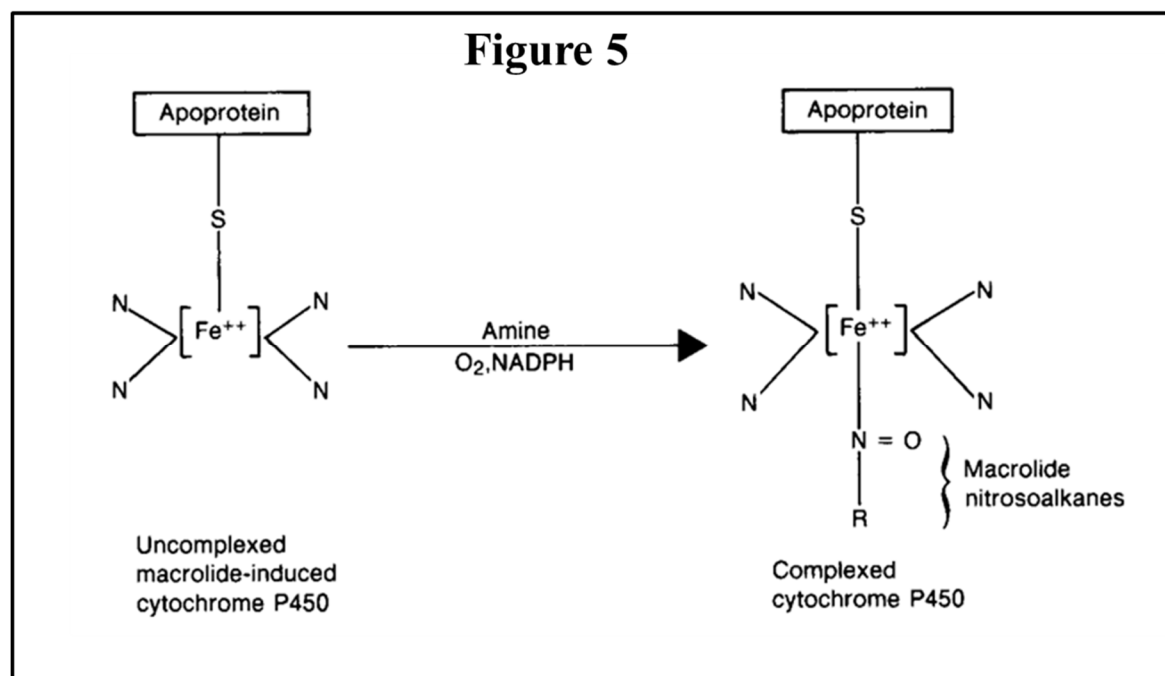
Figure 5. Metabolism of tertiary amine drugs such as macrolides. Macrolides consist of a large aglycone ring and 1 or more sugars, some of which are amino sugars, bearing a tertiary amine function. Drugs such as macrolide antibiotics are oxidised in the liver by a microsomal multienzymatic system with CYP450 as the terminal oxidase. Cytochrome P450 is comprised of different isozymes, each with the same haeme iron oxidising centre but varying apoprotein. The isozymes actively demethylate and oxidise the macrolide antibiotic into a nitrosoalkane which forms a stable, inactive complex with the iron [Fe++] of CYP450 [21].

Therefore, if CYP450 activities are modulating NO production to some extent by compound depletion or bioactive metabolite formation, some differential effects in NO production should be observed between in vitro models using cell lines or primary cultures. For this approach it

was essential using an inmunocompetent cell in vitro model but with   limited CYP450 expression compared with the in vivo situation or primary cell cultures.

2.1.2   Evaluation of immunomodulatory activity through NO production

Macrophages play a critical role in the initiation, maintenance, and resolution of inflammation. They are activated and deactivated in the inflammatory process. Activation signals include cytokines (interferon γ, granulocyte-monocyte colony stimulating factor, and tumor necrosis factor α), bacterial lipopolysaccharide (LPS), extracellular matrix proteins, and other chemical mediators (Figure 6).
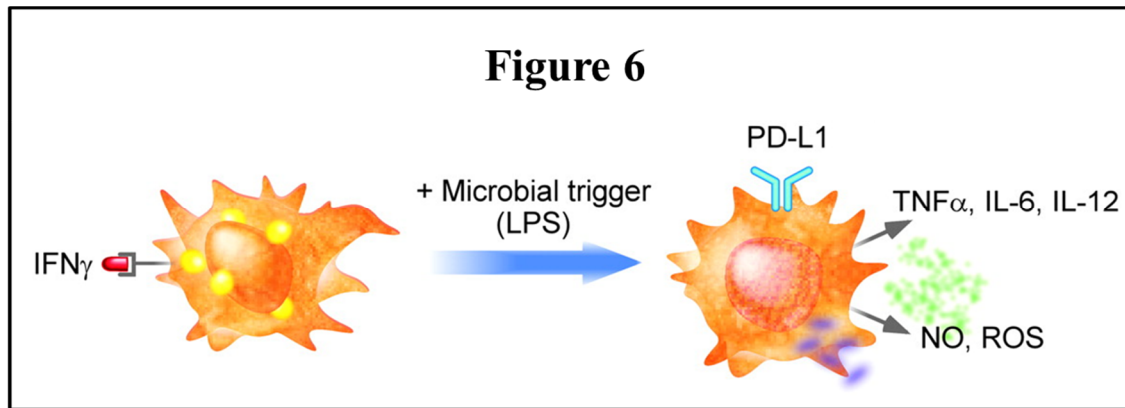
Figure 6. Macrophage activation contributes to functional heterogeneity. In response to cytokine signals, recruited and resident macrophages can undergo distinct activation programs. Stimulation with the Th1 cytokine IFNγ and microbial byproducts, such as LPS, promotes maturation of classically activated macrophages. While the respiratory burst, reactive oxygen species (ROS) and NO, promotes their microbicidal actions, secretion of proinflammatory cytokines, such as TNFα and IL-12, enhances cell-mediated immunity [22].

LPS is present in the outer membrane of the bacteria and plays a key role in mounting infection, leading to an immune response, and development of a strong inflammatory disorder. LPS is a potent inducer of monocytes and macrophages, which are key mediators of the innate immune response. Stimulation of cells by LPS leads to a cascade of intracellular signaling events that ultimately result in secretion and production of cytokines and other inflammatory mediators constituting the pro-inflammatory response [23]. In particular, macrophages play an important

role in the modulation of inflammation and immune response to maintain a defensive reaction. During an inflammatory response, activated macrophages secrete NO via the inducible isoforms of NOS (iNOS) and large amount of pro-inflammatory mediators and cytokines, tumor necrosis factor alpha (TNF-α), and IL-6, etc [24]. Because activated macrophages produce a wide range of biologically active molecules participated in inflammation outcomes, they represent a valuable tool for investigating inmunomodulatory response [25]. Specifically the quantitation of NO in LPS stimulated RAW 264.7 murine cell line has proven to be an important tool for in vitro studies of immunomodulation [26][27][28], having particular advantages over other cells generated from primary bone marrow cell populations or directly isolated from murine bones. These include their ready access and availability, simple culture that can generated large amounts of study material and close correlation in characteristics, gene expression, signaling, and developmental or functional processes with either directly isolated from murine bones or formed in vitro from primary bone marrow precursor cells [29]. However, it has been previously described that cultured cells displayed a low drug-metabolizing capacity as consequence of a decrease in CYP450 gene transcription that could be linked to decreased CYP450 expression and functionality of these cells [30].

Metabolism issues of a drug may affect to CYP450 inhibition and hence its half-life and often determines whether it will be effective and safe. For this reason, candidate drug compounds are often screened early in the discovery process for the most critical drug metabolism in vitro tests which are described in more detail in the following sections. A common system for measuring hepatic metabolism uses liver microsomes, a subcellular fraction containing major drug-metabolizing enzymes, including the CYP450 family and flavin monooxygenase [31].

2.1.3 CYP450 reversible inhibition

CYP450 are a family of enzymes which play a major role in the metabolism of drugs. The *in vitro* studies using hepatic microsomal fractions have historically provided critical and basic information on drug metabolism by CYP450, which is essential for prediction of the in vivo state [32]. Among the most critical determination within in vitro drug metabolism we can find the evaluation of the inhibition of CYP450. Assessment of the potential of a compound to inhibit a specific CYP450 enzyme is important as co-administration of compounds may result in one or both inhibiting the other's metabolism. This may affect plasma levels in vivo and potentially lead to adverse drug reactions or toxicity. The gold standard for CYP450 inhibition assays uses specific probe substrates, HLM and LC-MS as detection technique (Figure. 7). In the CYP450 Inhibition assay, a decrease in the formation of the metabolites compared to the vehicle control is used to calculate an IC_{50} value (test compound concentration which produces 50% inhibition). Typically the compounds can be categorized into the following classification bands:

- Potent inhibition $IC_{50} < 1\,\mu M$
- Moderate inhibition IC_{50} between 1 and 10 µM
- No or weak inhibition $IC_{50} > 10\,\mu M$
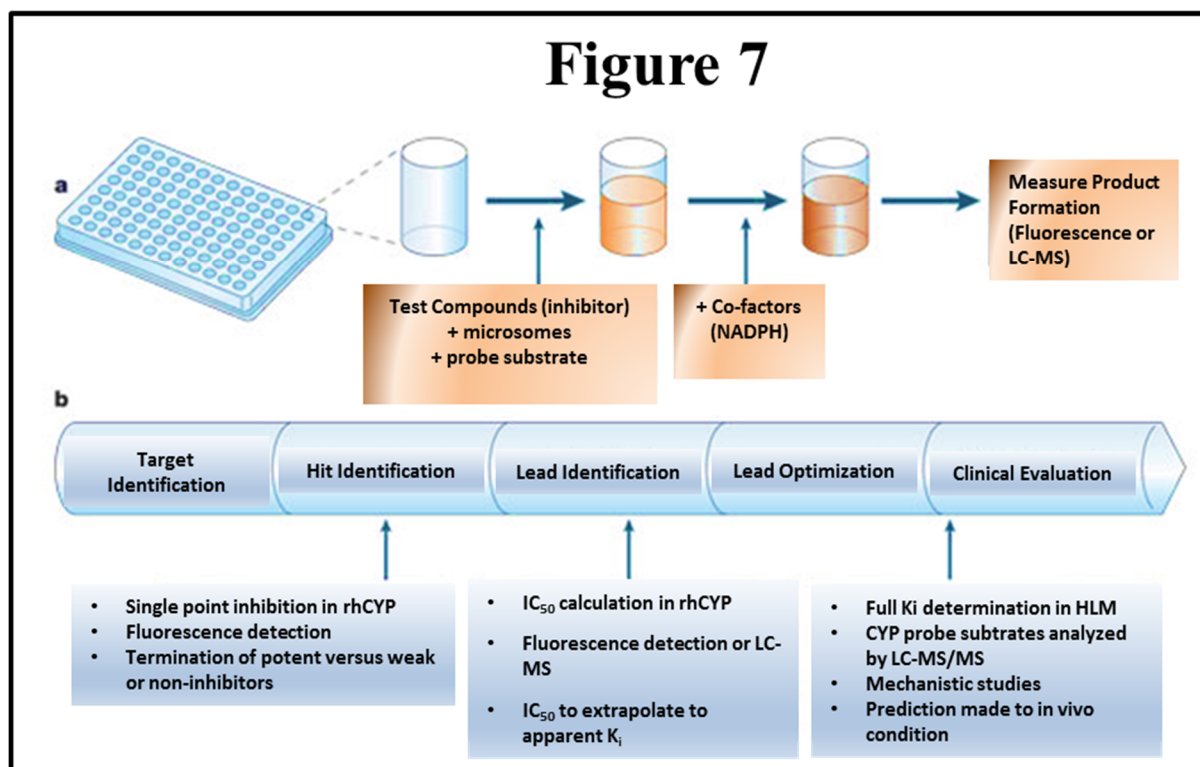
Figure 7. Assessing drug–drug interaction potential for new chemical entities at stages in drug development. a) A typical in vitro CYP450 inhibition assay. **b)|** Stages in drug development at which *in vitro* data are used to predict in vivo drug inhibition. Typically, the experimental robustness of the studies listed will yield results that possess the required level of detail to aid in decision making at that juncture in vitro. Restated, in vitro drug–drug interaction studies carried out in later stage drug development require high-quality and consistent data, as these studies ultimately influence the design of clinical trials compared with CYP450 inhibition screening in early lead identification, in which the goal is focused more on identifying issues associated with a particular chemistry series. Collectively, drug–drug interaction studies represent a crucial mechanism for assessing potential drug candidates and for aiding in the development of mechanisms for predicting and retrospectively explaining in vivo drug performance. LC–MS, liquid chromatography–mass spectrometry; rhCYP, recombinant human cytochrome P450 [33].

The inhibition of CYP450 can be reversible (competitive or non-competitive) or irreversible.

Irreversible inhibition usually derives from activation of a drug by CYP450 into a reactive

metabolite, which tightly binds to the enzyme active site, leading to a long lasting inactivation.

In competitive inhibition, binding of the inhibitor to the enzyme prevents the binding of the

substrate to the active site of the enzyme (Figure 8). This generally is believed to be the result

of the inhibitor sharing some degree of structural similarity with the substrate(s) of that

CYP450 isoform. Depending on the substrate specificity of the CYP450, some of which exhibit relatively little apparent specificity, the structural similarities between the competitive inhibitor and the substrate whose metabolism is inhibited may or may not be apparent. Although the competitive inhibitor may be a substrate also for the CYP450 that it inhibits, that is not necessarily the case. The competition by the inhibitor for occupancy of the CYP450 active site may involve simple competition for binding to a lipophilic domain in the active site or it may involve hydrogen bonding or ionic bonds with specific amino acid residues in the active site. This type of inhibition is most commonly observed when two different substrates of the same CYP450 enzyme are present. Competitive inhibition is encountered relatively frequently in drug metabolism studies both when using microsomal preparations or purified reconstituted enzyme systems in vitro as well as in metabolism studies performed in vivo. Since many of the CYP450 have numerous drugs as substrates, competition of various drugs for metabolism by a specific CYP450 is a common occurrence leading to drug–drug interactions in patients who are simultaneously administered several different drugs [34].
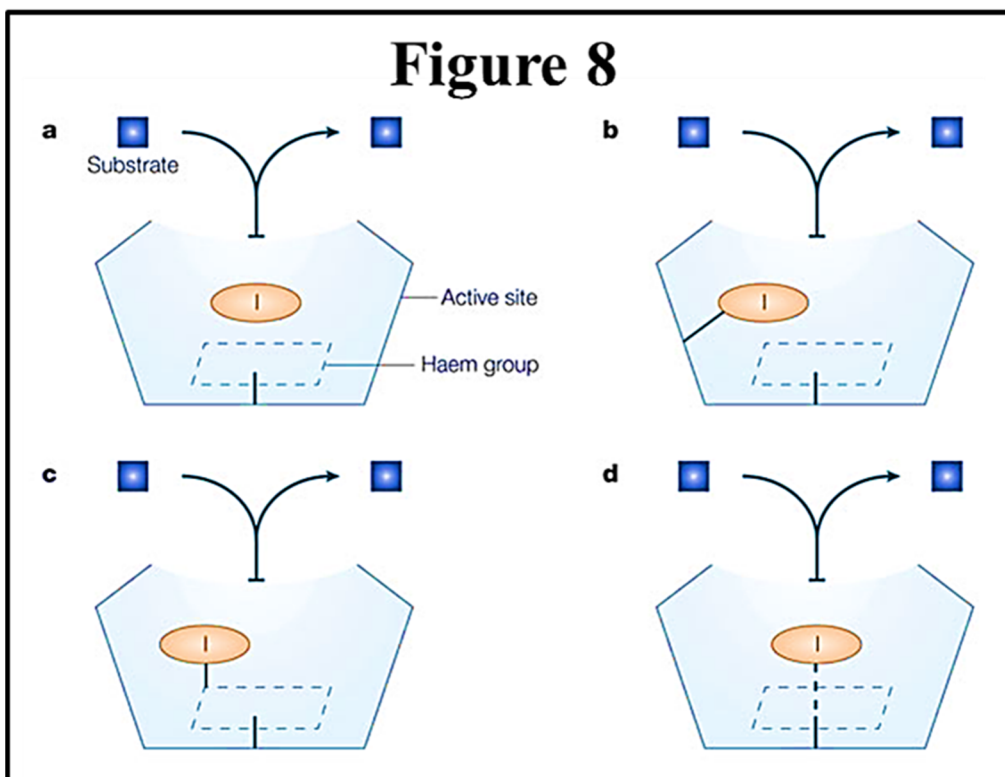
Figure 8. Possible mechanisms of inhibition for the cytochrome P450s. a) Reversible inhibition, in which the inhibitor interacts with the enzyme in a manner that blocks access of the drug to be metabolized to the active site of the enzyme. **b)** Irreversible inhibition, in which the inhibitor is activated by the enzyme to form a reactive intermediate that covalently binds to the apoprotein. **c)** Irreversible inhibition, in which the inhibitor is activated by the enzyme to form a reactive intermediate that covalently binds to the prosthetic haem group. **d)** Quasi-irreversible inhibition, in which the inhibitor is activated by the enzyme to form an intermediate that results in the destruction of the prosthetic haem group (metabolic intermediate complex) [33].

2.1.4 CYP450 Time dependent inhibition

A second category of inhibitors includes time dependent inhibitors: Among them we can find a category of inhibitors that bind irreversibly to the prosthetic heme or to the protein, or that cause covalent binding of the heme prosthetic group, or its degradation product to the apoprotein. These compounds require metabolic activation by the CYP450 and are part of a class of inhibitors commonly referred to as "catalysis-dependent", "suicide", or "mechanism-based" inactivators [35–37]. Mechanism-based inactivation is generally regarded to be a

relatively unusual occurrence with most enzymes. However, it is observed in reactions catalyzed by CYP450 in somewhat higher frequency than would normally be expected, possibly as a result of the reactivity of the oxygenated intermediates formed during the course of the oxygenation reactions. The utility of mechanism based inactivators in the design of new drugs that are highly selective for a given CYP450 enzyme has attracted great interest recently since, in principle, these compounds could be designed so that they would only inhibit the target enzyme [35]. These inactivators also have attracted considerable interest as a result of their utility in elucidating enzyme mechanisms. Finally, a great deal of effort has been expended on the development of mechanism-based inactivators as inhibitors of specific CYP450 enzymes that can be used as diagnostic tools to identify which form(s) of the CYP450 are involved in catalyzing a particular reaction in microsomal preparations. These compounds result in the formation of covalent bonds that cannot be broken to regenerate catalytically active enzyme. Although the onset of inhibition by these compounds may occur in vivo more slowly than that observed with reversible inhibitors, the final effect of the mechanism based inactivators is generally much more profound and inhibition of drug metabolism can be reversed only by the synthesis of new, catalytically active CYP450. A variety of compounds have been shown to be good mechanism-based inactivators for CYP450. These include: 1) acetylenes and terminal alkyl and aryl olefins such as 2-ethynylnaphthalene, 9-ethynylphenanthrene, 5-phenyl-1-pentyne, 10-undecynoic acid, and 17a-ethynyl-estradiol; 2) a variety of organosulfur compounds such as disulfiram, cimetidine, dialkylsulfides, parathion, diethyldithiocarbamate, isothiocyanates, thioureas, and xanthates; 3) halogenated compounds such as chloramphenicol and N-monosubstituted dichloroacetamides; 4) 1-aminobenzotriazole and its N-aralkylated derivatives; and 5) furanocoumarins such as methoxypsoralins, L-754, 394 (a Merck compound synthesized as a potential HIV protease inhibitor) and bergamottin (5,21,22). Reactions that result in the mechanism-based inactivation of CYP450 involve the

formation of a complex between the CYP450 and a reactive intermediate that can then either react with the CYP450 to form a covalent adduct resulting in inactivation or it can dissociate resulting in product formation and the regeneration of the native catalytically active enzyme. The derivation of the various kinetic constants for this type of reaction has been described. The potential of enzyme inhibition of a drug is frequently quantified in terms of IC_{50} values. Although this is a suitable quantity for reversible inhibitors, concerns arise when dealing with irreversible or mechanism-based inhibitors (MBIs). IC_{50} values of MBIs are time dependent, causing serious problems when aiming at ranking different compounds with respect to their inhibitory potential. As a consequence, most studies and ranking schemes related to MBIs rely on the inhibition constant (KI) and the rate of enzyme inactivation (Kinact) rather than on IC_{50} values [38].

As pointed out by Ortiz de Montellano and Correia [39], mechanism-based inactivators may exhibit better enzyme specificity than reversible inhibitors since: 1) the initial binding of the inhibitor to the specific CYP450 enzyme must satisfy all of the constraints imposed on reversible inhibitors; 2) the inhibitor must be acceptable as a substrate for that CYP450 due to the requirement for catalytic activation to a reactive species; and 3) the formation of the reactive species during metabolism leads to an irreversible modification of the enzyme that permanently removes it from the pool of active enzymes. The apparent flexibility of the active sites of many of the CYP450, as evidenced by the sizes and numbers of different substrates they can metabolize, offers the possibility of designing many different mechanism-based inactivators having a variety of potentially reactive moieties These inhibitors are of substantial interest not only for studies probing the structures, mechanisms of action, and biological roles of specific CYPP450, but also because of their potential as modulators of CYP450 activity that can be

used as therapeutic agents in a manner analogous to the way inhibitors of the steroidogenic CYP450s have been used to treat endocrine disorders and as anticancer agents [34].

2.1.5 Metabolic Stability

In general, the function of metabolic clearance is to convert a lipophilic molecule into a more polar and more aqueous soluble metabolite that can then be eliminated in the bile and/or urine. The liver possesses the highest levels of the major and most commonly involved drug metabolizing enzymes [33]. Hence, the metabolic stability refers to the susceptibility of compounds to biotransformation into metabolite as function of incubation time (Figure. 9).
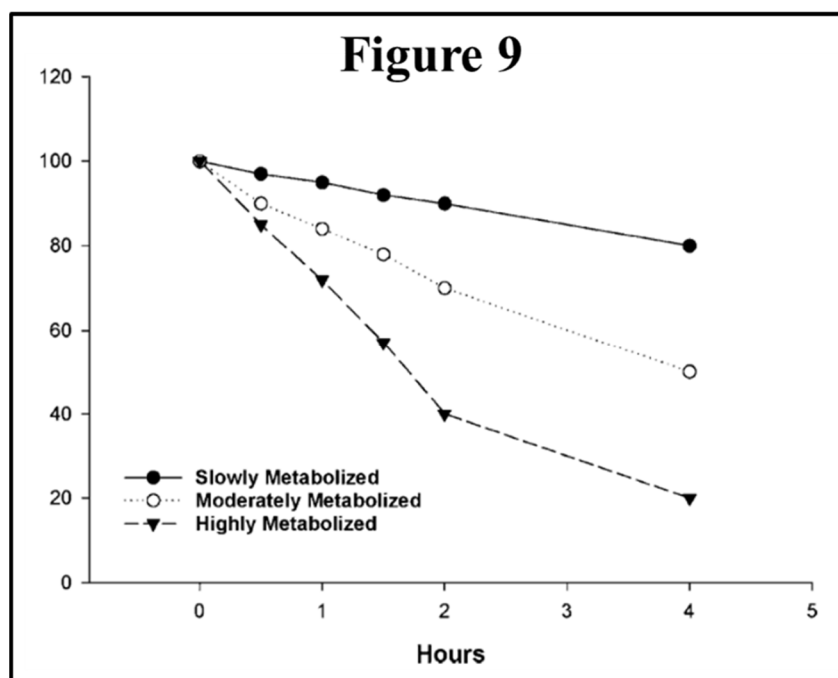
Figure 9. Theoretical stability of three compounds in the presence of suspended hepatocytes. The disappearance of the compounds at different rates allows the compounds to be assigned rankings, such as slowly metabolized, moderately metabolized, and highly metabolized [40].

Metabolic stability results are usually reported as measures of intrinsic clearance, from which secondary pharmacokinetic parameters such as bioavailability and half-life can be calculated [41]. This is done simply using simple liver microsomal assays are very useful for differentiating compounds with rapid turnover from those with no measurable turnover.

Intrinsic clearance or CLint can be defined as the proportionality constant between the concentration of substrate at the enzyme and its rate of metabolism in the absence of physiological constraints: a rate or metabolic half - life of metabolism to calculate the intrinsic clearance of a drug that in turn is scaled to predict its in vivo clearance in the animal or human. In general, if the in vitro assays correctly predict the in vivo clearance measured in animal models, then there is some confidence that the same will hold true for the prediction in humans.

2.1.6 Metabolite Elucidation

Mass spectrometry (MS) and nuclear magnetic resonance (NMR) are critical to the success of drug metabolism studies. NMR spectroscopic techniques are most often used to confirm and elucidate metabolite identification in drug metabolism studies. Liquid chromatography (LC)-NMR is a good choice for these studies, but MS has advantages over NMR with respect to sensitivity, smaller sample size, and greater speed compared with NMR. LC-MS-NMR has become a commercially available technique and is used in the late discovery stages to confirm and characterize metabolites. LC-MS is an analytical technique that still shows room for development; already, significant improvements have been made in sensitivity and resolution. It is probably the most powerful technique currently available for pharmaceutical analysis, and has significantly accelerated the drug discovery and development process. LC-MS has become the dominant technique for performing almost all of the analyses involved in drug metabolism studies, and is likely to remain the principal tool for such studies.

The major aim of LC-MS is the application of its analytical power to create straightforward, sensitive, fast, and reliable data. Improved hardware and software for LC – MS have led to greater sensitivity, greater ease - of - use, and improved post - analysis of data such as electron impact, chemical ionization, atmospheric pressure chemical ionization (APCI), fast atom bombardment, thermospray, gas chromatography – mass spectrometry and electrospray

ionization (ESI) are used in absorption, distribution, metabolism, and excretion - toxicity (ADMET) studies. Metabolite characterization ion trap ("MS^n" — this refers to multistage tandem mass spectrometry (MS/MS) experiments where n is the number of product ion stages (progeny ions)) and quadrupole time of flight (QTOF)-MS are widely used; QTOF-MS has advantages for metabolite identification over MS^n or triple quadrupole MS, including fast mass spectral acquisition speed with high full - scan sensitivity, enhanced mass resolution, and accurate mass measurement capabilities which allow for the determination of elemental composition. Exact mass measurement is a valuable tool for solving structure elucidation problems by helping to confirm elemental composition, and is also invaluable in eliminating false positives and determining nontrivial metabolites. Accurate mass measurements are routine experiments performed by modern mass spectrometers. The accuracy of a measurement refers to the degree of conformity of a measured quantity to its actual true value. Data-dependent scans on QTOF provides a highly useful tool. Increasing sample complexity, sample volume restrictions, and throughput requirements necessitate that the maximum amount of useful information is extracted from a single experiment. Information dependent adquisition (IDA) or data - dependent scans enable intelligent MS and MS/MS acquisitions to be performed automatically on multiple co-eluting components. IDA is able to make intelligent decisions about which ions to select for MS/MS using its inherent high resolution (HR), exact mass measurement capability, and full mass range. By utilizing high resolution, accurate mass spectrometry, specificity is improved without compromising on sensitivity. Greater confidence in structural elucidation can occur as both MS precursor and 'MS/MS' products ions can only be rationalized with a very small number of elemental combinations – therefore increasing the confidence in structural assignment (Figure 10) [42].
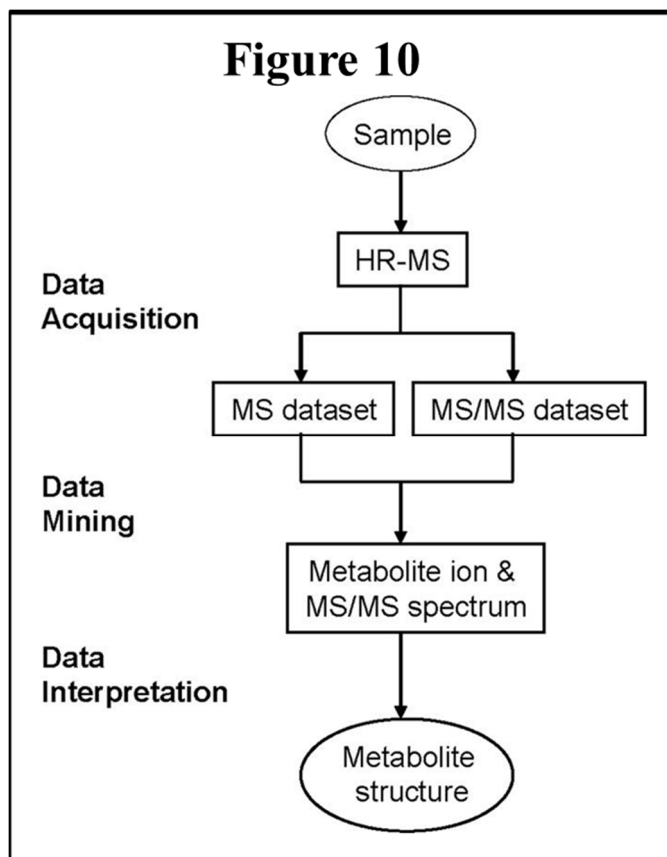
Figure 10. General scheme of HR-MS-based approaches to drug metabolite detection and identification [43]**.**

2.1.7 Drug Solubility

In order for an orally administered compound to act, it must dissolve in the aqueous environment of the gastrointestinal tract and within the cytoplasm when the target is intracellular. The partition coefficient of a compound is directly related to its aqueous solubility — all else equal within a series. The more lipophilic a compound is, the lower is its aqueous solubility. Poor solubility can limit the absorption of compounds from the gastrointestinal tract, resulting in reduced oral bioavailability. It may also necessitate novel formulation strategies and hence increase cost and delays. Moreover, compound solubility can affect other in vitro assays. Poor aqueous solubility is the largest physicochemical problem hindering oral drug

activity — hence on completion of compound synthesis, the determination of aqueous solubility is a priority. Solubility data may prove critical in rationalizing disparate results in other bioassays (Figure 11) [44].
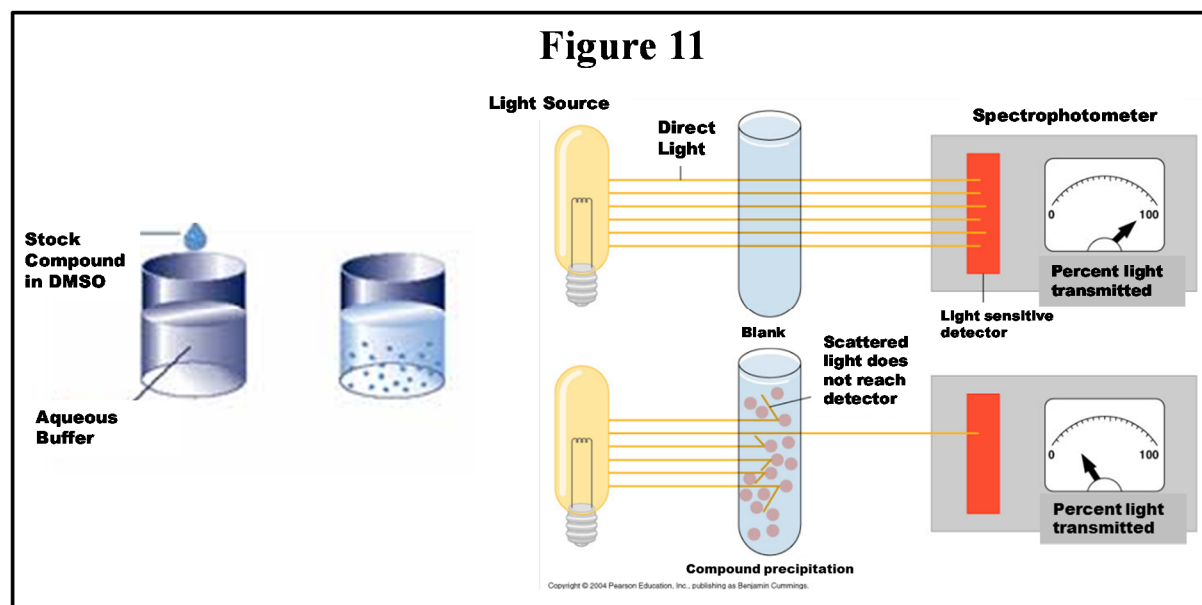
Figure 11

Figure 11. Estimating compound precipitation by indirect method. A spectrophotometer is used to determine turbidity ("cloudiness") by measuring the amount of light that passed through a suspension of compounds. More precipitated compound = more turbidity; more turbidity = less light passing through the suspension (absorption and transmission (T) spectra represent equivalent information and one can be calculated from the other through a mathematical transformation. A transmission spectrum will have its maximum intensities at wavelengths where the absorption is weakest because more light is transmitted through the sample. An absorption spectrum will have its maximum intensities at wavelengths where the absorption is strongest). %T is percent transmission - fewer precipitated compound present (less turbidity) will allow more light to pass through, the %T is higher when the cell number is lower. Absorbance is the opposite of %T. More light is absorbed when more precipitated compound is present.

For example, a compound must be soluble in the assay buffer used to measure activity. Poorly soluble compounds within a series are more likely to have variable solubility in different buffer systems used in common bioassays, which can confound the SARs that are critical for effective lead optimization. In fact, some have shown that determination of the effective concentration of compounds in bioassays reveals marked errors in potency measurements due to marked underestimation of the actual concentration of compound that is in solution in the bioassay,

particularly when a single concentration is used to assess activity by extrapolated IC$_{50}$ values [45].

Therefore the integration of the results from immunomodulatory activity and drug metabolism tests for selective compounds (imidazoles & macrolides) along with other results from other fully functional cell models (primary alveolar macrophages) represents a useful approach to enhance the knowledge about the role of CYP450mediated drug metabolism in the pharmacological modulation of NO production.

2.2 A high throughput screening platform for the assessment and discovery of immunomodulator molecules.

2.2.1 Targets for the assessment of immunomodulatory activity

Modulation of the immune system involves induction, expression, amplification or inhibition of any phase of the immune response, and as such the immune system could be modulated through various mechanisms such as complement activation/inhibition, lymphocyte proliferation, macrophages stimulation/inhibition or influencing the cytokine production by various immune cells [46]. During the inflammatory process, large amounts of pro-inflammatory mediators such as NO and prostaglandin E2 are generated by iNOS and COX-2. Expression of COX-2 during inflammation is controlled by cytokines and bacterial products, such as LPS. LPS is a potent inducer of systemic inflammatory responses, which can be mediated via induction of oxidative stress. This event may lead to tissue damage and increased epithelial permeability. Free radicals and reactive oxygen metabolites trigger and/or amplify inflammation via the upregulation of expression of a number of genes, including nuclear factor kappa-light-chain-enhancer of activated B cells (NF-κβ). Activation of NF-κβ in turn leads to amplification of the inflammatory response by upregulating production of several proinflammatory cytokines and enzymes, such as IL- 1, IL-6, TNF-α, and iNOS.

Inflammation can also be induced by biochemical and pharmacological agents from the environment, in addition to a diverse array of cell types and soluble mediators including cytokines. The immune system of mammals is comprised of a complex array of cells and molecules, which interact to provide protection from invading pathogenic microbes through mediation of T cells that include Th1 and Th2. Besides this, it is clearly demonstrated that other subpopulations such as Th17 and regulatory T cells maintain immunological tolerance (Petersen et al. 2012). Th1 cells produce pro-inflammatory cytokines such as interferon gamma (IFN-γ), TNF-α, IL-1 and IL-2, IL-8 and COX-2. Th2 cells, on the other hand, express anti-inflammatory cytokines, namely IL-4, IL-5, IL-6 and IL-10, etc [47].

2.2.2 Approaches to evaluate immunomodulatory properties

The principal purpose of any in vitro model is to simplify experimental variables to effectively isolate different components of organs or organ structures for study under well-controlled and easily assessed conditions. How accurately these conditions must duplicate in vivo conditions depends on the study design and desired outcomes. Not every in vitro assay must necessarily recapitulate in vivo physiology. Different in vitro models may reflect different levels of cellular organization and behavior, and provide different degrees of in vivo-relevant information. Exploitation of in vitro cell culture systems has proven to be a valuable tool to study cell biological, physiological and pathological processes for over a century, but as any tool, is subject to limitations, distractions, artifacts, and misleading results when removed from physiological context without validation or justification. Intact functional organs in vivo exhibit extensive interrelationships and crosstalk from multiple different cell types and dynamics that modulate all physiological processes. This feedback mechanism is lost when individual cell types are cultured in vitro. All cell, tissue, or organ cultures seek a minimalist approach that on one hand facilitates their simplified assessment isolated from the dynamic in

vivo context, but on the other hand restricts the depth of conclusions that can be drawn from the work. General agreement exists that no in vitro culture will ever completely represent whole animal experiments, and there are many cases in basic science where such fidelity is unnecessary [48]. Despite different triggering events, a common feature of inflammation diseases is immune activation [49]. Therefore, several approaches might be use to explore ways to inhibit or modulate inflammation through the main anti-inflammatory target proteins, such as iNOS and interleukin-8 (IL-8), among many others thought to contribute to tissue damage. NO regulates numerous physiological processes including neurotransmission, smooth muscle contractility, platelet reactivity and the cytotoxic activity of immune cells. Because of the ubiquitous nature of NO, inappropriate release of this mediator has been linked to the pathogenesis of a number of disease states. This provides the rationale for the design of therapies that modulate NO concentrations selectively. The inhibitors of iNOS are potentially beneficial agents in the treatment of conditions associated with an overproduction of NO, including septic shock, neurodegenerative disorders and inflammation. In turn, the pro-inflammatory chemokine IL-8, produced by macrophages and other cell types, exposed to inflammatory stimuli, is also an attractive target for inflammation treatment [50].

RAW 264.7 murine macrophage-like cells have previously been used to evaluate the anti-inflammatory activity of solvent plant extracts, whereby inflammatory mediators and pro-inflammatory cytokines represent the main readouts. TNF-α is a pleiotropic cytokine, produced principally by monocytes and macrophages, which plays a pivotal role in host immune responses while NO and COX-2 are two important inflammatory mediators to test the anti-inflammatory activity of solvent extracts and have been shown to plays a pivotal role in regulating various biological activities in vascular, neural, and immune systems. Infected macrophages mediate host defense functions such as antimicrobial and anti-tumor activities through production of NO; however excessive production lead to tissue damage and several

inflammatory disorders [46]. Hence that the production of NO from LPS stimulated RAW 264.7 macrophages, it has been considered an appropriate in vitro model for the evaluation of immunomodulatory properties [51–53].

Adherence of bacteria to epithelial cells is an important step in colonization and immune modulation in the large bowel.Caco-2 cells (derived from human colon adenocarcinoma) have gained enormous popularity as a reliable and high-throughput in vitro model system to investigate how environmental factors affect cytokine expression to Caco-2 cells [54] [55]. This cytokines produced by intestinal epithelial cells may function as signals to neighbouring immune and inflammatory cells. Other investigators demonstrated that production of the neutrophil and T-lymphocyte chemotactic cytokine IL-8 by intestinal epithelial cells using four colonic adenocarcinoma cell lines, T84, CaCo-2, HT29 and SW620, as a model system [56]. These cell lines secreted substantial amounts of IL-8 if stimulated with IL-1β, TNF-α or IFN-γ, except CaCo-2 cells, which responded only to IL-1β (Figure. 12) [57]. IL-8 and possibly other chemokines generated by colonic adenocarcinomas may help to attract tumour-infiltrating leucocytes. Possibly, normal intestinal epithelial cells also have the potential to secrete this potent chemoattractant and thus might contribute to inflammatory responses of the intestinal mucosa, for example in inflammatory bowel disease [56].

Even though NO's involvement in the production of IL-8 has been studied in different cell types and tissues, the mechanism of action has not been clarified yet. However, the results suggest that the production of IL-8 is regulated by similar transcription factors to those responsible for the increased expression of iNOS [58]. Therefore, the correlated measurements of NO and IL-8 productions provide information not only on the compounds' ability to inhibit the activity of iNOS and thus the production of NO, but also on the potential mechanism of action to interfere with the expression of inducible inflammatory mediators.
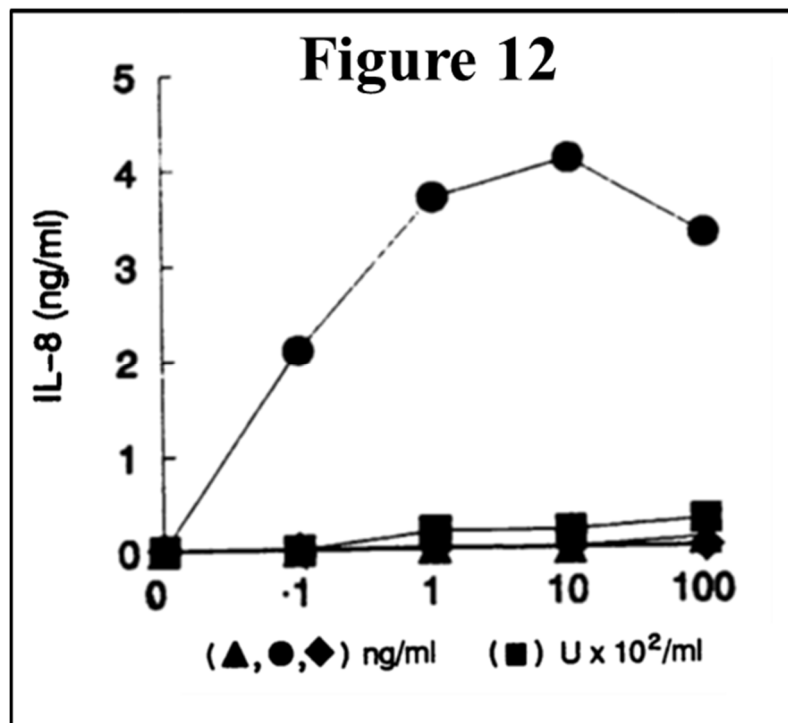
Figure l2. Dose-dependent stimulation of lL-8 secretion in colonic epithelial cell lines by TNF-α, lL-lβ, LPS and IFN-γ. Confluent monolayers CaCo-2 cells were stimulated for 16 hour with either TNF-α (triangles), IL-1β (circles) or LPS (diamonds), added as final doses in ng/ml as indicated on the horizontal axis. The final concentration of lFN-y (squares) is given in U x 10^2/ml also on the horizontal axis [59].

2.2.3 Characteristics of chemical diversity found in natural products and synthetic libraries

Several classes of drugs, such as corticosteroids, non-steroidal anti-inflammatory drugs and biologics are used to treat inflammatory disorders. However, all these drugs possess several adverse side effects, such as gastrointestinal ulceration, bleeding, and platelet dysfunction due to the inhibition of COX-1-derived prostanoids, or cardiovascular side effects due to inhibition of prostacyclin formation. Therefore, there is a continuous need to search for more effective and safer anti-inflammation agents which is a key objective for the pharmaceutical industry.

Current thinking in the generation of drug leads embodies the concept of achieving high molecular diversity within the boundaries of reasonable drug-like properties. It has long been recognized that natural-product structures have the characteristics of high chemical diversity,

biochemical specificity and other molecular properties that make them favourable as lead structures for drug discovery, and which serve to differentiate them from libraries of synthetic and combinatorial compounds. Various investigators have worked to measure by means of computational chemistry those desirable chemical features that distinguish natural products from other sources of drug leads [60, 61]. They examined representative combinatorial, synthetic and natural product compound libraries on the basis of molecular diversity and 'drug-likeness' properties such as molecular mass, number of chiral centers, molecular flexibility as measured by number of rotatable bonds and ring topology, distribution of heavy atoms, and Lipinski-type descriptors. Other investigators have differentiated natural products, trade drugs or other synthetic molecular libraries on the basis of scaffold architecture and pharmacophoric properties, or other molecular descriptors [62, 63]. These studies reveal that natural products typically have a greater number of chiral centers and increased steric complexity than either synthetic drugs or combinatorial libraries. Although drug and combinatorial molecules tend to contain a significantly higher number of nitrogen-, sulphur- and halogencontaining groups, natural products bear a higher number of oxygen atoms. Multivariate statistical analysis of molecular descriptors shows that natural products differ significantly from synthetic drugs and combinatorial libraries in the ratio of aromatic ring atoms to total heavy atoms (lower in natural products), number of solvated hydrogen-bond donors and acceptors (higher in natural products) and by greater molecular rigidity. Natural-product libraries also have a broader distribution of molecular properties such as molecular mass, octanol–water partition coefficient and diversity of ring systems compared with synthetic and combinatorial counterparts. Indeed, less than one-fifth of the ring systems found in natural products are represented in current trade drugs. A perhaps unexpected finding is that of other investigators who revealed that the fraction of natural product structures with two or more 'rule-of-five' violations is quite low (approximately 10%) and equal to that of trade drugs [64]. In this regard, natural products or

natural product-derived compounds offer great structural diversity, which is not commonly seen in synthetic compounds. Natural products offer an alternative source of highly underexplored chemical entities with privileged bioactive molecules that could be used as templates for the synthesis of novel drugs. The possibility of obtaining them by scaling up the fermentations of the producing microbial strain is an additional advantage that microbial natural products offer as compared to those from other sources, such as plants or marine invertebrates. After elucidation of the molecular structures of many natural products, chemists are often able to propose a total synthesis, rather than isolate them from their natural sources, thereby markedly reducing the cost of mass drug production (Figure 13).
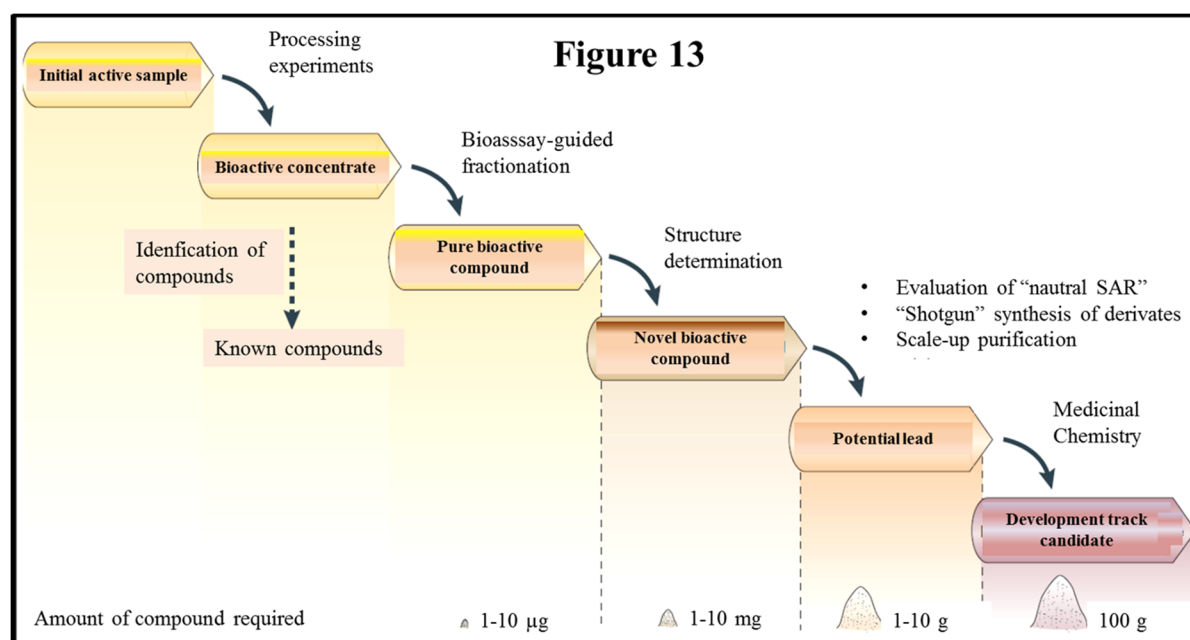
Figure 13. Chemical process for natural product discovery. The natural product is extracted from the source, concentrated, fractionated and purified yielding essentially a single biologically active compound. Identification of known compounds, thereby avoiding replication of previous efforts, has been greatly aided by directly coupled LC-MS systems and natural-product databases. De novo structure determination of compounds that are novel has been revolutionized by advances in spectroscopic techniques, particularly in high-resolution nuclear magnetic resonance technologies. Although the determination of complex structures is technically challenging, it is no longer a major impasse in the drug discovery process. In those cases in which the biological activity profile meets criteria for potency and selectivity, preliminary structure–activity relationship (SAR) studies are conducted and the purification process is scaled up. Once the feasibility of modulating biological response through synthetic modification is established, the hit is declared a lead and proceeds onward for additional optimization by traditional medicinal chemistry.

It has been estimated that about 60% of the drugs available now, including household names such as artemisinin, camptothecin, lovastatin, maytansine, paclitaxel, penicillin, reserpine, and silibinin, were directly or indirectly derived from natural products [65]. Microbes are the leading producers of useful natural products. Natural products from microbes and plants make excellent drugs. Significant portions of the microbial genomes are devoted to production of these useful secondary metabolites. A single microbe can make a number of secondary metabolites, as high as 50 compounds. The most useful products include antibiotics, anticancer agents, immunosuppressants, but products for many other applications, e.g., antivirals, anthelmintics, enzyme inhibitors, nutraceuticals, polymers, surfactants, bioherbicides, and vaccines have been commercialized. Microbes are the leading producers of useful natural products [65]. In this regard and based on more than fifty years of cumulative experience in the pharmaceutical industry and with international collaborations, Fundación MEDINA continues creating, improving and characterizing a high quality Natural Products Extract Collection for HTS Drug Discovery. This precious resource is open to worldwide discovery initiatives focused on novel therapeutic approaches and clinical development of medicinal agents. Fundación MEDINA offers the scientific community an integrated solution for natural products discovery derived from a superbly diverse, laboratory-optimized and well-maintained microbiological arsenal resulting in a collection of samples thoroughly annotated with chemical and biological data. Fundación Medina's Natural Products Collection (http://www.medinadiscovery.com) with 190,000 microbial strains and >130,000 extracts covers an uncommonly broad chemical space resulting from a variety of fermentation products. Innovative semi-automated methodologies for automated extraction and purification techniques are continuously integrated with the generation of specific collection modules by combining, among others: (i) Filamentous fungi, actinomycetes and other bacteria as secondary

metabolite sources; (ii) Different extraction protocols based on nature of starting materials (resin pre-adsorption of diluted, watery broths; two-phase solvent extractions for lipid rich fungal strains and aqueous-based extracts for actinomycetes); (iii) Automated fractionation protocols tailor-made for different starting materials (chromatography on highly retentive resins, gel filtration, regular reverse-phase separations); and (iv) Samples segregated into organized subsets for maximizing ease of use by biologists and chemists. In addition, collection samples have been annotated with anti-infective, cytotoxic and various biochemical data of use in deciphering new activities [66, 67].

2.2.4 Inmunomodulator compounds from natural products

The immune system is a sophisticated defense system present in all vertebrates which plays a central role in the etiology as well as the pathophysiological mechanisms of many diseases. Innate immunity, an ancient form of host defense, was evolved to enable, through multiple mechanisms, protection against bacterial or viral infections as well as tissue inflammation. Modulation of the immune response to alleviate diseases has long been of interest where natural products represent the ideal alternative to conventional chemotherapy for treatment of various diseases. Currently, there is a considerable interest in identifying novel immunomodulators particularly of plant origin and searching for novel natural immunomodulators represents a real need for patients having inflammatory/ immunological disorders. Various plants are believed to promote and maintain positive health since a plethora of plant derived components have been claimed to modulate the immune response and exhibit significant anti-inflammatory effects. Work done in recent years has shown that many plants have the ability to modulate different cells of the immune system [68, 69]. Several plants have been reported as immunodulators and were shown to directly stimulate the immune system, while others were shown to have immunosuppressive activities [46]. Research on immunomodulation by natural

products or synthetic derivatives is of key interest for anti-infective therapy for a number of reasons. Many plant remedies well-known in traditional medicine or refined natural products in clinical use exert their anti-infective effects not only (if at all) by directly affecting the pathogen. At least part of their effect is indirect, by stimulating natural and adaptive defense mechanisms of the host. These findings have now given many empirical therapies a rationale, scientific basis and thereby a means for 'intelligent' improvement. In discovering the molecular mechanisms by which known remedies exert their effects, chosen elements further down the 'chain of command' might be synthesized and applied directly for more rapid and selective cure, omitting unwanted side effects. The direct use of recombinant cytokines, often in combination with antibiotics, is one consequence of this rationale. A great variety of plant species contain products with immunomodulatory potency, mostly by activating macrophage functions. Among the less known are *Aloe barbadensis, Asphodelaceae* and *Codonopsis pilosula Campanulaceae*, as an alternative for Panax ginseng extracts; *Quillaia saponaria, Rosaceae; Vinca minor, Apocyanaceae; Uncaria tomentosa, Rubiaceae; Trichosanthes kirilowii, Curcubitaceae; Tecoma lapacho, Bignoniaceae; and Pelargonium reniforme, Geraniaceae*. Certain fungi such as *Lentinula edodes, Tricholomataceae; Paxillus involutus, Paxillaceae*; and *Schizophyllum commune, Schizophyllaceae*; yield extracts with similar general immunostimulatory effects [70].

Several reviews have recently been published on natural anti-inflammatory compounds, underlining the potential that these products offer in identifying and developing novel bioactive compounds into drugs for the treatment of inflammatory diseases [71].

Nevertheless, these reviews have been devoted exclusively to plants and no mention is made of molecules from marine or microbial sources [72]. Interestingly, the three prominent categories of natural product compounds identified from these reviews (poliphenolics, terpenoids and fatty acids) are commonly produced in microbial fermentations [73]. The

bioactivities of these classes of compounds are exhibited through the down regulation of different types of inflammatory mediators, highlighting the importance of microbial fermentations as potential biofactories for the production of natural anti-inflammatory metabolites of highly diversified chemical structures. The possibility of obtaining them by scaling up the fermentations of the producing microbial strain is an additional advantage that microbial natural products offer when compared to natural compounds from other sources. However, as with natural products, the search for active compounds from whole crude extracts is both time-consuming and capital-intensive. For this reason, it is critical to develop quick, efficient, high-throughput primary screening assays integrated with chemistry platforms for early de-replication of known compounds, in order to guarantee that only extracts with relevant pharmacological properties are selected for further study [65]. HTS is one of the newest techniques used in drug design and may be applied in biological and chemical sciences. This method, due to utilization of robots, detectors and software that regulate the whole process, enables a series of analyses of chemical compounds to be conducted in a short time and the affinity of biological structures which is often related to toxicity or activity to be defined. It is possible using such the appropriate approaches to examine 100,000 compounds /extracts per day. The HTS method is more frequently utilized in conjunction with analytical techniques such as NMR or coupled methods e.g., LC-MS/MS. Series of studies enable the establishment of the rate of affinity for targets or the level of toxicity. Moreover, researches are conducted concerning conjugation of nanoparticles with drugs and the determination of the toxicity of such structures. For these purposes there are frequently used cell lines. Due to the miniaturization of all systems, it is possible to examine the compound's toxicity having only 1–3 mg of this compound. Determination of cytotoxicity in this way leads to a significant decrease in the expenditure and to a reduction in the length of the study (Figure 14) [65].
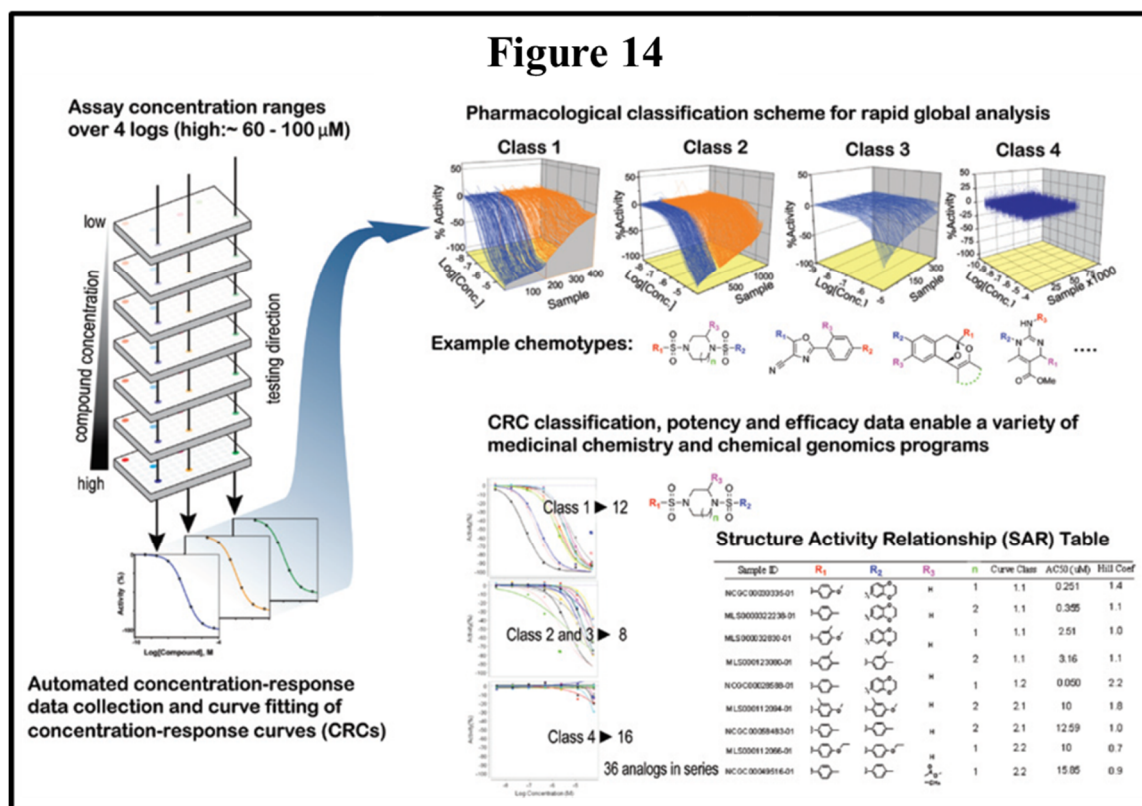
Figure 14

Figure 14. HTS paradigm. HTS allows researchers to obtain dose-response relationships during their initial screen of compounds. By varying the concentrations of compounds being screened, researchers can quickly construct response curves. Based on these patterns of activity, they can group compound classes based on their activity profiles and build structure-activity relationships [74].

Natural products and their derivatives have historically been invaluable as a source of therapeutic agents. However, in the past decade, research into natural products in the pharmaceutical industry has declined, owing to issues such as the lack of compatibility of traditional natural-product extract libraries with high-throughput screening. The underlying reasons for these industry trends are as much commercial as they are scientific, particularly in the case of research into infectious disease. As a result of these factors, today's drug discovery environment calls for rapid screening, hit identification and hit-to-lead development [75].

2.2.5 Chemical process for natural product discovery.

The natural product is extracted from the source, concentrated, fractionated and purified yielding essentially a single biologically active compound. Identification of known

compounds, thereby avoiding replication of previous efforts, has been greatly aided by LC-MS systems and natural-product databases. De novo structure determination of compounds that are novel has been revolutionized by advances in spectroscopic techniques, particularly in HR NMR technologies (Figure 15).
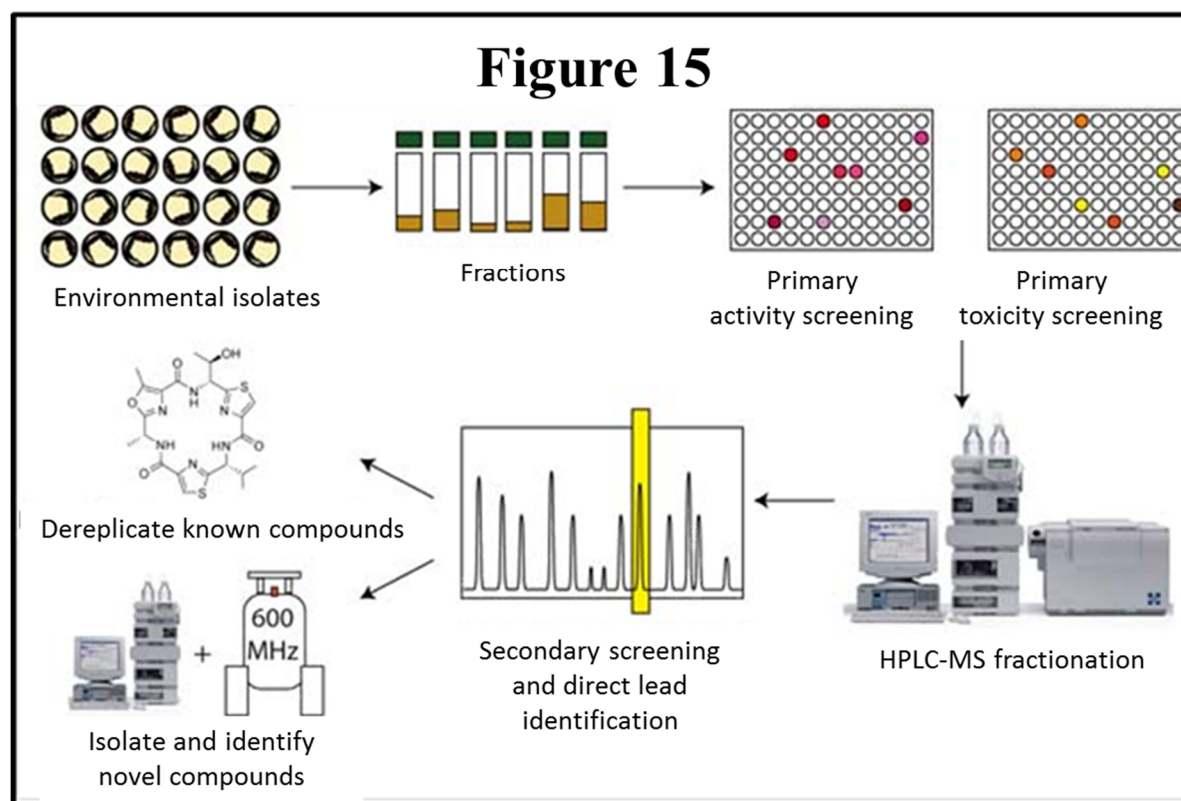
Figure 15. This flow chart outlines the drug discovery pipeline for microbial natural products.

Although the determination of complex structures is technically challenging, it is no longer a major impasse in the drug discovery process. In those cases in which the biological activity profile meets criteria for potency and selectivity, preliminary SAR studies are conducted and the purification process is scaled up. Once the feasibility of modulating biological response through synthetic modification is established, the hit is declared a lead and proceeds onward for additional optimization by traditional medicinal chemistry. In this environment, traditional resource intensive natural-product programmes that are based on extract-library screening,

bioassay-guided isolation, structure elucidation and subsequent production scaleup face a distinct competitive disadvantage when compared with approaches that utilize defined synthetic chemical libraries. However, emerging trends, coupled with unrealized expectations from current research & development strategies, are prompting a renewed interest in natural products as a source of chemical diversity and lead generation [75].

2.2.6   New trends in natural products drug discovery

Drugs developed from microbial natural products are in the fundaments of modern pharmaceutical companies. Despite decades of research, all evidences suggest that there must remain many interesting natural molecules with potential therapeutic application yet to be discovered. Any efforts to successfully exploit the chemical diversity of microbial secondary metabolites need to rely heavily on a good understanding of microbial diversity, being the working hypothesis that maximizing biological diversity is the key strategy to maximizing chemical diversity [76]. The question of why secondary metabolites are produced by living organisms continues to evade us and is vigorously debated. It has been proposed that some of the higher eukaryotes such as plants and animals produce secondary metabolites as a way to defend themselves from predators; microorganisms would produce them to defend from other organisms that surround them or use them as signaling molecules with other organisms. However, it is hard to unequivocally prove either of these hypotheses and only circumstantial evidence has been proposed. Until we understand the reason why these secondary metabolites are produced and how they are used by the producing organisms, the debate as to what organisms should be screened for what drug targets is nothing more than a random approach and mainly based on previous successes. Nevertheless, natural products have taught us numerous lessons, as nicely summarized by Clardy and Walsh [77]. It is unreasonable to expect that all natural products will interact with specific and required biological targets, and actually

only a small percentage do. Of those which do interact, only even smaller numbers will have drugable properties and can be converted into drugs. Therefore, to identify a natural product-biological target pair, one needs to have specific biological assays that can selectively detect these compounds from the mixture of many others. Therefore, the success of natural products drug discovery depends on the availability of highly robust, sensitive and high throughput biological screening assays. Tight coupling of robust assays with broad biodiversity and efficient natural products chemistry is the key to success of natural products programs, as exemplified by the discovery of platensimycin by Wang et al. [78]. Lack of efficiency in any of the pieces can significantly derail natural products programs. Recently, significant improvements have been seen in all aspects of the technologies and disciplines associated with natural products (microbiology, natural products chemistry and assay technologies). Those groups who can combine them effectively at one place will have the potential to make a profound impact on the discovery of natural product drugs and leads [76]. Crucial breakthroughs in separation and structure- determination technologies have lowered the hurdles inherent in screening mixtures of structurally complex molecules. A greater understanding of the exquisite specificity ingrained in secondary metabolites through the evolutionary process has focused attention on their roles as mediators of protein–protein interactions in vital cellular processes, and advances in synthetic chemistry have revolutionized the processes of material supply and the modulation of biological activity through structural modifications. Furthermore, our ability to model the binding of these evolved, privileged structures with their targets enables the design of simpler mimetics that have superior properties. Efforts to expand the impact of natural chemical diversity on the drug discovery process follow two main chemistry-driven paths. One seeks to simplify crude mixtures, as well as enhance the impact of minor components in assays, through the creation of fractionated natural-product libraries. The other approach uses the power of combinatorial synthesis to

amplify the structural context in which the unique features of natural products are expressed. The confluence of these technologies with advances in genomics, metabolic engineering and chemical synthesis offer exciting new possibilities to exploit the remarkable chemical diversity of nature's 'small molecules' in the quest for new drugs [64].

2.3 <u>Evaluation of the effect of compound aqueous solubility in CYP450 reversible inhibition assays.</u>

2.3.1 Approaches to CYP450 reversible inhibition assessment

In the drug discovery process, it is important to determine possible drug-drug interactions of new drug candidates mediated by CYP450 inhibition. These drug-drug interactions may lead to toxicity due to the elevation in plasma levels of one to the drugs involved in the interaction [79]. Monitoring the inhibitory potency of these compounds on CYP450 activity using well-characterized CYP450 substrates helps predict these drug-drug interactions (DDI). In early drug discovery programs, the potential of CYP450 inhibition of new chemical entities is frequently quantified in terms of IC_{50} values. A risk classification of potential inhibitors as low ($IC_{50}<1$ μM), medium (1 μM$<IC_{50}<10$), or high ($IC_{50}>10$ μM) is often sufficient for ranking and prioritizing compounds [80].

The liver is the predominant organ in which biotransformation of foreign compounds takes place, although other organs may also be involved in drug biotransformation. Ideally, an in vitro model for drug biotransformation should accurately resemble biotransformation in vivo in the liver. Several in vitro human liver models have been developed in the past few decades, including supersomes, microsomes, cytosol, S9 fraction, cell lines, transgenic cell lines, primary hepatocytes, liver slices, and perfused liver. In vitro CYP450 inhibition assays developed for the purpose, including those using fluorogenic substrates and recombined human CYP450 enzymes (Figure 16), which are characterized by high throughput capability and low

operation cost.

Figure 16

Discovery

Lead selection | Optimization

Preclinical development

Clinical development

Phase I / Phase II / Phase III

IND First-in-human study

NDA approval

In vitro high throughput assays

In vitro definitive assays

Clinical assays

Reversible inhibition assay
- rhCYP-fluorescent assay
- HLM LC-MS cocktail assay
- HLM SPE-MS assay

- HLM LC-MS assay
- HLM SPE-MS assay

- Plasma LC-MS assay with a single or multiple probe substrate(s) co-administered with a test drug

Time-dependent inhibition assay
- HLM IC_{50} shift assay
- HLM assay with a single concentration pre-incubation

- HLM K_I and K_{inact} measurement assay

Figure 16. Assessment of CYP450 inhibition in drug discovery and development. The data generated from these assays are mainly used to support selection of clinical candidates, regulatory submissions for investigational new drug (IND) applications, and the design of clinical DDI studies [81].

Microtiter plate assays are carried out using a nonspecific fluorescent substrate and a single rhCYP450 enzyme. After 10 – 30 - min incubations, results are quickly recorded using a plate reader. The rhCYP450 - fluorescent assay is a fast, easy operation that does not use MS, and it has been widely used for HTS for a large number of compounds in lead selection and optimization [82–84]. Results from the assays allow for the termination of new chemical entities that are strong inhibitors of major CYP450 enzymes for progression. In addition, structure – activity relationships can be developed for a large set of CYP450 inhibition data, which can facilitate the design of alternate agents that have no or reduced CYP450 inhibitory potency. Fluorescent assays are especially applicable to the determination of structure, CYP450

inhibitory activity relationships, and rank order of compounds that have the same chemotypes, knowledge of which helps medicinal chemists to design compounds with better CYP450 inhibition profiles. However, since most probe substrates employed in fluorescent assays are not CYP450 enzyme - specific, these assays cannot be used with HLM. It has been reported that the rhCYP450 - fluorescent assay generated more false - positive results than HLM - based assays in comparison with CYP450 inhibition data observed in clinical studies [85]. In addition, rhCYP450 - fluorescent assays are not suited for compounds that have strong fluorescent responses [86]. As a result, in the later stages of drug discovery, CYP450 inhibition assays that employ HLM and CYP450 probe substrates are often performed (Figure 16). CYP450 inhibition assays using selective probe substrates and HLM followed by LC-MS analysis of metabolites of the probe substrates have been developed and validated for the definitive evaluation of drug candidates for their inhibitory effects in late discovery and drug development [87–89]. Results from HLM-LC-MS assays provide some key drug metabolism and pharmacokinetic information affecting the selection of clinical candidates, the design of clinical DDI studies, and regulatory filings for new drugs [81]. In order to develop a continuum for studies with recombinant systems to HLM and ultimately to in vivo DDI prediction, a basic quantitative approach has been proposed based on scaling the expressed enzyme activity using the relative abundance of specific P450 enzymes in liver microsomes determined by immunoquantitation. The normalization process is relatively straightforward; the rate of reaction as measured by the metabolite formation in a recombinant CYP450 is multiplied by the mean specific content of the corresponding CYP450 in native HLM [90].

In summuary, the most widely accepted approach for in vitro evaluation of CYP450 inhibitory potential requires the use of HLM as the enzyme source, with "drug-like" substrates, using LC-MS to quantify the enzymatic activity. However, this methodology is expensive and time-consuming, and therefore does not deliver the high throughput typically required in the drug

discovery process. Alternatively, several high throughput methodologies have been developed using fluorogenic probe substrates and recombinant CYP450 enzymes [91].

Interestingly, it has been demonstrated that IC_{50} values obtained for certain compounds in cytochrome P450 inhibition assays may vary considerably depending on the assay methodology used [85].

2.3.2 Key factors affecting inhibition measurements

Several factors, such as enzyme source, enzyme concentration or substrate specificity, are usually considered responsible for such variations.

2.3.2.1 Purified or rhCYP450 enzymes

Numerous human CYP450 enzymes have been cloned and heterologously expressed individually in various cell types [90, 92, 93]. Microsomes from these cells, which contain a single human CYP450 enzyme with NADPH – CYP450 reductase with or without cytochrome b5 are commercially available (e.g., Gentest Corp., Panvera Corp., and Oxford Biomedical Research Inc.). One of the attractive features of recombinant enzymes is that metabolism studies with drug candidate can be greatly simplified and the involvement of particular CYP450 can be quickly assessed. However, the major disadvantage of recombinant CYP450 enzymes is that they differ in their catalytic competency, and they are not expressed in cells at concentrations that reflect their levels in native HLM. Furthermore, the recombinant CYP450 enzymes are usually expressed with much higher levels of NADPH – CYP450 reductase than those present in HLM. In addition, cytochrome b5 coexpression can affect the kinetics of drug metabolism by certain CYP450 enzymes. Therefore, simple evaluation of metabolism by recombinant CYP450 enzyme does not necessarily provide the extent to which that particular drug candidate contributes to the CYP450 inhibitition [90].

2.3.2.2 Human liver microsomes

In hepatocytes, cell membrane can present a barrier for both substrate and selective inhibitors to entry into the cell, making it difficult to study DDI. Subcellular fractions, in particular, HLM, may be the optimal in vitro system for this purpose. HLM are a rich source of heme - containing metabolic enzymes, including CYP450 enzymes, flavin-containing monooxygenase (FMO), uridine diphosphate glucuronosyltransferase (UGT), glutathione S-transferases, esterases, and microsomal epoxide hydrolase [90].

HLM still account for the most popular in vitro model, providing an affordable way to give a good indication of the CYP450 and UGT metabolic profile. The large availability of HLM and their simplicity in use contribute to the popularity of this in vitro model. HLM consist of vesicles of the hepatocyte endoplasmic reticulum and are prepared by differential centrifugation and thus contain almost only CYP450 and UGT enzymes. Liver preparations, other than from fresh human liver, can also be used (e.g., liver slices, liver cell lines, and primary hepatocytes) for preparation of microsomes. The CYP450 and UGT enzyme activity can be measured by various model substrates. In commercially available HLM, the major advantages of microsomes are low costs, simplicity in use, and they are one of the best-characterized in vitro systems for drug biotransformation research. However, some major drawbacks exist. First, it should be noted that results obtained with microsomes cannot be used for quantitative estimations of in vivo human biotransformation, because CYP450 and UGTs are enriched in the microsomal fraction and there is no competition with other enzymes. This results in higher biotransformation rates in HLM compared to the human in vivo situation, but also compared to primary hepatocytes and liver slices. Additionally, the absence of other enzymes (e.g., NAT, GST, and ST) and cytosolic cofactors can leave metabolites formed in intact liver cells unnoticed [94].

However and in spite of such differences related to biotransforming enzymes in quantitative

and qualitative terms, our hypothesis is that the physicochemical properties of the tested compounds, such as their aqueous solubility, may also play a key role in IC_{50} value variations across methodologies.

When HLM are used for CYP450 inhibition experiments, the excess of lipids in the assay can increase the apparent aqueous solubility of lipophilic compounds. Actually, the solubility of the test compounds remains the same while the concentration of the free test compound decreases. The decreased free concentrations during the incubation result in an apparent increase in the IC_{50} value. In contrast, when rhCYP are used, the higher specific enzymatic content results in a much smaller amount of lipids in incubation, thereby minimizing the partitioning of test compounds in incubation and the uncertainty in test compound concentration [95]. According to the hypothesis that the phospholipid component of microsomes is the primary contributor to the non-specific binding of inhibitors, the physicochemical properties of the compounds, such as aqueous solubility, might have a strong influence on their behavior in the different assays.

2.3.3 Drug solubility

In order for an orally administered compound to act, it must dissolve in the aqueous environment of the gastrointestinal tract and within the cytoplasm when the target is intracellular. The partition coefficient of a compound is directly related to its aqueous solubility — all else equal within a series. The more lipophilic a compound is, the lower is its aqueous solubility. Poor solubility can limit the absorption of compounds from the gastrointestinal tract, resulting in reduced oral bioavailability. It may also necessitate novel formulation strategies and hence increase cost and delays. Moreover, compound solubility can affect other in vitro assays. Poor aqueous solubility is the largest physicochemical problem hindering oral drug activity — hence on completion of compound synthesis, the

determination of aqueous solubility is a priority.

Solubility data may prove critical in rationalizing disparate results in other bioassays. For example, a compound must be soluble in the assay buffer used to measure activity. Poorly soluble compounds within a series are more likely to have variable solubility in different buffer systems used in common bioassays, which can confound the SARs that are critical for effective lead optimization. In fact, some have shown that determination of the effective concentration of compounds in bioassays reveals marked errors in potency measurements due to marked underestimation of the actual concentration of compound that is in solution in the bioassay, particularly when a single concentration is used to assess activity by extrapolated IC_{50} values (Popa - Burke *et al.* , 2004).

2.3.3.1 Automated Methods Used to Determine Drug Solubility

Compound solubility is usually determined by either kinetic or thermodynamic methods. Kinetic assessments, which start from a solution of dissolved compound, are now common in an early discovery setting. Often a turbidimetric end point is used for the KS measurements. Thermodynamic assessments, where a saturated solution of a compound in equilibrium is prepared from solid, are considered to be the gold standard and take into consideration the crystal lattice of the compound, and therefore, the dissolution rate of the compound. Throughput is generally lower than kinetic measurements and larger quantities of analytical grade of compound are ideally

used for these studies. For this reason, thermodynamic assays are usually performed in early development (rather than in the earlier discovery stages) to confirm earlier KS results, to rule out potential artifacts, and to generate quality solubility data with crystalline material to support the best selection of potential clinical candidates.

[44]. Basically, the difference between the two approaches lies in the fact that the solid

compound is introduced into the aqueous medium for determination of thermodynamic solubility whereas the pre-dissolved compound is taken as the starting material for assessing KS [96]. Both – kinetic and thermodynamic solubility assays – rely on measurement of concentration of the saturated aqueous phase. This can be either done by HPLC- and UV-methods. Whereas UV-methods generally are much faster and allow higher throughput, they are generally not able to detect impurities such as degradation products, starting materials or by products from synthesis in the compounds. Such impurities might influence results directly as they also contribute to UV-absorption which represents the basis for calculation of solubility from these assays. In contrast, HPLC based methods for determination of solubility require more time for analytical determination of concentration but provide information on purity [96]. Accordingly, assays to determine thermodynamic solubility answer the question: "To what extent does the compound dissolve?" Vice-versa, KS answers the question: "To what extent does the compound precipitate?" From this it becomes obvious that thermodynamic solubility should be the gold standard for optimizing compounds for solubility targeting, e.g. as solid oral formulations to be used during clinical development and for marketing. By contrast, methods for determining thermodynamic solubility are generally much more labor-intensive than methods for assessing KS [96]. Since the majority of described HT-assays in discovery set-ups use dimethyl sulfoxide (DMSO) stock solutions for logistic reasons, it becomes beneficial if these DMSO stocks can also be used for the determination of solubility. For determination of KS, the compounds are introduced into the aqueous solvents predissolved in organic solvents. Therefore KS clearly reflects a situation close to that found in many high-throughput screens and does answer the question of whether a compound precipitates in the high-throughput screen [97]. Methods that use turbidimetric detection techniques are now becoming more popular as they bypass the need for HPLC analysis. Turbidimetry measures the onset of precipitation by either absorbance or

nephelometry (light scattering) and is often used as the end point for KS determination. These techniques are amenable to high - throughput format with rapid data generation and require only small amounts of test compound, usually from readily available DMSO stock solutions [98]. An additional advantage of the turbidimetric method is that it is easily temperature controlled and incubations can be performed and monitored at physiological temperature. A number of automated methods based on KS have been developed, which have dramatically increased the throughput of solubility assessment. A brief overview of the methods can be found in a previous work by Kerns and collaborators [99].

2.3.4 Glycogen synthase kinase 3 (GSK3) Inhibitors

In 1988, Ishiguro and his colleagues identified a protein kinase (activity) associated with brain microtubules which phosphorylated tau in more than one residue modifying its electrophoretic mobility [100]. This kinase was designated as tau protein kinase, but when it was further characterized, two different proteins were observed in the original protein fraction. These kinases were called tau protein kinase I and tau protein kinase II, further identified as GSK3 and CDK5. Dysregulation (usually increase) of GSK3 activity is believed to play a role in different and important disorders like cancer [101], heart disease [102] and neurodegenerative disorders [103]. More recently, the requirement of GSK3 for a type of human leukemia has been reported, suggesting GSK3 as a candidate drug target for the treatment of this cancer [104]. Recently, an association of a GSK3 polymorphism with Alzheimer disease and with frontotemporal dementia has been reported. In this way, there are small compounds like thiazoles, thiadiazolidinones, maleimides, used as GSK3 inhibitors. Some of these inhibitors, developed by several pharmaceutical companies, have reached the clinic [105]. Interestingly these categories of compounds are nitrogen heterocycle containing drugs and it is known that the loaning extent of nitrogen electronic pair to

CYP3A4 heme group was critical in the development of CYP3A4 inhibition [106]. Additionally, the incorporation of nitrogen-based aromatic heterocycles was previously shown to modulate potency, spectrum of activity and hydrosolubility when compared with other fused-heterocycles [107]. Together, these categories of compounds may constitute an appropriate approach to evaluate the influence of aqueous solubility in CYP3A4 reversible inhibition.

2.4   A novel in vitro approach for simultaneous evaluation of CYP3A4 inhibition and kinetic aqueous solubility.

2.4.1   Drug-Drug Interactions

Drug discovery is a long, intensive, and expensive process and there is tremendous pressure to maximize efficiency and minimize the time it takes to discover and bring a drug to the market. In order to do this, it is necessary to identify steps in the discovery and development process where changes can be made to increase efficiency and save time [108]. In this regard, drug metabolism assessment represents an essential stage of the process, the main goal of which is the multi-parameter optimization of candidate compounds for interaction with the desired target and minimal off-target activities, while imparting drug-like properties on the candidate compounds. Within drug metabolism, drug-drug interactions (DDI) remain a major regulatory hurdle which can lead to early termination of development, refusal of approval, prescribing restrictions or the withdrawal of the drugs from the market. CYP450 are recognized as playing an important role in clinically relevant DDI as a result of which new chemical entities are typically subjected to high-throughput CYP450 inhibition screening [80, 83, 109]. The inhibition of metabolism by cytochrome P450 enzymes is a principal mechanism for such interactions.

2.4.2 Approaches to evaluate CYP450 inhibition

It is well established that appropriate *in vitro* assays are useful predictors of the potential for in vivo interactions and represent an important experimental approach in drug development. In vitro drug interaction data can be used to guide the design of clinical drug interaction studies, or, when no effect is observed in vitro, the data can be used in place of an in vivo study to assert that no interaction will occur in vivo. In the most frequently applied high throughput method, CYP450 activity from recombinant enzymes results in oxidation of a pro-fluorescent molecule which then breaks down to give a fluorescent product (usually a hydroxycoumarin, fluorescein or resorufin analogue) that can then be detected directly using a fluorescence plate reader (Figure 17). This method has the advantage of being a fast and cost-effective way of performing thousands of IC_{50} determinations per year [86]. One of the limitations of this approach is that measurements can be subject to interference from test inhibitors which are either fluorescent or cause fluorescence quenching. However, although these effects are sometimes observed, in practice their frequency is usually acceptably low. These systems investigate the potential of test compounds to inhibit the metabolism of a probe substrate by the main CYP450 isoforms providing, as a final outcome, the concentration of a test compound causing 50% inhibition (IC_{50}) of the probe substrate metabolism, which is deemed sufficient for ranking and selection purposes in early discovery screening.
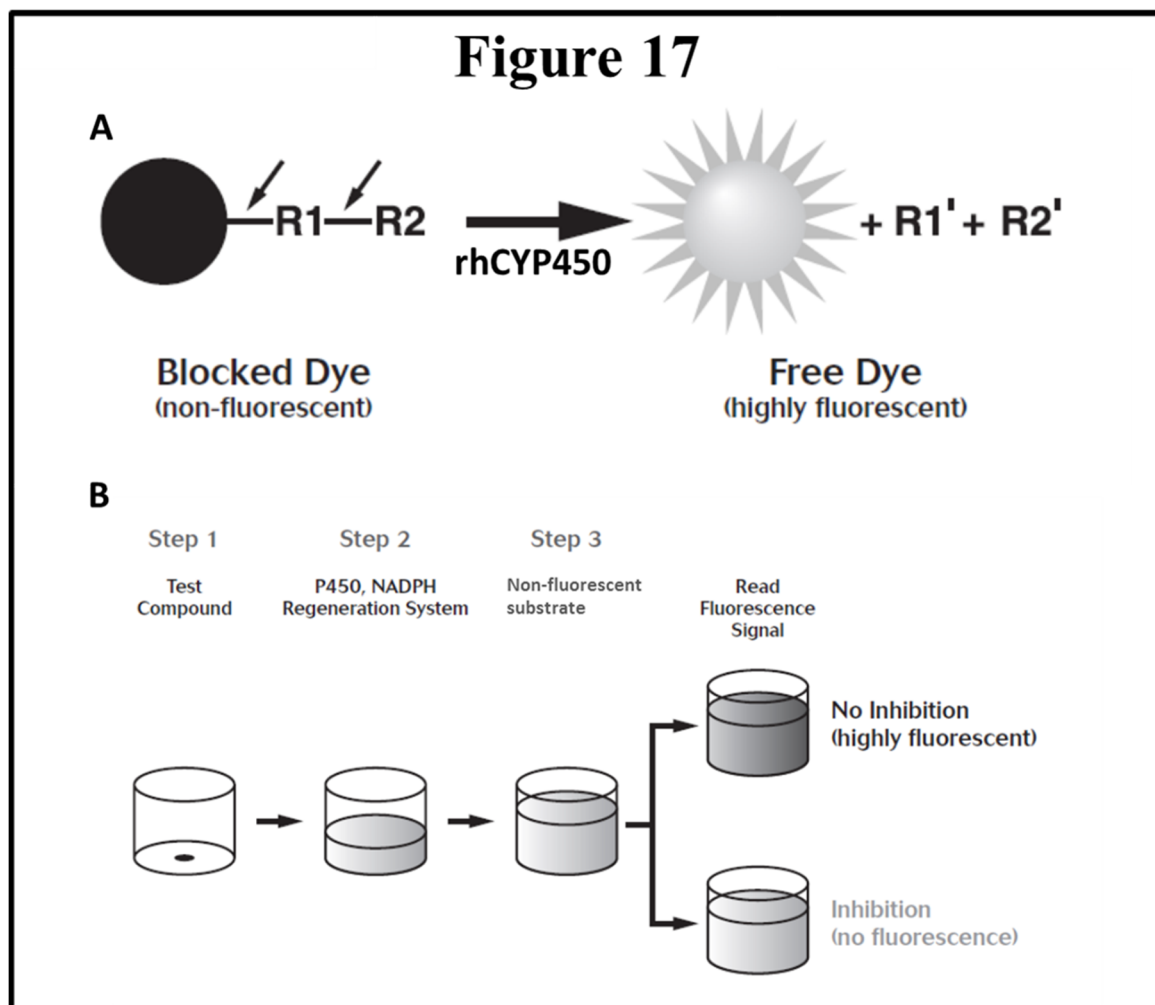
Figure 17 A) Schematic of the Metabolism of the Fluorogenic "Blocked" Dye into a Fluorescent Metabolite. B) A schematic representation of an end-point CYP450 reaction. In end-point mode, the test compounds are first combined with the rhCYP450 reagents and the NADPH regeneration system (consisting of glucose- 6-phosphate and glucose-6-phosphate dehydrogenase). The regeneration system converts NADP+ into NADPH, which is required to start the CYP450 reaction. After a brief pre-incubation, the background fluorescence is measured. The enzymatic reaction is initiated by the addition of the non- fluorescent substrate and the background fluorescence of the sample is measured within 2-3 minutes after this addition. After incubation time, the addition of a stop reagent is added, the fluorescence is measured.

2.4.3 Solubility issues in candidate compound libraries

The general routine in early screening assays is to perform a serial dilution of the test compounds in DMSO (or other organic solvent) from library stock solutions in order to maximize the opportunity for the test compounds to be in solution before being added to the

incubation mixture, to be as independent as possible from the other measurements. Nevertheless, the highly lipophilic nature of many early lead compounds results in frequent solubility problems when test compounds are dispensed into aqueous solutions. It is therefore important to consider the effect of test compound precipitation after addition to the incubation mixture. At this point, it is worth remembering that the term "Molecular Obesity" is introduced to describe the general tendency in drug discovery settings to build potency into molecules through the use of lipophilicity which leads to drug candidates with low aqueous solubility [110]. This trend towards lower solubility compounds was attributed to the introduction of HTS and combinatorial chemistry as well as new targets requiring more lipophilic molecules for efficient target affinity. As a result, the limited solubility of compounds can interfere with the results of biological screening as it may lead to the precipitation or aggregation of compounds, causing underestimated activity, reduced HTS–hit rates, variable data, inaccurate SAR, discrepancies between enzyme and cell assays and inaccurate *in vitro* ADME–Tox testing [45, 111]. Thus, solubility should be tested under assay conditions either before or in parallel to biological screening [112]. The aqueous solubility in the majority of drug discovery settings is commonly determined by means of a KS. Typically, small volumes of the stock solution are added incrementally to the aqueous (buffered) solution of interest until the solubility limit is reached. The resulting precipitation is detected optically, and the KS is defined as the concentration preceding the point at which precipitation occurs. In summary, KS assays are appropriate for solubility screening up to lead optimization. Assays have minimal compound requirements, are fast, suitable for HTS and cover the required concentration range in assays used in early discovery.

Both CYP450 inhibition potential and aqueous solubility are compound properties which are routinely determined for candidate optimization using HTS in separate *in vitro* models and that

means parallel consumption of time, staff resources and materials such as reagents, plates or liquid handling station consumables. Furthermore, and more importantly, data generation and management are usually performed in very different timeframes, which may result in a more difficult integration of the final outcome of both determinations.

In this regard, it seems reasonable to develop a new HTS strategy in which CYP450 inhibition and KS could be determine in the same assay procedure. This may result in a significant reduction in resources used since the consumption of time, staff availability, material and hardly exceeds that of an individual separate in vitro model for the evaluation of CYP450 inhibition. Furthermore, the sequential data acquisition within a short period of time from CYP450 inhibition and solubility readouts would enable the integration and synchronization of data management which eventually provide a better understanding of CYP450 inhibition data according to a real situation of test compounds in assay solution.

3 OBJECTIVES

The main objectives of this Thesis were:

1. The main objective of this work to was to assess *in vitro,* the implication of the CYP450 activities in the modulation of NO production.

2. To developed and validate a high-throughput screening (HTS) platform for the assessment of immunomodulatory properties and discovery of inmmunomodulator molecules.

3. To assess how compound aqueous solubility contributes to the potential variation in IC_{50} between different approaches for CYP450 inhibition assessment.

4. To develop and validate a Novel In vitro Approach for simultaneous evaluation of CYP3A4 inhibition potential and kinetic aqueous solubility (NIVA-CYPI-KS) using fluorogenic substrate and turbidimetric or kinetic measurements respectively.

4 MATERIALS AND METHODS

4.1 Integrated Evaluation of Immunomodulatory Activity and Hepatic Drug Metabolism

To this end, we used an immunocompetent in vitro model, but with limited CYP450 functionality, LPS stimulated, cultured cell lines of RAW 264.7 [113, 114]. These results were compared with those retrieved from literature using primary cultures of alveolar macrophages, in which the pattern of CYP450 expression was found to closely resemble the expression pattern in lung tissue [115, 116]. In order to correlate NO measurements with CYP450 activity, we assessed the aforementioned dual inhibitors (Imidazole derivates and selected macrolides) in classical in vitro models for drug metabolism assessment, such as CYP450 reversible and time-dependent inhibition, aqueous solubility and microsomal stability with metabolite identification [117–121].

4.1.1 Reagents

Fetal bovine serum (FBS), L-glutamine, sodium pyruvate, MEM non-essential amino acids, penicillin–streptomycin, and TrypLE Express were purchased from Invitrogen Gibco, Inc. (Life Technologies, Carlsbad, CA). NP40 was purchased from Thermo Scientific (Rockford, IL). Diphenyl tetrazolium bromide (MTT) and methyl methane sulfonate (MMS) were obtained from Sigma Aldrich. The commercial compounds evaluated in this work, ketoconazole, miconazole, clotrimazole, erythromycin (ERY), roxythromycin (RXT), azythromycin (AZT) and clarithromycin (CLT), were obtained from Sigma Aldrich (St. Louis, MO). Human recombinant c-DNA expressed CYP3A4 at 1 nmol/mL was obtained from

Gentest Corporation. Pooled HLM were obtained from Becton Dickinson Gentest (Woburn, MA).

4.1.2 Test Compound Preparation for NO assay

Commercial test compounds were prepared as follows: test compounds were provided in powder form and dissolved in 100% DMSO at 25 mM in 96-well plates. Serial dilutions of test compounds in 100% DMSO were carried out on a Biomek FX workstation coupled with a stacker carrousel (Beckman Coulter Inc. Brea, California). Final working solutions were prepared from serial dilutions in 100% DMSO (20 µL) which were combined with water (80 µL). Initial concentrations and dilution patterns were adjusted for each compound depending on the calculated solubility values and expected response in NO production related studies in order to optimize their IC_{50} calculation from a titration curve with 10 concentration levels (macrolides and imidazole derivatives at concentration levels from 0.48 to 250 µM and from 0.019 to 10 µM, respectively). All compounds were tested in triplicate in two different days for every methodology studied.

4.1.3 Cell cultures

The mouse macrophage cells, RAW 264.7 (ATCC® TIB-71™) and the human colon adenocarcinoma cells, Caco-2 (ATCC® HTB-37™), were obtained from ATCC and cultured in Dulbecco's Modified Eagle Medium (DMEM), supplemented with 10% FBS and 2 mM l-glutamine, in a humidified 5% CO2 atmosphere at 37 ºC. All cell handling steps were carried out using the SelecT automated cell culture system.

4.1.4 NO assay

The following procedure is an adaptation to the 96-well format of a methodology previously described [114]. RAW 264.7 cells were seeded into 96-well plates at a density of 20×10^3 cells

per well and grown to approximately 50% of confluence (24 h). They were cultured for another 24 hours with each of the extracts described above (5 µL of 2 × whole broth extraction (WBE) at 20% DMSO were dispensed into 190 µL of fresh medium using Perkin Elmer Evolution P3, Waltham, MA, obtaining a final extract concentration of 1/20 × WBE). Afterwards, these cells were stimulated with LPS (5 µL of 6 µg/mL were dispensed using a Thermo Scientific Multidrop Combi dispenser, MTX Lab Systems, Vienna, VA). Untreated (5 µL of 20% DMSO, microbial extract vehicle) and unstimulated (5 µL of purified water, LPS vehicle) cells were used as negative controls (n=4) while untreated but stimulated cells were used as positive controls (n=4) in each assay plate. After 24 h, supernatants were collected and centrifuged at 10,000 × g for 5 min, and nitrite levels were measured in 100 uL of supernatant according to the Griess assay [122] using a Thermo Scientific Multidrop Combi dispenser and PerkinElmer EnVision Multilabel Reader (Waltham, MA). After discarding the remaining supernatant, the cell viability was examined in the remaining cells through the 3-(4, 5-dimethylthiazolyl-2)-2, 5-diphenyltetrazolium bromide (MTT) test described elsewhere [123] and also using a Thermo Scientific Multidrop Combi dispenser and PerkinElmer EnVision Multilabel Reader.

4.1.4.1 Data Analysis

Pure compounds and extract activities were calculated automatically using the Genedata Screener software (Genedata AG, Basel, Switzerland), and the percentage inhibition of each extract (or compound) was determined by Equation 1, integrated in the Genedata Screener software: Percentage inhibition of production of either NO or IL-8:

$$\text{Equation 1}: Percentage\ of\ inhibition = [1 - (\frac{Abs_{well} - Abs_{neg}}{Abs_{pos} - Abs_{neg}})] * 100 \ (1)$$

where Abs_{well} is the absorbance measured per specific well, and Abs_{pos} and Abs_{neg} are the average absorbance measured for the positive and negative controls, respectively.

4.1.4.2 Determination of IC$_{50}$ of inhibitor controls for NO production.

The IC$_{50}$ values of commercially known inhibitors of NO production (dexamethasone, cortisol and cyclosporine A) were obtained from dose–response curves in the NO assay described above. Compound concentrations were started at different levels in order to optimize IC$_{50}$ calculation and two-fold serial dilutions were performed (DMSO concentration below 0.5%). The IC$_{50}$ values were calculated as the compound concentration which inhibits the production of NO by 50% using Gene Data Screener software.

4.1.5 Assessment of CYP3A4 reversible inhibition and aqueous solubility

See section 4.4.3 Novel in vitro approach for simultaneous CYP-inhibition and turbidimetric solubility evaluation (NIVA-CYPI-KS).

4.1.6 Assessment of CYP3A4 time-dependent inhibition

Experiments were designed according to previous works with minor modifications [124]. Briefly, pre-incubation mixtures contained hrCYP3A4 (25 pmol/mL), NADPH-regenerating system (1 mM NADP, 10 mM glucose 6-phosphate, 2 IU/mL glucose 6-phosphate dehydrogenase, 5 mM MgCl$_2$), test compound solutions (ERY, RXT, CLT, AZT and ketoconazole) in at least five different concentrations, and phosphate buffer (0.1 M, pH 7.4) in a total volume of 500 µL. At 0, 5, 10, 15, 20, 25 or 30 min, BFC (dissolved in AcN) was added so that the final concentration of BFC in the incubations was 25 µM. Incubations were allowed to proceed for a further 15 min at 37°C. Reactions were terminated with the addition of 75 µL of a STOP solution of AcN containing 0.5 M Tris base using a Multidrop Combi liquid dispenser. Then fluorescence for 7-HFC formation was determined using 430 nm as excitation and 535 nm as emission wavelengths by an EnVision multilabel plate reader. Stock solutions of macrolides were prepared in DMSO/AcN [35:65] [v/v] in order to minimize the DMSO final content in enzyme incubations and added to the pre-incubation mixtures so that the

concentration ranges were: ERY, RXT and AZT, from 0.133 to 32.5 µM; CLT, from 0.06 to 16.2 µM; ketoconazole, from 0.0021 to 0.512 µM. The DMSO content in incubations was kept at 0.35% throughout the experiment. Control samples were prepared in the absence of test compounds by adding solvent alone. Regarding the data analysis, the mean value of 7-HFC formation expressed as a percentage of control was used to estimate the rates of enzyme inactivation (Kinact) and the kinetic constants of inhibition (KI) according to related works [38][125]. In outline, the observed inactivation rate constant at each macrolide concentration was calculated from the initial slopes of the remaining enzyme activity, plotted semi-logarithmically against the pre-incubation time. Non-linear regression analysis of the negative slopes against inhibitor concentration enables Kinact and KI to be calculated. Verapamil (tested at concentrations ranging from 0.279 to 68 µM) was used as positive control.

4.1.7 Simultaneous determination of in vitro metabolic profiling and metabolic stability

Test compounds (ERY, RXT, CLT and AZT) were incubated in HLM at an initial substrate concentration of 1 µM in a 96-well format. Standard high-throughput incubation conditions were used with time points of 0, 15, 30, 45, 60, and 90 minutes. Protein concentration was used at 1 mg/mL, and NADPH was present at 4 mM. Reaction was quenched using an equal volume of AcN and then diluted 1:1 with water prior to analysis by liquid chromatography coupled to high resolution mass spectrometry (LC-HRMS). In the case of the chromatography, the incubations were analyzed using an Agilent Series 1290 LC system (Agilent Technologies, Santa Clara, CA, USA). All analyses were performed using a Supelco Discovery HS C18 (2.1×50 mm) 3 µm column that was held at 30°C. Solvent A contained water with 0.1% formic acid and solvent B contained AcN with 0.1% formic acid, and the flow rate was set at 400 µL/min. The gradient elution was performed as follows: 0–0.5 min 0% eluent B; 0.5–7 min 100% eluent B; 7-9 min 100% eluent B; 9-9.2 min 0% eluent B; and 9.2-10.5 min 0% eluent

B. An AB SCIEX TripleTOF 5600 quadrupole-time-of-flight mass spectrometer (Q-TOF-MS) in positive ESI mode (AB SCIEX, Concord, ON, Canada) was used with a generic method for data acquisition on all compounds and samples. The method consisted of a time of flight mass survey scan (TOF MS), followed by two information-dependent acquisition (IDA) TOF MS/MS scans. The mass range was m/z 100–1000 for both MS and MS/MS. An accumulation time of 100 ms was used for each scan. Mass defect-triggered IDA was used for the MS/MS scans (collision energy of 35 eV with a spread of +/-10 eV). External mass calibration was performed automatically using a calibrant delivery system. Data processing was performed using MultiQuant Software and MetabolitePilot Software (AB SCIEX, Concord, ON, Canada) to process the TOF MS data and generate all quantitative information. An extracted ion current (XIC) window of ± 10mDa was used for all compounds. Peak areas were used to plot the Ln % remaining relative to t = 0. The slope of the natural log of the percent remaining versus time was calculated to determine the first-order rate constant (k) and the half-life ($T_{1/2}$) of the test compounds according to equation 2:

$$Half\ life\ (T1/2) = 0.693/k \text{ (min) Eq.(2)}$$

Tentative metabolite identification was performed using MetabolitePilot Software (AB SCIEX, Concord, ON, Canada) for predicted and unpredicted metabolites, including fragment ion interpretation from precursor high resolution MS/MS spectra and potential cleavage metabolites. As a result, a confirmation score (from 0 to 100) is provided to rank metabolite peak identification. In addition, formation rates of the metabolites were correlated to different incubation times to investigate metabolite stability.

4.1.8 Production of RXT main hepatic metabolites

In order to provide a large enough amount of RXT main hepatic metabolites, large-scale human microsomal incubations were performed. Incubations were carried out in glass tubes containing HLM (2 mg of protein/mL), 5 mM $MgCl_2$, 2 mM NADPH, 500 μM RXT, and 50 mM phosphate buffer (pH 7.4) in a total volume of 50 mL. After incubation in a 37°C water bath shaker for 240 min, the reactions were terminated by adding 50 mL of ice-cold AcN. The mixture was vortexed for 3 min and centrifuged at 3750 rpm for 15 min. The supernatant was collected and dried under nitrogen gas flow. The residue was reconstituted with 100 mL of water. This concentrate was applied to a pre-conditioned Waters Oasis HLB solid phase extraction (SPE) on 96-well plates (30 mg). The pre-conditioning step included washing with 1 mL each of neat methanol and 20% aqueous methanol. The loaded cartridge was washed with water, after which the metabolites were eluted using 1 mL of methanol. After evaporation of SPE elution and further reconstitution in 50 mL of water, liquid-liquid extraction (LLE) was also applied as an isolation step. The RXT metabolites extract was contacted with an organic solvent [(methyl-ethyl ketone), 1:1] and shaken vigorously for 10 min. Both SPE and L/L procedures were optimized for achieving maximum recuperation of main RXT metabolites which had been previously described [126]. Centrifugation of the liquid mixture at 805 g for 15 min separated the organic layer from the aqueous layer. Samples from both layers were analyzed for metabolite content by LC-HRMS. The aqueous layer was dried under N_2 current and further reconstituted in 5% aqueous methanol for subsequent preparative HPLC isolations which were performed using an Atlantis T3 column, 10×250 mm, 5-μm particle size. For isolation of metabolites, the mobile phase consisted of a linear gradient from 5% to 95% of mobile phase B (AcN containing 0.1% formic acid) in 25 min. The flow rate was 2.3 mL/min and UV absorbance was monitored at 290 nm. Fractions were automatically collected every 0.25 min and further analyzed by LC-HRMS using a fast gradient in 3.5 min in order to assess

the metabolite purity and fraction enrichment. At this point, it is important to mention that in parallel, we carried out blank (not containing RXT) large-scale incubations that were equally subjected to SPE, LLE and semi-preparative HPLC fractionation in order to be used as false positive controls in the biological activity assessment.

4.2 Optimization and Validation of HTS Platform Using Microbial Extract for the assessment and discovery of immunomodulator molecules.

In vitro studies were performed to evaluate immunomodulatory properties of microbial extracts, both in LPS–stimulated RAW 264.7 cells for NO production (see section 4.1.4) and IL-1β stimulated – Caco-2 cells for IL-8 production.

4.2.1 Microbial Extracts Collection

For the primary screening campaign, a subset of the MEDINA microbial natural product collection consisting of 5,976 non-cytotoxic microbial extracts (3,568 from actinomycetes and 2,408 from fungi) was used. This subset of extracts was previously found to inhibit by less than 20% the growth of hepatic tumoral HepG2 cells when tested at a final concentration of $1/40 \times$ WBE for 24 hours.

The microbial extracts were obtained from a selection of producing strains that were cultivated for 7 and 14 days at 28°C in the case of actinomycetes, and for 21 and 28 days at 22°C for fungi. The secondary metabolites in the broths were extracted with acetone (1:1) by mixing 10 mL of culture broth with 10 mL of acetone and shaking in an orbital shaker (Adolf Kuhner AG, Birsfelden, Switzerland) for 1 hour. The extracts were then centrifuged at $1500 \times g$ for 15 min and the supernatants were transferred to 16 mm glass tubes. DMSO was then added to each extract and organic solvent and part of the water were evaporated down to half of the original

fermentation volume under warm N_2 stream, to attain a final crude concentration of $2 \times$ WBE and 20% DMSO. Five copies of one hundred microliters (500 µL) of these crude extracts were stored at -20°C in 96-well ABgene plates (AB-0756) until needed. One of them was used to carry out the screening.

4.2.2   Primary Screening and Dose Response Experiments

All of the microbial extracts were used first in the primary screening assayed against the macrophages model at single concentration ($1/20 \times$ WBE) in duplicate (Figure 18A) and those exhibiting inhibition of NO production ≥80% and cell viability ≥75% were selected as hits and confirmed in triplicate (Figure 19B). The extracts selected from this stage were then tested in a 5-point dose response assay for potency determination (Figure 18C); the first point was the initial dilution previously described for each assay ($1/20 \times$ WBE), and the 4 subsequent points were twofold serial dilutions from each point. Extracts which exhibited a minimum of 70% inhibition at initial dilution ($1/20 \times$ WBE) in dose response experiments were selected for de-replication (Figure 18D) by low resolution LC-MS.
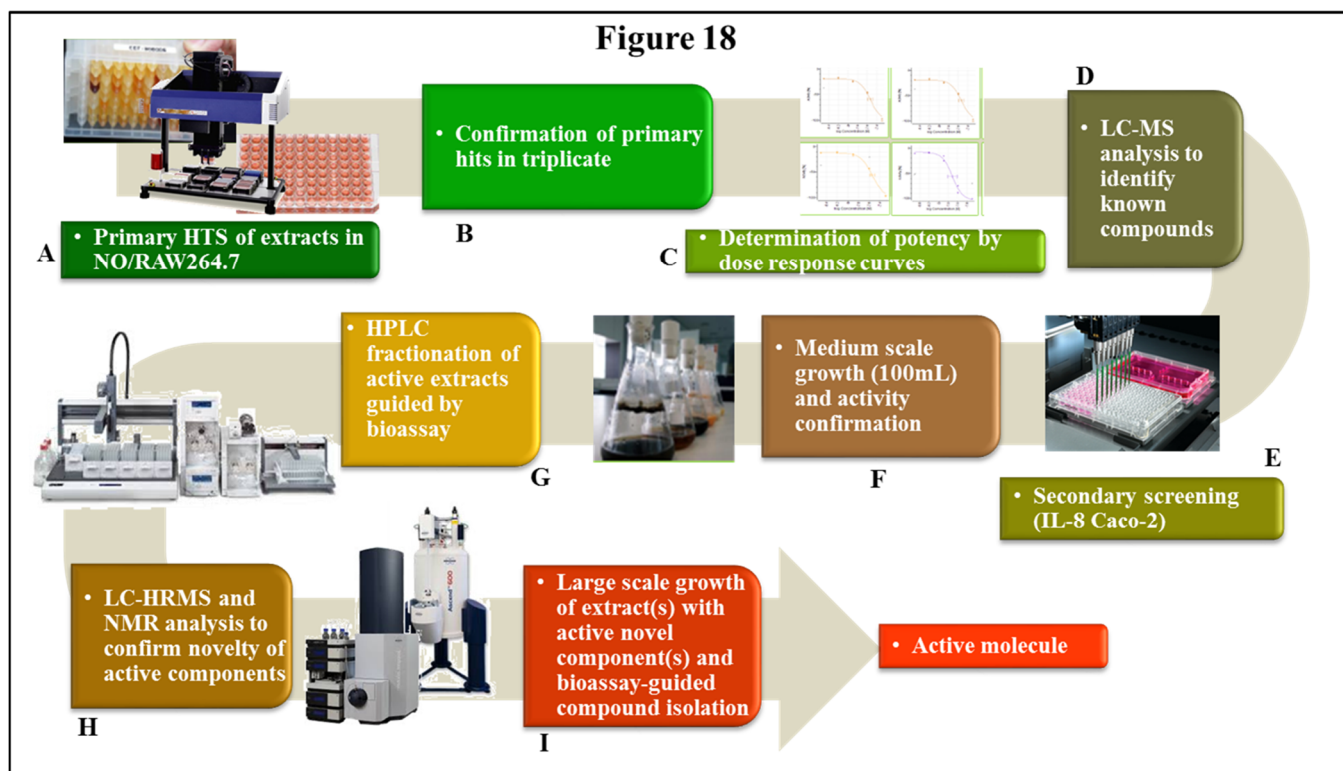
Figure 18. Schematic representation of the HTS and integrated de-replicating chemistry platform used in discovering immunomodulatory molecules from microbial extracts.

(A) Microbial extracts are first screened against the NO assay in duplicate. (B) The extracts meeting selection criteria (inhibition of NO production ≥80% and cell viability ≥75%) are confirmed in triplicate. (C) The confirmed extracts are tested in a NO 5-point dose response assay for potency determination. Extracts exhibiting at least 70% inhibition at initial dilution (1/20 × WBE) in dose response experiments are selected for de-replication by low resolution LC-MS. (D) UV-Mass spectra of the selected extracts are compared to the UV-LC-MS data of known metabolites stored in a proprietary database. Only extracts without positive metabolite identification in the spectral data base are selected as potentially not containing known active components. (E) The extracts selected at this stage are tested against the Caco-2 model in a 5-point dose response pattern in duplicate for confirmation of activity. Those meeting the selection criteria (inhibition of IL-8 production ≥60% at 1/20 × WBE and cell viability ≥75%) are (F) regrown in medium scale format (100 mL) and the bioactivity confirmed. (G) The extracts from confirmed re-growths are subjected to bioassay-guided fractionation applying the primary and secondary screening paradigm. (H) Active fractions from this stage are then analyzed by LC-HRMS and NMR. (I) The extracts in which novel components are confirmed are regrown in 1 L volumes for the purification of the active compounds by bioassay-guided compound isolation.

4.2.3 LC-MS and Database Matching of Known Secondary Metabolites (De-replication)

Two microliters (2 µL) of the selected extracts were analyzed by LC-MS. Analysis was performed on an Agilent (Santa Clara, CA) 1100 single quadrupole LC-MS, using a Zorbax SB-C8 column (2.1 × 30 mm), maintained at 40°C with a flow rate of 300 µL/min. Solvent A consisted of 10% acetonitrile and 90% water with 1.3 mM trifluoroacetic acid and 1.3 mM ammonium formate, whereas solvent B was 90% acetonitrile and 10% water with 1.3 mM trifluoroacetic acid and 1.3 mM ammonium formate. The gradient was started at 10% B and went to 100% B in 6 min; it was kept at 100% B for 2 min, and was returned to 10% B for 2 min to initialize the system. Full diode array ultraviolet (UV) scans from 100 to 900 nm were collected in 4 nm steps at 0.25 s/scan. The eluting solvent was ionized using the standard Agilent 1100 ESI source adjusted to a drying gas flow of 11 L/min at 325°C and a nebulizer pressure of 40 psig. The capillary voltage was set to 3500 V. Mass spectra were collected as full scans from m/z 150 to 1500, with 1 scan every 0.77 s, in both positive and negative modes. Database matching was performed using an application developed in-house, in which the diode array detection, retention time, and positive and negative mass spectra of the active samples were compared to the UV-LC-MS data of known metabolites stored in a proprietary database and in which metabolite standard data were obtained using the exact same LC-MS conditions as the samples under analysis. More information about this proprietary data base such as number and main classes of compounds and how it was built can be found in a previous work by Pérez-Victoria and collaborators [127]

4.2.4 Assays for IL-8 regulation assessment in IL-1β stimulated Caco-2 cells

The following procedure is an adaptation to the 96-well format from a methodology previously described [114]. Caco-2 cells were seeded into 96-well plates at a density of 20×10^3 cells per

well and grown to approximately 50% confluence (24 hours, 37ºC and 10% CO2). Then, they were pre-incubated for 24 hours with each of the extracts described above (5 µL of 2 × WBE at 20% DMSO were dispensed into 190 µL of fresh medium using Perkin Elmer Evolution P3, obtaining a final extract concentration of 1/20 × WBE). Afterwards, cells were stimulated with IL-1β (5 µL of 2 ng/ml were dispensed using a Thermo Scientific Multidrop Combi dispenser) for 24 h. Untreated (5 µL of 20% DMSO, microbial extract vehicle) and unstimulated (5 µL of purified water, IL-1β vehicle) cells were used as negative controls (n=4) while untreated but stimulated cells were used as positive controls (n=4) in each assay plate. The supernatants (100 µL) were then collected, centrifuged at 10,000 × g for 5 min, and stored at -80ºC until IL-8 determination by ELISA (Biosource, InvitrogenTM) was performed. Cell viability was examined using the MTT test described elsewhere [123].

4.2.5   Cell Based Caco-2 Model - Secondary Screening Assay

Extracts with LC-MS profiles suggestive of not containing known compounds were tested against the Caco-2 model in a 5-point dose response dilution pattern in duplicate for confirmation of activity (Figure 18E). The first point was the initial dilution previously described for each assay (1/20 × WBE), and the 4 subsequent points were twofold serial dilutions from each point. Those exhibiting inhibition of IL-8 production ≥60% and cell viability ≥75% at initial dilution were selected for medium scale-up fermentation and bioactivity confirmation.

4.2.6   Medium Scale-up Fermentation and Fractionation Guided by Bioassay

Extracts with confirmed activity in secondary screening were regrown in 100 mL volume (Figure. 18F). An equal volume of acetone was added to each 100 mL fermentation, and the mixture was homogenized and shaken in a Kühner shaker at 220 rpm for 3 h. From each extract, 13 mL were transferred into separate glass tubes and evaporated under a N$_2$ stream until only

3.2 mL remained (extract concentration $2 \times$ WBE). From each of these glass tubes, $5 \times 520\,\mu L$ extract volumes were transferred onto 5 ABgene plates (AB-0756) using a Multiprobe II liquid handler (PerkinElmer). Aliquots from 1 of these 5 ABgene plates were bio-assayed to confirm activity (Figure. 18F) before storing the plate at -20°C, as a reference plate. The remaining 4 ABgene plates of each extract identified as active were centrifuged, each of the extracts was pooled together in a glass vial and loaded onto a 10 g SP207ss charged column, and the flow-through was collected and stored at -20°C. The column was then washed with an equal volume of Milli-Q water, and the aqueous flow-through was also collected and saved in a new glass vial at -20°C. The column was finally eluted to dryness with 20 mL of acetone. The collected solutions were evaporated under a N_2 gas stream to yield a dry crude extract. Each crude extract was then reconstituted in 400 µL DMSO, and half of this volume was injected and separated into 80 fractions (Figure. 18G) using a linear gradient of 5–100% acetonitrile–water with 0.1% trifluoroacetic acid in reverse-phase, semi-preparative, high-performance liquid chromatography (HPLC) using Agilent column Zorbax RX-C8, 5 µm, 9.4×250 mm, with UV detection at 210 nm (Gilson, Middleton, WI). The 80 fractions collected were evaporated to dryness in an ABgene plate using a Genevac evaporator (Genevac, Ipswich, UK). These fractions were then reconstituted in 30 µL of DMSO and 150 µL of Milli-Q water to make a final solution at 20% DMSO concentration. The fractions were then tested for activity following the previously described screening paradigm. Active fractions from this stage were then analyzed by LC-HRMS and NMR (Figure. 18H). The extracts in which novel components are confirmed will be then regrown in 1 L volume for the purification of the active compounds by bioassay-guided compound isolation (Figure 18I).

4.2.7 Growth Scale-up Bioassay-Guided Purification (in collaboration with MEDINA Microbiology and Chemistry Departments)

One of the hit extracts containing compounds of interest detected in the previous step was growth again at 1 L scale using the appropriate production conditions. The producing organism (CF-097474) was isolated from the surface-disinfected stems and leaves of Juniperus thurifera collected in Peralejos de las Truchas, Guadalajara, Spain, using a method for isolating fungal endophytes. Frozen stock cultures in 10% glycerol (-80ºC) are included in the collection of Fundación MEDINA. Total genomic DNA was extracted from mycelia grown on YM agar. The 28S rDNA fragments, containing D1-D2 and ITS regions, were PCR amplified, and sequence aligned [128]. Sequence homology searches in public databases (www.fungalbarcoding.org; NCBI) indicated that the fungus had affinities to the species Seimatosporium lichenicola CBS 506.71. Extensive taxonomical analysis placed this strain in the Seimatosporium genus (data not shown). Seimatosporium sp. (CF-097474) was fermented by inoculating ten mycelial agar plugs into SMYA medium (Bactoneopeptone 10 g; maltose 40 g; yeast extract 10 g; agar 3 g; water 1 L) in an Erlenmeyer flask (50 mL medium in a 250 mL flask). The flask was incubated in a rotary shaker at 220 rpm at 22ºC with 70% relative humidity (RH). After growing the seed stage for 7 days, a 3 mL aliquot was used to inoculate each flask of the production medium CYS80 (sucrose 80 g; corn meal 50 g; yeast extract 1 g; water 1 L). Ten flasks (100 mL medium per 500 mL Erlenmeyer flask) were incubated at 22ºC with 70% RH in a rotary shaker at 220 rpm for 14 days. A 1 L fermentation was carried out for purifying the compounds. An equal volume of acetone was added to the growth broth and the mixture was homogenized by shaking in a Kühner cabinet at 220 rpm for 3 h. The remaining solution was filtered and the acetone was evaporated under a N_2 stream. This solution was loaded (with continuous 1:1 water dilution, discarding the flow-through) on a column packed with SP-207SS reversed phase resin (brominated styrenic polymer, 65 g) previously

equilibrated with water. The loaded column was further washed with water (1 L) and afterwards eluted at 10 mL/min on an automatic flash-chromatography system (CombiFlash Rf, Teledyne Isco) using a 30-minute step gradient from 10% to 100% acetone in water with a final 100% acetone step (for 12 min.) collecting 19 fractions of 20 mL. Fractions were submitted to be tested in the primary screening and fraction number 9 (gradient step at 40% acetone) showed the desired activity. Fraction number 9 was subjected to semi-preparative HPLC (Agilent Zorbax RX-C8, 9.4 × 250 mm, 5 µm; 3.6 mL/min, UV detection at 210 nm, gradient water + 0.1% trifluoroacetic acid:acetonitrile + 0.1% trifluoroacetic acid from 5% to 100% acetonitrile for 35 min) yielding a fraction eluting at 15.0 min that retained the target activity and that was further purified by semi-preparative HPLC (Agilent Zorbax RX-C8, 9.4 x 250 mm, 5 µm: 3.6 mL/min, UV detection at 210 nm, gradient water + 0.1% trifluoroacetic acid:acetonitrile + 0.1% trifluoroacetic acid from 25% to 40% acetonitrile for 35 min) to yield 2.5 mg of mixture of epimers TAN-2483A and TAN-2483B [129].

4.2.8 Evaluation of Antimicrobial Activity

The antimicrobial activity of the fractions was evaluated using a broth microdilution technique against various clinically relevant strains (all from Fundación MEDINA's collection). Antibacterial susceptibility was tested against *Pseudomonas aeruginosa* PAO1, *Acinetobacter baumannii* CL5973, *Escherichia coli* MB2884 (wild type), *Escherichia coli* MB5746 (envA/tolC) and *Meticillin-resistant Staphylococcus aureus* MB5393, while antifungal susceptibility was tested against *Candida albicans* MY1055. Previously described methods were used to test for antimicrobial and antifungal activities [130]. Experiments were made in triplicate and on different days. The Genedata Screener software was used to process and analyze the data.

4.3 Compound Aqueous Solubility Assessment in Cytochrome P450 Inhibition Assays

For this purpose 42 compounds were selected from the Instituto de Quimica Médica - CSIC (IQM-CSIC) drug discovery research program as lead compounds targeting different GSK3 enzymes for the treatment of neurodegenerative diseases, along with 20 commercial specific inhibitors of different CYP450 isoforms. We determined the IC_{50} value of each molecule in 2 different CYP450 inhibition assays, using hrCYP / fluorometric or HLM- LC/MS-MS methodologies. In parallel, we determined the aqueous solubility by turbidimetric measurement for each molecule considered. Experiments were made in duplicate and on different days

4.3.1 Test Compounds & Reagents

Nicotinamide adenine dinucleotide phosphate reduced tetrasodium salt, standard CYP450 probe substrates (testosterone, diclofenac and dextromethorphan), LC-MS/MS internal standards (cortisone and levallorphan) and CYP450 control inhibitors (ketoconazole, quinidine, sulfaphenazole) were obtained from Sigma Aldrich (St. Louis, MO). LC-MS/MS internal standard 4'-hydroxydiclofenac 13C6 was purchased from Toronto Research Chemicals (Toronto).

The fluorogenic reagents, 7-Benzyloxy-4-(trifluoromethyl) coumarin (BFC), 7-methoxy-4-trifluoromethylcoumarin (MFC), and 3-[2-(N,N-diethyl-N-methylamino)ethyl]-7-methoxy-4-methylcoumarin (AMMC), were obtained from BD GentestCorp (Woburn, MA).

IQM drug discovery compounds were obtained from the Instituto de Química Médica - CSIC (IQM-CSIC) library. All test compounds were provided in powder form and dissolved in 25 mM and 10 mM DMSO stock solutions and 1/2 serially diluted in DMSO.

For CYP inhibition assays, several concentrations were prepared and diluted with acetonitrile [35:65] [v/v] in order to minimize the final DMSO content in enzyme incubations. The same stock solutions were used for the comparisons of CYP inhibition assays and KS assays.

Human liver microsomes (mixed gender, pool of 22) were purchased from BD Gentest Corp (Bedford, MA). The recombinants isoforms of CYP3A4+OR, CYP2D6+OR, CYP2C9+OR, were purchased from BD Gentest Corporation. The marketed compounds evaluated in these assays were obtained from Sigma Aldrich.

Before CYP450 inhibition reactions, reaction times and microsomal protein concentrations were verified to be within the limits of kinetics linearity (not shown). All probe substrate concentrations selected for these determinations were approximately equal to the apparent reaction Km. All compounds were tested in triplicates in every methodology studied.

4.3.2 CYP450 inhibition assay by HLM- LC/MS-MS method

Incubations for evaluating CYP450 inhibition were conducted in a 96-well plate format at 37°C. The final incubation (200 µL total volume) contained 0.25 mg/mL of HLM protein in 100 mM potassium phosphate buffer (pH 7.4), 1 mM NADPH, and test compound at 0.078, 0.313, 0.625, 1.25, 2.5, 5, 11, 22, 44 and 88 µM. The probe reaction for CYP3A4 was conducted with 50 µM testosterone and HLM protein for 15 min. In the case of CYP2D6, the probe reaction was conducted with 22 µM dextromethorphan for 15 min. The CYP2C9 probe reaction was conducted with 10 µM diclofenac for 15 min.

Test compounds in DMSO/AcN (v/v) (2 µL) were combined with 98 µL NADPH solution, and reactions were initiated by the addition of 100 µL of enzyme – substrate solution. Reactions were terminated with the addition of a quench solution (90 µL) of acetonitrile containing

internal standards for LC-MS/MS (60 ppb cortisone, 100 ppb 4′-hydroxydiclofenac 13C6, 60 ppb levallorphan).

Control inhibitors, such as ketoconazole for CYP3A4, quinidine for CYP2D6, or sulfaphenazole for CYP 2C9, were included in all incubation plates. The final DMSO content was established at 0.35% for all isoforms. Reaction supernatants, clarified by 10 min of centrifugation at 3717 g (4°C), were analyzed by LC/MS-MS for relative quantification of the metabolites (6β-hydroxytestosterone, 4′-hydroxy-diclofenac, or dextrorphan) generated from the corresponding probe substrates.

4.3.3 LC/MS-MS analysis

Quantitative analysis of probe substrate metabolites in quenched reaction supernatant was performed using a Shimadzhu AD10 liquid chromatography equipped with an API4000 (triple quadrupole) mass spectrometer (AB SCIEX). Chromatographic separation was achieved using a Discovery HS C18 (50 mm length, 2 mm internal diameter, 5 µm particule size) column (Supelco, Torrance, CA) preceded by a Discovery HS C18 precolumn. The column temperature was held at 25°C. The mobile phase consisted of 2 solvents: (A) water/methanol 90/10 (v/v) in 0.1% formic acid and (B) AcN/water in 0.1% formic acid. Mobile phase B was held at 10% for 0.5 minutes, then increased to 45% B for 1.50 minutes. Solvent composition was held for 0.30 minutes, increased again to 95% B for 2.30 minutes and held for 0.50 minutes, and returned to 10% B for 0.10 minutes for re-equilibration, being held for 0.61 minutes. Total run time was 3.51 minutes, with a flow rate of 1mL/minute.

The mass spectrometer was operated with an atmospheric pressure chemical ionization probe in positive mode using multiple reaction-monitoring scanning mode. Integration of reaction product and internal standard peak areas was performed using Analyst software (AB SCIEX).

4.3.4 CYP450 inhibition assay by hrCYP fluorometric method

Fluorometric CYP450 inhibition assays were conducted at 37ºC in 96-well, flat-bottom, black polystyrene plates. Incubation mixtures containing CYP protein, substrate, and potassium phosphate buffer (pH 7.4) were prepared with the following final concentrations: CYP3A4, 25 pmol/mL, 20 µM BFC in 175 mM buffer; CYP2D6, 20 pmol/mL 1.5 µM AMMC in 25 mM buffer; and CYP2C9, 25 pmol/mL, 50 µM MFC in 25 mM buffer. Reaction times were verified to be within the limits of kinetics linearity (not shown). All probe substrate concentrations selected for these determinations were approximately equal to the Km. Test compounds dissolved in DMSO/AcN (v/v)(2 µL) were combined with 98 µL NADP/ cofactors solution, and reactions were initiated by the addition of 100 µL of enzyme – substrate solution. Incubation times for CYPs 3A4, 2D6, and 2C9 were 15, 30 and 45 minutes, respectively. Then fluorescence was determined in a Tecan Ultra Evolution reader, using the following excitation/emission wavelengths: CYP3A4 (430/535 nm), CYP2D6 (360/465 nm), and CYP2C9 (430/535 nm). Two separate control incubations for fluorescent interference and quenching interference containing test compound (88 µM) and recombinant enzymes (at the same concentration as the inhibition incubations) were included for each compound tested. A compound was excluded from the data set if the fluorescent signal from the control incubation was >30% of the dynamic window for the reaction, as evidence of fluorescence interference. Conversely, a known amount of product metabolite was added to quenching control positions post-incubation. This determined whether the production of metabolites from potential inhibitors could result in the quenching of signal of product metabolite in relative fluorescence units (RFU) produced for a known amount, established in the absence of potential inhibitors. If the fluorescent signal from the control incubation was <30% of the known fluorescent signal for post-incubation addition of metabolite product, as evidence of quenching interference, the IC_{50} value for those potential inhibitors was not calculated.

The key differences between the 2 CYP450 inhibition methodologies (fluorescence and LCMS) are summarized in Table 1.

4.3.5 Calculation of IC$_{50}$ values in CYP450 inhibition assays

The equation used for normalization for CYP450 inhibition data is as follows:

$$\%PC = \frac{(X-NC)}{(PC-NC)} * 100$$

where %PC is the percentage of remaining activity at a particular concentration after normalization, NC is the median of the measured signal values for the negative control wells on a plate, PC is the median of the measured signal values for the positive control wells on a plate, and X is the measured raw signal value of a well. The normalized data were fitted by the smart engine embedded in the core of Screener GeneData using a 4-parameter logistic fit to determine the IC$_{50}$.

Table 1. Summary of Key Assay Conditions in the 2 CYP450 inhibition methodologies.

Assay Approach	hrCYP/Fluorogenic	HLM/LC-MS/MS
Isoform/Concentration (pmol/ml)	CYP3A4/25	CYP3A4/16 (a)
Total Protein Concentration (mg/ml)	0.11	0.25
Substrate/ Concentration (µM)	BFC/20	Testosterone/50
Isoform/Concentration (pmol/ml)	CYP2C9/25	CYP2C9/14.4 (a)
Total Protein Concentration (mg/ml)	0.14	0.25
Substrate/ Concentration (µM)	MFC/50	Diclofenac/10
Isoform/Concentration (pmol/ml)	CYP2D6/20	CYP2D6/1.6 (a)
Total Protein Concentration (mg/ml)	0.11	0.25
Substrate/ Concentration (µM)	AMMC/1.5	Dextromethorphan/20

hrCYP = human recombinantly expressed CYP450 isoforms; HLM = human liver microsomes;
LC-MS/MS = Liquid chromatography coupled to mass - mass spectrometry; (a) Calculated based on the total CYP450 content of 330 pmole/mg (BDBiosciences. Lot. Number 59488) and distribution of each isoenzyme [131] (3A4=20%, CYP2C9=18%, CYP2D6=2).

4.3.6   Conventional separate in vitro model for KS evaluation (CSIVM-KS)

The KS assay was conducted in 96-well, flat-bottom, transparent polystyrene plates (Costar 9018, Corning, Tewksbury MA). Six ½ serial dilutions of an initial 10 mM test compound solution were prepared in DMSO. As currently practiced, 2 µL of a concentrated stock solution of the test compound in DMSO is added to a 198µL of 100 mM potassium phosphate buffer

(pH 7.4) solution to give a final DMSO concentration of 1% in each well and a final test compound concentration ranging between 3.12 µM and 100 µM. Three replicates of each test compound were prepared per concentration. After a 2-hour incubation period, to avoid missing slow precipitation which might affect the outcome of a biochemical experiment, absorbance is measured at 620 nm by an EnVision multilabel plate reader. The KS is estimated from the concentration of test compound that produced an increase in absorbance above the background levels (typically 1% DMSO in buffer).

4.4 A novel in vitro approach for simultaneous evaluation of CYP3A4 inhibition and kinetic aqueous solubility (NIVA-CYPI-KS)

To establish the suitability of this NIVA-CYPI-KS, we selected a set of 11 commercial compounds with reported data as potential CYP3A4 inhibitors, and we simultaneously evaluated their potential and aqueous solubility, using both the NIVA-CYPI-KS and separate conventional methodologies. In addition, five lead compounds from MEDINA in-house research were tested in the NIVA-CYPI-KS to assess the potential benefits of this new approach.

4.4.1 Compounds and reagents

Nicotinamide adenine dinucleotide phosphate (NADP) sodium salt, Glucose-6-phosphate monosodium salt, glucose-6-phosphate dehydrogenase, potassium phosphate buffer and magnesium chloride were obtained from Sigma Aldrich. The CYP3A4 non fluorescent probe substrate BFC and its corresponding fluorescent reaction product were obtained from Gentest Corporation (Woburn, Massachusetts). Human recombinant c-DNA expressed CYP3A4 microsomes at 1 nmol/ml were obtained from Gentest Corporation. Lead compounds evaluated in this work were obtained from Fundación MEDINA (Granada, Spain). The commercial compounds evaluated in this work (erythromycin, verapamil, ethynilestradiol, miconazole,

bromoergocriptine, nicardipine, clotrimazole, itraconazole, roxythromycin, cimetidine, nifedipine and ketoconazole) were obtained from Sigma Aldrich (St. Louis, MO).

4.4.2 Test Compound Preparation

For CYP3A4 inhibition evaluation in the conventional separate model and also for the simultaneous evaluation of CYP3A4 inhibition and solubility using NIVA-CYPI-KS, we used the same solutions of commercial compounds, which were prepared as follows: test compounds were provided in powder form and dissolved in 100% DMSO at 25 mM in 96-well plates. Serial dilutions of test compounds in 100% DMSO were carried out on a Biomek FX workstation coupled with a stacker carrousel (Beckman Coulter Inc., Brea, California). Considering their previously reported CYP3A4 inhibition potential, commercial compounds were prepared at different initial concentrations and dilution factors in order to optimize their IC_{50} calculation from a titration curve with 8 concentration levels (Figure 19A). Diluted compounds in 100% DMSO (35 µL) were combined with acetonitrile (65 µL) on 96-well microtiter plates (AB-0765, Thermo, Waltham, MA) by a Perkin Elmer Evolution P3 liquid-dispensing instrument (Waltham, Massachusetts) in order to minimize the final DMSO content in enzyme incubations (Figure 19B). Regarding the lead compounds from Fundación MEDINA research programs, they were also prepared at 25 mM stock solution from pure powder material. Stock solutions were ½ serially diluted in DMSO to achieve titration curves comprising 8 concentration levels. Further dilutions with AcN of these DMSO solutions were carried out as previously described in this section for commercial compounds. Therefore, the concentration levels of drug discovery compounds in the novel approach experiments ranged from 86 to 0.65 µM. All compounds (commercial and Fundación MEDINA) were tested in triplicate in every methodology studied.
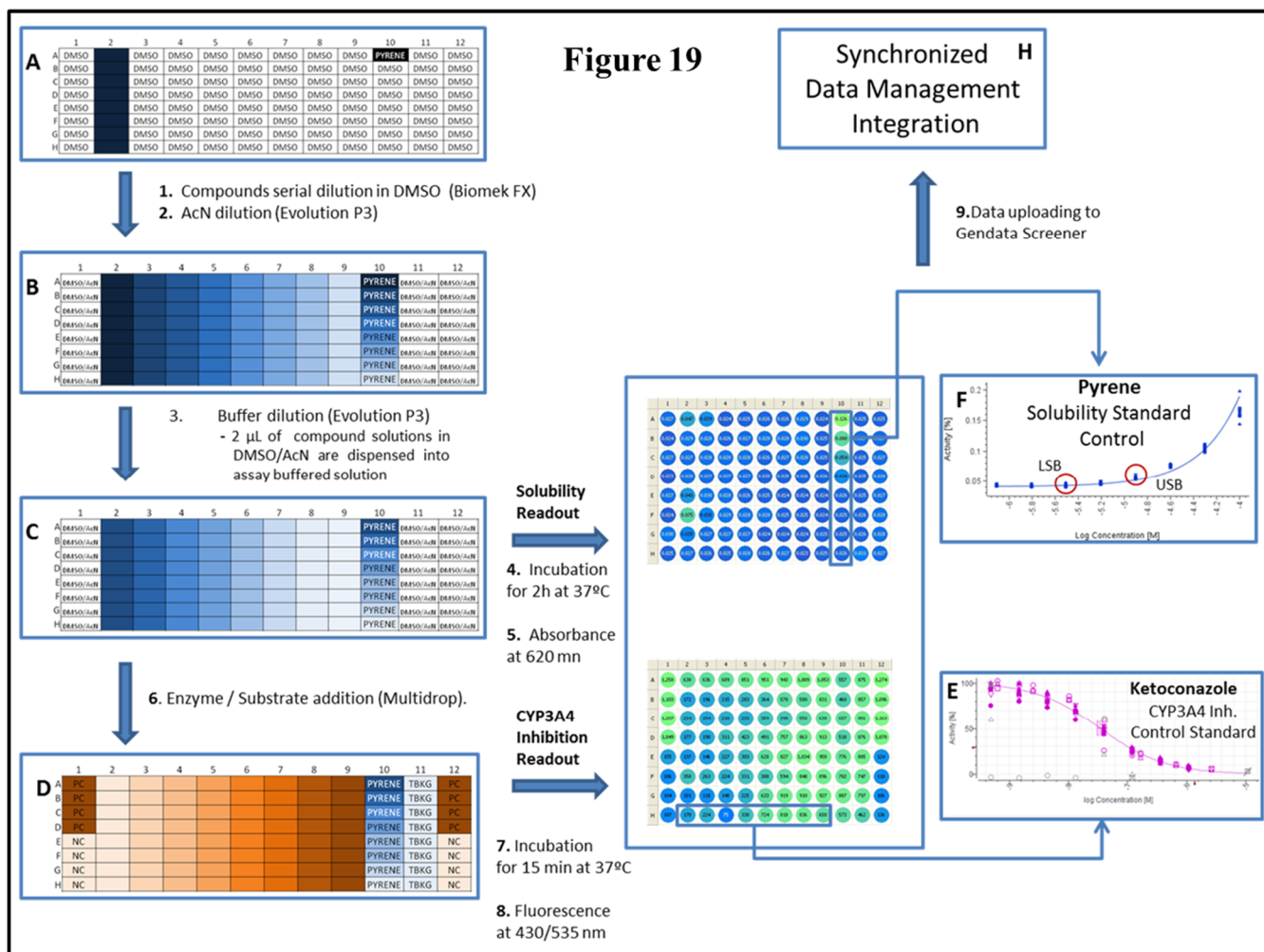
Figure 19. Assay scheme for novel In vitro approach for simultaneous evaluation of CYP3A4 inhibition and kinetic aqueous solubility (NIVA-CYPI-KS). DMSO stock solutions of test compounds are serially diluted with DMSO from column 2 to column 9. The DMSO stock solution of pyrene is serially diluted with DMSO in column 10 from row A to row H. Columns 1 and 11 contain organic solvent assay control. (B) Serially diluted test compounds, standard assay solubility controls are further diluted with AcN. (C) 2 µL of DMSO/AcN solutions are dispensed into assay buffered solution representing 90% of final volume. (D) Initiation of enzymatic reaction is achieved by the addition of 10 µL enzyme / substrate solution and 10 µL NADPH regenerating system solution. PC (Positive control for enzyme activity), NC (Negative control for enzyme activity), TBKG (Turbidimetric background). (E) Reference inhibitor ketoconazole was included in every assay plate to monitor CYP3A4 activity. (F) Pyrene, a highly lipophilic and very low water solubility compound, was used to monitor turbidimetric detection in every assay plate. USB: Upper solubility bound. LSB: Lower solubility bound. (H) Graphic user interface of GeneData Screener® allows simultaneously reviewing the readouts for solubility and CYP3A4 inhibition, enabling the integration and synchronization of data management which eventually provides a better understanding of CYP450 inhibition data according to a real situation of test compounds in assay solution.

4.4.3 Conventional separate in vitro model for CYP-inhibition evaluation (CSIVM-CYPI)

Before CYP450 inhibition reactions, reaction times and microsomal protein concentrations were verified to be within the limits of kinetic linearity (data not shown). Probe substrate concentration selected for these determinations was approximately equal to the apparent reaction Km [132]. CYP3A4 inhibition studies were conducted by quantification of non-fluorescent substrate (BFC) transformation to a fluorescent product (7-HFC), which is mediated by CYP3A4. Incubation mixtures were prepared as follows: CYP3A4 enzyme, substrate, and potassium phosphate buffer (pH 7.4) were prepared with the following final concentrations: CYP3A4, 25 pmol/mL, 20 µM BFC in 175 µM potassium phosphate buffer. Test compounds dissolved in DMSO/AcN [35:65] [v/v] (2 µL) were transferred onto black 96-well plates with a clear flat bottom (3650 Corning, Tewksbury MA) containing NADPH generating system (1.33 mM NADP, 3.54 mM glucose-6-phosphate, 0.4 U/ml glucose-6-phosphate and 3.3 mM $MgCl_2$) in a potassium phosphate buffer (pH 7.4) (98 µL) using a Perkin Elmer Evolution P3 liquid handling station. Reactions were initiated by the addition of enzyme-substrate buffered solution (100 µL) using a Thermo Multidrop Combi liquid dispenser (Waltham, MA). Reaction mixtures were incubated with shaking for 15 min at 37ºC. Reactions were terminated with the addition of 75 µl of a STOP solution of AcN containing 0.5 M Tris base. Then fluorescence was determined using 430 nm as excitation and 535 nm as emission wavelengths in Perkin Elmer EnVision multilabel reader. Fluorescence signals were used to estimate IC_{50} as described in the data analysis section. Regarding the experimental design of incubation plates, eight positive controls (no inhibitor incubations) were included in each assay plate to assess the maximum amount of fluorescent product formed and, conversely, eight negative controls (no NADP incubations) were included to assess the contribution of assay regents to fluorescent readout in each assay plate. Control incubations for fluorescent

interference and quenching interference were carried out for each test compound in separate assay plates, containing test compound at maximum dose, recombinant enzyme and no substrate.

4.4.4   Conventional separate in vitro model for KS evaluation (CSIVM-KS)

The KS assay was conducted in 96-well, flat-bottom, transparent polystyrene plates (Costar 9018, Corning, Tewksbury MA). Six ½ serial dilutions of an initial 10 mM test compound solution were prepared in DMSO. As currently practiced, 2 µL of a concentrated stock solution of the test compound in DMSO is added to a 198µL of 100 mM potassium phosphate buffer (pH 7.4) solution to give a final DMSO concentration of 1% in each well and a final test compound concentration range between 3.12 µM and 100 µM. Three replicates of each test compound were prepared per concentration. After a 2-hour incubation period, to avoid missing slow precipitation which might affect the outcome of a biochemical experiment, absorbance is measured at 620 nm by an EnVision multilabel plate reader. The KS is estimated from the concentration of test compound that produced an increase in absorbance above the background levels (typically 1% DMSO in buffer).

4.4.5   Novel in vitro approach for simultaneous CYP450-inhibition and turbidimetric solubility evaluation (NIVA-CYPI-KS)

The experiments for simultaneous determination of CYP3A4 inhibition and aqueous solubility were conducted at 37°C using white flat bottom 96-well plates with clear bottom polystyrene plates (Costar 3632, Corning, Tewksbury MA). Incubation mixtures containing CYP3A4 protein, substrate, and potassium phosphate buffer (pH 7.4) were made at the same reagent concentrations and kinetic conditions as the CSIVM-CYPI experiment previously described. Test compounds dissolved in DMSO/AcN [35:65] [v/v] (2 µL) were combined with a 180 µL potassium phosphate buffer (pH 7.4) using an Evolution P3 liquid handling station (Figure.

19C). Then the plates were incubated for 2 hours at 37°C to allow slow compound precipitation. Thereafter, absorbance was measured at 620 nm by an EnVision multilabel plate reader. Absorbance signals were used to determine compound solubility limits. After that, 10 µl NADP / cofactors buffered solution and 10 µL of enzyme / substrate buffered solution were dispensed using a Multidrop liquid dispenser to trigger the enzymatic reaction (Figure. 19D). Plates were incubated at 37°C for 15 min. Reactions were terminated with the addition of 75 µL of a STOP solution of AcN containing 0.5 M Tris base using a Multidrop liquid dispenser. Then fluorescence was determined using 430 nm as excitation and 535 nm as emission wavelengths by an EnVision multilabel plate reader. Fluorescent signals were used to estimate IC_{50} values. Eight positive control wells (no inhibitor incubations) were included in each assay plate to assess the maximum amount of fluorescent product formed. Eight negative control wells (no NADP incubations) were included in each assay plate to assess the contribution of assay regents to fluorescent readout. Additionally, eight absorbance background control levels for turbidimetric assessment (potassium phosphate buffer at pH 7.4 and 2 µL DMSO/AcN [35:65] v/v) were included in each plate. Ketocnazole and pyrene were used as standard control for CYP3A4 inhibition and precipitation in KS determination respectively (Figure 19E&F).

4.4.6 Data management, data analysis and calculations for NIVA-CYPI-KS

Two main calculations lie at the core of the present work. One is the calculation of the IC_{50} parameters from the fluorescence layer, and the other is the calculation of solubility parameters from the absorbance values. All calculations of IC_{50} values and solubility limits were made using GeneData Screener application software. In the case of NIVA-CYPI-KS, this software tool was configured to integrate 2 different measured layers (absorbance at 620 nm before starting enzymatic reaction and fluorescence at final enzymatic incubation time) in a single graphical user interface (GUI) for each 96-well plate, enabling the simultaneous

synchronization and visualization of the CYP3A4 inhibition and aqueous solubility data (Figure 19H).

4.4.6.1 Calculation of IC$_{50}$ values in CYP450 inhibition assays

See section 4.3.5

Assay correlations (r2) were evaluated from best-fit linear regression analysis using log IC$_{50}$ values with Microsoft™ XLFit (version 4.0). General DDI risk binning is based on the criteria of IC$_{50}$<1 μM (high risk), 1 μM > IC$_{50}$ <10 μM (medium risk), or IC$_{50}$>10 μM (low risk).

4.4.6.2 KS limits calculation

As previously described in the CSIVM-KS section, turbidimetric solubility is generally assessed in terms of upper and lower bounds. These two values should be deduced in a straightforward way from the absorbance measurements versus compound concentration curve along with the values from the turbidimetric absorbance background controls (TBKG), which sets the baseline for calculating the two bounds. Intuitively, the curve is flat at lower concentrations and lies at the same level as that of the TBKG controls but it starts to rise at some point when moving towards higher concentration levels. This raising point, or elbow, is the one which defines the region where the lower and upper bounds are found. To determine this point in the curve, the tool combines two different approaches, taking advantage of the information provided by the TBKG wells along with the shape of the curve. For the first approach, the tool calculates a sort of Z score for each compound concentration from their respective raw absorbance data, by subtracting the TBGK median values and adding 3 times their standard deviation [133].

A new data layer is created with this value and, in principle, hopefully, the first point which meets the condition Z score > 0 when moving from lower to higher concentrations will indicate

where the curve elbow is. The addition of 3 times the standard deviation ensures that the system discards the random fluctuations or experimental error from the calculation. In any case, at times there is a greater fluctuation which causes this approach (on its own) to fail in a small percentage of cases because it misinterprets a rising slope as a small maximum. To overcome this limitation, a second approach was introduced that calculates two slopes at any point in the curve, by making the subtraction part of each point with the closest right/left neighborhood (S_0) and also taking into account the nearest right point slope (S_{+1}, slope of nearest point towards the highest concentration). The final criteria for determining where the curve elbow would be to identify the first point to the right that meets the criteria: $Z_{score} > 0; S_0 > 0; S_{+1} > 0$. The system automatically identifies this point (P_0) as the lower bound and the next one (P_{+1}) as the upper bound. All these calculations are made without human intervention at any step.

According to the KS classification bands established by Rogge and Taft [134], compounds can be categorized according to their KS into acceptable KS (>50 µM), marginal solubility (12-50 µM) and unacceptable solubility (<12 µM).

4.4.6.3 Kinetic solubility and CYP450 inhibition data integration

Since the fluorescence and absorbance readings obtained when using NIVA-CYPI-KS, albeit read in the same reader, are stored in different files, an automated tool was developed to unify both readings and incorporate them into the GeneData Screener system for further processing. GeneData Screener application allows the user to assign to every well in a plate as many different values as needed, regardless of whether they are raw or calculated data. Any kind of calculation can be defined in these logical structures called layers. This is one of the most important features which allowed us to integrate data from different evaluations in a single GUI. This facilitates the use of the linked values to perform operations such as flagging, ranking, filtering, masking, etc., on the samples, based on those single values or any other

logical ensemble. In any case, any change in the value of any layer is automatically reflected in the other layers (if any point in the solubility curve is masked, it will also be masked automatically in the CYP3A4 inhibition Dose/Response curve). The linked data are transferred to a corporate database where they can be monitored or used in subsequent experiments.

5 RESULTS and DISCUSSION

5.1 Effect of dual inhibitors on NO oxide production and correlated measurements of hepatic in vitro metabolism

5.1.1 CYP3A4 inhibition and aqueous solubility

Imidazoles derivates are prominent broad-spectrum oral antifungals that have been reported to be extensively metabolized by hepatic-microsomal enzymes to a large number of metabolites, interacting with major CYP450s at very low Ki values [135]. In turn, it has been shown that these drugs are able to inhibit the NO production in 2 different ways. On one hand they inhibit the induction of functionally active NO synthase in cell lines through a mechanism that differs from other known inhibitors of induction including glucocorticoids and actinomycin D which are likely to act via inhibition of gene expression and transcription. On the other hand they are also able to directly inactivate NO synthase by interacting with its heme moiety, inhibiting NO production in both mouse and human cell lines [136, 137]. Analogously, macrolides, a group of antibiotics whose activity is ascribable to the presence of the macrolide ring, have long been recognized from in vitro and in vivo studies to exert immunomodulatory and anti-inflammatory actions, via inactivation of NO production [138]. In turn, some macrolide antibiotics, such as, ERY, RXT and CLT, but not AZT, have also been found to form stable metabolic intermediate complexes with the iron (II) present in the heme group of CYP450 after being metabolized, leading to clinically relevant drug interactions in humans [18][19]. To further characterize the involvement of the CYP450 enzymatic system in immunomodulatory properties of the previously described molecules, we selected representative members of the 2 families of compounds (ketoconazole, miconazole and clotrimazole for the imidazole derivate family, and ERY, RXT, CLT and AZT for the macrolides family) to assess NO production in the LPS stimulated RAW 264.7 macrophages in vitro model. Therefore, taking into consideration that

a loss of biotransformation activity has been observed in cultured cells (RAW 264.7) caused by a decrease in CYP450 transcription in comparison with primary cell cultures (alveolar macrophages) or in vivo experimental systems, a differential response in NO production should be expected for dual inhibitors depending on the experimental model considered [113][139]. Thus, a compound being intensively metabolized by CYP450 should display a higher inhibition potential on NO production in this in vitro model with reduced CYP450 functionality. For contrary, a compound producing active metabolites via CYP450 should show a reduced potential to inhibit NO in comparison with other in vitro models with regular CYP450 functionality. Our results from the LPS stimulated RAW 264.7 macrophages in vitro model showed that the 3 members of the imidazole derivate family displayed moderate to weak inhibition potential on NO production (IC_{50} = 7.20, >10 μM and 7.35 μM, respectively. Table 2), which coincides with previous the results of works using cultured cell line models [140]. The in vivo results reported for related azole compounds (even at higher doses) showed no inhibition of NOS activity, supporting thereby our working hypothesis in which the diminished CYP450 activity in RAW 264.7 cells may have some influence on NO production [141]. In this case, the absence of compound depletion may contribute to the moderate IC_{50} values obtained in comparison with the complete lack of inhibition of NO production observed using an in vivo experimental systems. However and based on their demonstrated ability to interact with the heme moiety, we had expected a more intense potential to inhibit NOS in vitro. Our experiments for the parallel determination of CYP3A4 inhibition using isolated enzymes and aqueous solubility confirmed the strong potential of these compounds to inhibit enzymatic activity (IC_{50} = 0.14-0.0045 μM, Table 2) and their limited solubility (<10 μM, Table 2). The data showed that imidazole derivates exerted their inhibition ability on CYP3A4 in the soluble range, suggesting that their limited solubility (upper solubility limit from 10.35 to 34 μM) could

be related with the moderate ability to inhibit NOS in vitro and even with the lack of in vivo response.

Table 2. Summary of the results obtained in the different in vitro models for the selected compounds

Compound ID	CYP3A4 RI IC$_{50}$ (µM)	CYP3A4 TDI K$_{inac}$ / KI (min-1/µM)	Met. stability T$_{1/2}$ (min)	NO inhibition IC$_{50}$ (µM)	Solubility Range Lower Bound (µM)	Upper Bound (µM)
Miconazole	0.141	N.A.	N.A.	7.35	8.62	34.5
Clotrimazole	4.51E-3	N.A.	N.A.	7.21	2.59	10.3
Ketoconazole	3.32E-2	N.A.	N.A.	>10	2.59	10.3
ERY	3.21	9.45E-2 / 0.15 (6.39E-1)	21.66	>250	>86	>86
RXT	6.41	4.29E-2 / 0.29 (1.47E-2)	38.08	>250	>86	>86
CLT	4.03	3.99E-2 / 2.68 (1.49E-2)	50.59	>62.5	>86	>86
AZT	16.1	8.23E-2 / 7.35 (1.11E-2)	>60	>250	>86	>86
Ciclosporin A	N.A.	N.A.	N.A.	1.16	N.A.	N.A.
Dexamethasone	N.A.	N.A.	N.A.	7.21E-3	N.A.	N.A.
Verapamil	N.A.	0.121 / 0.791	N.A.	N.A.	N.A.	N.A.

RI: Reversible inhibition; TDI:Time dependant inhibition; T$_{1/2}$: Half-life, K$_{inac}$: Constant of inactivation; KI: Constant of inhibition. N.A. Not Applicable

Solubility is one of the important parameters to achieve the desired concentration of drug in systemic circulation for desired pharmacological response. The poor aqueous solubility is one of the mainr causes of low systemic exposure and, consequently, lack of in vivo activity [142]. In fact, low compound solubility might lead to erratic in vitro results, including discrepancies between isolated enzyme assays and more complex models such as microsomes or whole cell-based assays [143]. In this work, we have conducted, an extensive study of the effect of low solubility on the inhibition potential considering in vitro models of different complexity (see sections 2.3, 4.3 and 5.3). As a result, we concluded that compounds with low solubility, tended to yield higher IC$_{50}$ values in complex in vitro models due to nonspecific binding to lipophilic components not present in isolated enzyme incubations [144]. Therefore, it is reasonable to expect that the actual citoplasmatic concentration of imidazole derivatives in RAW 264.7 cells might be much lower than anticipated, and hence, might show artificially low inhibition of NO production. In fact, the IC$_{50}$ values (0.14 µM) obtained by other investigators for ketoconazole

on CYP3A4 activity using cryopreserved hepatocytes were 4-fold higher than those obtained in our experiment with recombinant CYP3A4 enzymes (0.033 µM)[145].

In the case of macrolides, other investigators have demonstrated that these compounds (ERY, RXT and CLT) could inhibit the production of NO in either primary cultures of stimulated rat pulmonary alveolar macrophages or stimulated animal models by down-regulation of NO synthase gene expression [42][32][20]. However, the therapeutic mode of action and the biotransformation of macrolides are not well understood and many questions remain unanswered, such as the role of NOS inhibition or the involvement of their main metabolites in the therapeutic response. Our results for macrolides in LPS stimulated RAW 264.7 cells in contrast with those from primary cultures, showed IC_{50} values higher that the highest noncitotoxic dose (Table 2). Only AZT and CLT had the ability to weakly inhibit the production of NO at the highest noncitotoxic dose (53.82% of control at 250 µM and 85.2% at 62.5 µM, respectively, as shown in Figure 20 right). This lack of potential activity to inhibit NO production in comparison with other experimental systems with drug metabolic competence also supported our previous working hypothesis and points towards the critical role of macrolides biotransformation via CYP450 in the inactivation of NO production. In order to check the extent of these interactions, we tested the CYP3A4 inhibitory potency and the solubility range of these macrolide members using NIVA (Table 2). As a result, the CYP3A4 activity was inhibited but to a lesser extent than with imidazole derivatives. Specifically ERY, ROX and CLT displayed, among them, very similar IC_{50} values, in the range of moderate inhibitors (from 1 to 10 µM, table 2) whereas AZT behaved as a weak inhibitor ($IC_{50} > 10$ µM, Table 2). These data confirm the differential ability of these compounds to inhibit CYP3A4 activity in a concentration dependent manner, which interestingly correlates reversely with their potential to inhibit NO production in LPS stimulated RAW 264.7 cells (Figure 20, left).

In terms of solubility, macrolide compounds presented solubility limit values >86 µM (Table 2) which suppress the effect of solubility issues in the observed results.

Figure 20. Dose-dependent effects of macrolide antibiotics.
Left: Release of NO from LPS-stimulated murine macrophages. The cells were incubated for 24 hours with various concentrations of ERY **(a)**, RXT **(b)**, CLT **(c)** and AZT **(d)**. Values represent the percentage of control of NO formation in the culture medium after addition of LPS The maximum dose in each case corresponds to the highest concentration yielding a cell cell viability ≥ 80% (i.e 250 µM for ERY, RXT and AZT and 62.5 µM. for CLT. Data are presented as mean. (n=3 for each point.)
Right: Human in vitro liver microsome stabilities (Data are means ± SEM; n = 3 for each time point) for ERY **(e)**, RXT **(f)**, CLT **(g)**, and AZT **(h)**.
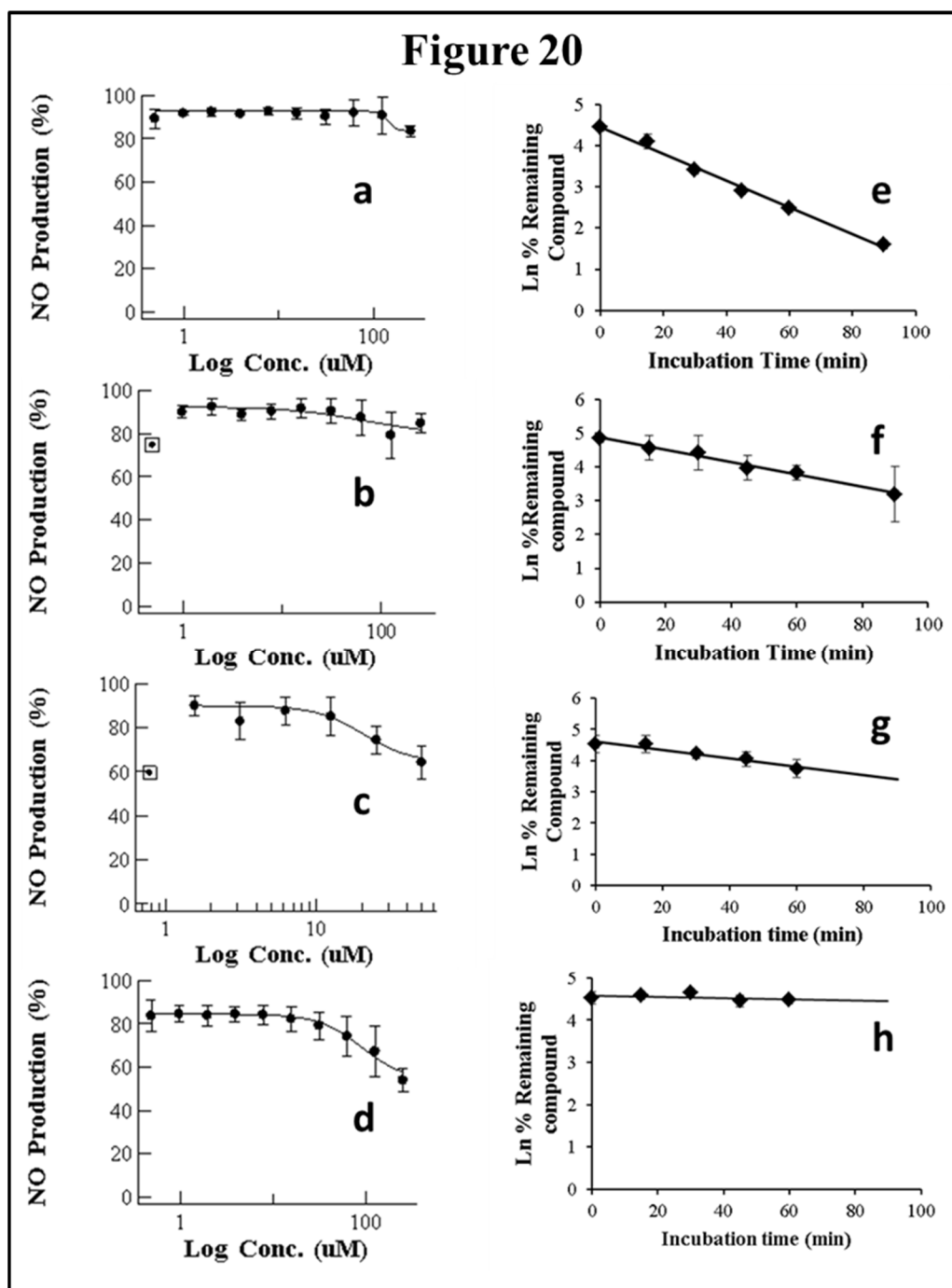
5.1.2 In vitro kinetics of CYP3A4 inhibition by macrolides

Macrolide antibiotics have been previously described as mechanism-based inactivators of CYP3A enzymes that exhibit varying degrees of inhibitory potency [146]. Mechanism-based inhibition often involves the metabolism of an inhibitor by CYP3A4 to a reactive metabolite, which inactivates the catalyzing enzyme in a concentration and time-dependent manner. The interaction between the inactivating species and the enzyme can either be covalent or non-covalent, involving binding to protein or heme moiety, respectively [124]. In order to establish the in vitro macrolide kinetic constants of CYP3A inhibition, these compounds (ERY, CLT, RXT and AZT) were estimated by varying the time of pre-incubation and the test compound concentrations (Figure 21). The two main kinetic parameters that characterize time-dependent inhibition (TDI) interactions are the maximal inactivation rate constant (K_{inact}) and the inhibitor concentration leading to 50% of enzyme inactivation (KI). The K_{inact}/KI ratio is commonly taken as an indicator of the in vitro potency of a mechanism-based inhibitor. The kinetic constants derived from the inactivation experiments are presented in Table 2. K_{inact} and KI values were in the range of 0.0399 to 0.0945 min−1 and of 0.146 to 7.349 μM, respectively, indicating that all 4 macrolides inhibited in a time dependent manner, the BFC conversion into 7-HFC in CYP3A4 human recombinant microsomes with an inactivation potency (K_{inact}/KI ratio) in the following order: ERY > RXT > CLT > AZT. Therefore, for these macrolide antibiotics, CYP3A4 is responsible for the production of active metabolites which might be central to inhibit NO production.
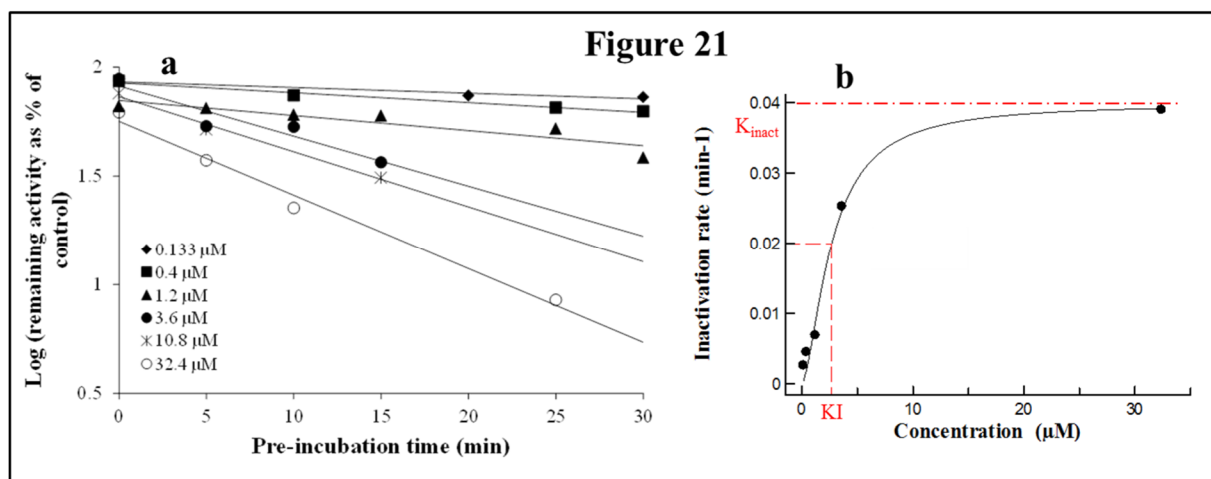
Figure 21. The macrolides CYP3A4 time dependent inhibition
Compounds were evaluated by pre-incubating a range of 6 test compound concentrations selected so as to achieve a scale from no inactivation to maximal inactivation, for 6 differing pre-incubation times (including 0 min) with hrCYP3A4 and NADPH. Following the pre-incubation, an aliquot of the pre-incubation was diluted with buffer containing a specific cytochrome P450 probe substrate (7-HFC) and NADPH for a specific incubation time (data are singletons for each time and concentration point). **(a)** Inactivation plot (natural logarithm of the % remaining activity versus pre-incubation time) for CLT. The least-squares regression analysis enables determining the negative slope of the logarithm of the % remaining activity versus pre-incubation time. **(b)** The non-linear regression analysis of the negative slopes against inhibitor concentration enables K_{inact} and KI to be calculated. The K_{inact} is the maximal rate of enzyme inactivation at a saturating concentration of inhibitor, and KI is the concentration of inhibitor which gives half the maximal rate of inactivation. Similar time- and concentration-dependent inhibition profiles were observed for ERY, RXT and AZT (data not shown).

Hence, important conclusions can be drawn: First, although ERY, RXT and CLT achieved very similar IC_{50} values from CYP3A4 reversible inhibition, we can observe a clear shift in K_{inact}/KI ratio from ERY and RXT (0.64 and 0.14 $min^{-1}/\mu M$, respectively) to CLT and AZT (0.014 and 0.010 $min^{-1}/\mu M$, respectively). These results indicate that product metabolites from ERY and RXT are much more potent inhibitors than those produced from CLT and AZT, which is in line with the differential CYP3A4 inhibition potency observed for the macrolides in the clinic [124].

Second, it makes sense to consider that in other experimental systems with full metabolic competence, these product metabolites might also bind irreversibly to NOS causing its

inactivation. This idea is further supported by other works which demonstrated the ability of main metabolites of RXT and other macrolide antibiotics to form inhibitory P450-Fe2+-complexes [124][146].

Third, the inability of RAW 264.7 cells to produce these active metabolites might partially explain the lack of NO inhibition observed for macrolides in this cell line.

5.1.3 Macrolide in vitro metabolic stability

The HLM incubations represent an accepted model for understanding the metabolism of pharmacologically active compounds including the quantitative and qualitative assessment of metabolites [147]. This approach enables assessing the in vitro biotransformation rate (metabolic stability) of parental compounds as well as the profile of the main breakdown products by utilizing high resolution mass spectrometry (HRMS) since structural elucidation can be achieved from both full scan mass spectrometry (MS) of precursor and collision-induced dissociation (CID). The in vitro metabolic stability, expressed as intrinsic half-life ($T_{1/2}$) of selected macrolide antibiotics, was investigated in HLM. Following incubation, all 4 macrolides displayed different $T_{1/2}$ values in the range of 21 to >60 min. This value increased in the order ERY <RXT < CLT < AZT (Table 2 and Figure 20, right). These results indicate that the biotransformation rate of ERY and, consequently, the metabolite formation rate is about double that of RXT and CLT, while non-detectable biotransformation was observed for AZT at the referred incubation times. Pointing in the same direction as TDI results, these data also showed that compounds undergoing more intense biotransformation (ERY and RXT) did not affect NO production in RAW 267.4 cell lines (Figure 20, left) while those displaying higher microsomal stability (CLT and AZT) exerted a certain degree of inactivation in NO production (Figure 20, right). This fact suggests that the reduced expression CYP450 isoform

and the subsequent lack of reactive metabolites might be the cause of the inability of ERY and RXT to inhibit NO production in RAW 267.4 cell lines.

5.1.4 RXT metabolite profile in HLM incubations.

Although a larger quantity and distribution of metabolites is expected for ERY based on our stability and TDI results, the more abundant previous information relating to in vivo and in vitro metabolism as well as the increasing interest aroused by RXT's anti-inflammatory and immunomodulatory properties in clinical practice, led us to select this macrolide to explore its in vitro metabolic profile in detail [138][18]. The characterization of the in vitro metabolism of RXT was done using the LC-HRMS data obtained from the metabolic stability incubations using HLM. As a result, in addition to unchanged RXT, a total of 5 stable potential metabolites were found (Table 3 and Figure 22 a).

Table 3. Summary of key LC/HRMS data of in vitro metabolites after RXT incubation with HLM

Peak ID	Description	Formula	m/z	Mass error (ppm)	R.T. (min)	Peak Area	Area (%)	Score (%)
	RXT (Parent)	$C_{41}H_{76}N_2O_{15}$	837.5331	1.5	4.12	7.78E+05	65	93.9
M1	ERY oxime	$C_{37}H_{68}N_2O_{13}$	749.4805	1.5	3.64	2.37E+05	20	93.7
M2	Demethylatied + Hydroxylated RXT	$C_{40}H_{74}N_2O_{16}$	839.5118	0.8	3.52	8.74E+04	7	86.1
M3	N-mono-demethylated RXT	$C_{40}H_{74}N_2O_{15}$	823.5169	0.9	3.68	3.57E+04	3	95.5
M4	Mono hydroxylated RXT	$C_{41}H_{76}N_2O_{16}$	853.527	0.3	3.74	2.46E+04	2	79.3
M5	Demethylated ERY oxime	$C_{36}H_{66}N_2O_{13}$	735.4638	0.1	3.56	2.82E+04	2	81.5
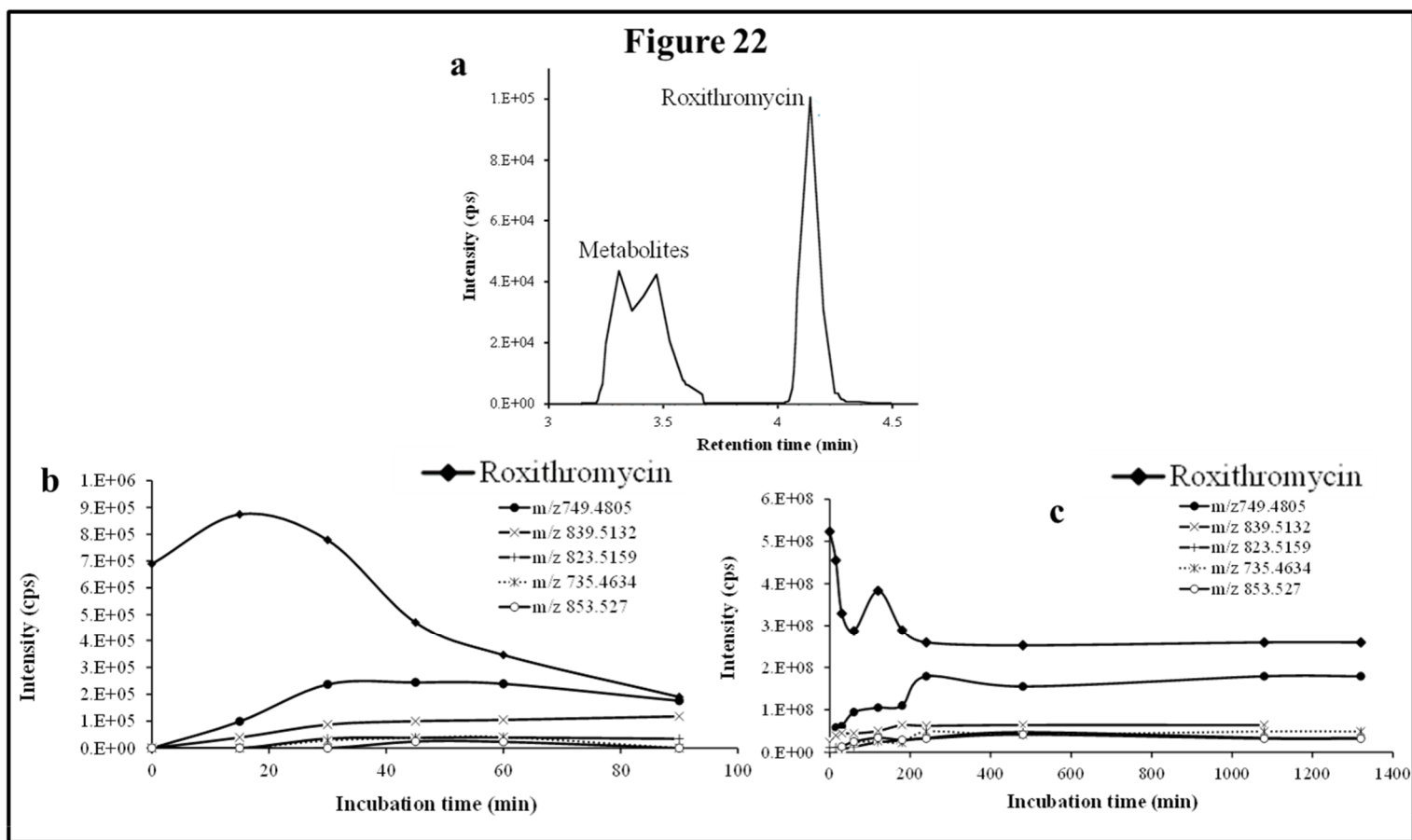
Figure 22. Time course of RXT incubations with HLM.
(a): Representative combined extracted ion chromatogram (XIC) of RXT and its metabolites at 30 min incubation time. The main peak at 4.12 min was identified as RXT by direct comparison with the authentic standard. The rest of peaks correspond to RXT metabolites, which were not observed in the control samples. (b): Time course of RXT in small scale incubation. (c): Time course of RXT in large scale incubation (data are singletons for each incubation time).

Besides the metabolites of RXT identified by other investigators [126] (i.e. ERY oxime at m/z 749, demethylated ERY oxime at m/z 735 and N-mono-demethylated RXT at m/z 823), we identified another 2 stable biotransformation products (hydroxylated RXT at m/z 853 and demethylated and hydroxylated RXT at m/z 839). The molecular structure elucidation of the potential metabolites was carried out by fragment interpretation of CID spectral data with the assistance of chromatographic behaviors and basic rules of drug metabolism and is discussed in the following sections. The relative content of each metabolite was estimated with reference to RXT on the basis of peak area of their $[M+H]^+$ ion, selected from ion monitoring chromatograms. According to this criteria, metabolite M1 (ERY oxime at m/z 749) is the main biotransformation product (20%) of RXT in HLM incubations. The relative contents for the rest of metabolites (M2-M5) ranged from 7 to 2% (Table 3) of RXT peak area and are shown in Figure 22b. Although not shown in this work, we also investigated the metabolic profile of the rest of macrolide members and these results will be presented shortly in a new publication. However, we will briefly mention that for ERY and CLT the main biotransformations consisted of demethylation and oxidations in the deoxy sugar moieties while no modifications were observed in the macrocyclic lactone ring. In contrast, for RXT, as stated above, the main biotransformation took place in the N-oxime ether side chain attached to the lactone ring, rendering an oxime functional group. This metabolism feature leads to a higher exposition of imime moiety (carbon–nitrogen double bond) which is also observed in imidazole derivates and suggests that this biotransformation may have a key role in differential clinical effects observed for RXT [138].

5.1.5 Isolation and structural elucidation of roxithromycin metabolites

Establishing the pharmacological properties of metabolites from active compounds has traditionally been a topic of great interest of the pharmaceutical industry. However, obtaining the standards of metabolites to be used in pharmacological assays can be difficult and therefore, expensive to chemically synthesize. As an alternative approach, the biological generation and isolation of metabolites from source material obtained from in vivo or in vitro studies has proven to be useful for the production of isolates in the nanomole range [147, 148]. In order to isolate the main microsomal metabolites of RXT with the objective of assessing their involvement in NO modulation, we carry out a large scale incubation, as described in Methods and Materials section. The RXT metabolite profiling was monitored at different incubation times and the same main metabolites with very similar formation rates to those of small scale incubations were obtained (Figure 22c). After SPE and LLE for isolation of the main RXT metabolites, semi-preparative HPLC chromatography was used to obtain fractions containing RXT metabolites. After several steps of isolation and purification guided by the XIC of previously observed metabolites, we achieved 1 mg of a highly enriched fraction (at elution time of 12.5 min) in 2 main metabolic products (M1&M5, Figure 23a).
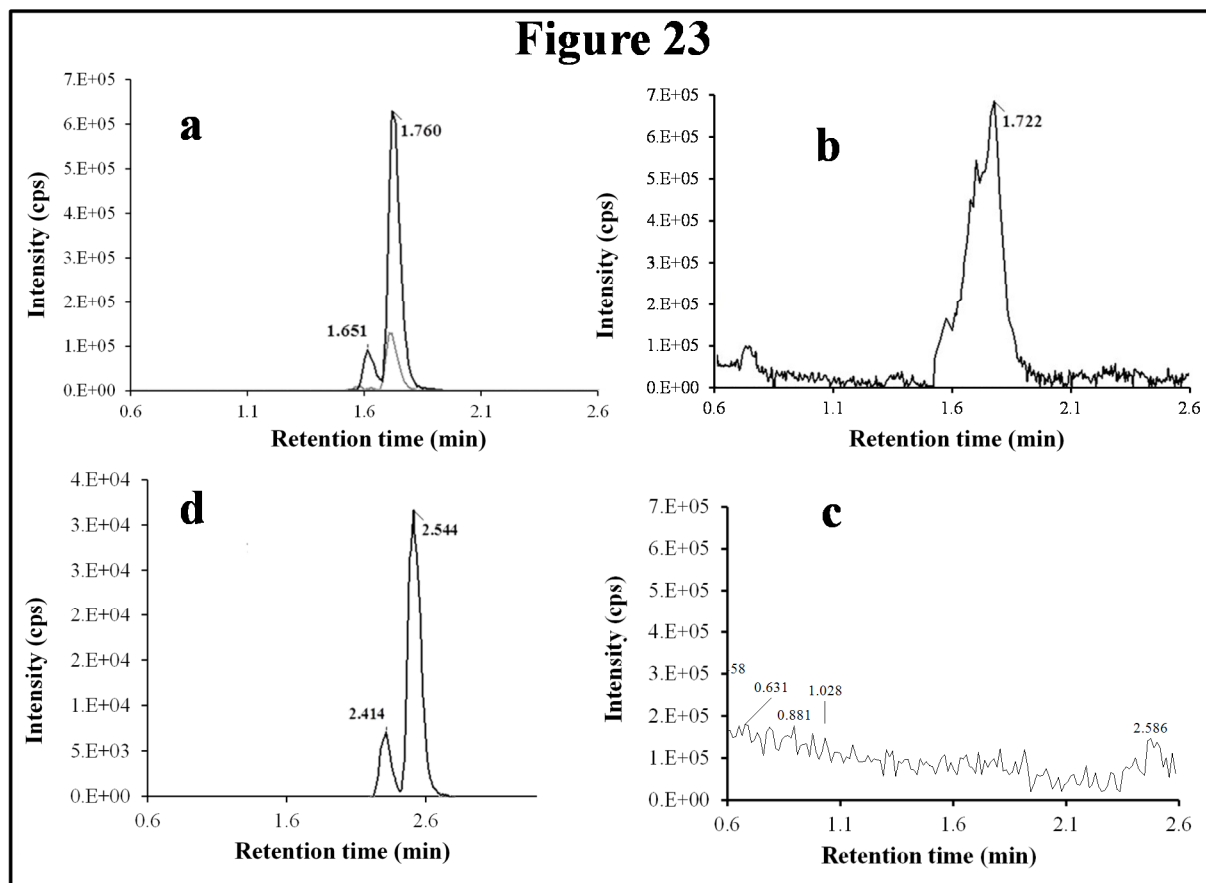
Figure 23

5.1.5.1 Figure 23. LC-HRMS chromatograms of RXT metabolite isolation using fast gradient separation.

(a) Extracted ion chromatogram (XIC) for expected RXT metabolites showed 3 main peaks: 2 peaks at m/z 749.4805 (in black color line) at 1.65 and 1.76 min corresponding to (Z)-ERY-oxime and (E)-ERY-oxime (M1), respectively and 1 peak at m/z 735.4638 (in light grey color line) and 1.76 min, corresponding to metabolite M5. Although very weakly the corresponding (Z) isomer was also observed at 1.65 min. **(b)** TIC (50-1000 Da) of semi-preparative fraction enriched (at elution time 12.5) in main RXT metabolites (M1&M5). **(c)** Total ion chromatogram (TIC) (50-1000 Da) of semi-preparative fraction from blank incubation at 12.5 min elution time. **(d)** XIC of RXT reference substance showed 2 peak at m/z 837.5331 corresponding to RXT (2.54 min) and its Z-stereoisomer (2.41 min), which were not observed in the metabolite enriched fraction, ensuring the absence of parental drug.

As previously described, purity was assessed by comparison of the detector response of the metabolites in the incubation matrix to the response of a blank incubation matrix at the same elution time (Figure 23b and 6c) [43]. The assessment by total ion chromatogram (TIC) delivered a purity of 93% for the RXT metabolites contained in that fraction, which is in line

with the general purity target for library compounds for activity screening [149]. The identification of these metabolites was achieved by comparative fragment ion interpretation with parent drug RXT (chemically designated as (*E*)-ERY-9-[*O*-[(2-methoxyethoxy)methyl]oxime]) reference substance, and previous results from other investigators using LC-MS and NMR [126]. Briefly, full scan high resolution mass spectra of RXT reference substance provided 2 chromatographic peaks with a 5-fold intensity ratio, at identical m/z 837 but with different retention times (2.41 and 2.54min, see Figure 23d). Both chromatographic peaks displayed the same MS/MS fragment ions at m/z 679, 558, 540, and 158 (Figure 24a), suggesting they were stereoisomers with tertiary amino groups in their structure. They were thus identified as RXT and its Z-stereoisomer. For metabolite M1, we also observed 2 chromatographic peaks at retention times of 1.65 and 1.76 min, displaying a 7-fold intensity ratio (Figure 23a). They also showed identical protonated molecular ions [M+H]$^+$ at m/z 749 as well as identical MS/MS fragment ions, indicating they were also stereoisomers. Their protonated molecular ions were 88 Da lower (characteristic loss of the alkylether side chain) than the one of the parent drug, indicating they were *O*-dealkylated metabolites. The MS/MS spectra of both peaks (parent ion at *m/z* 749) gave fragment ions at m/z 591, 434 and 158 Da (Figure 24b). The ion at m/z 591was 158 Da lower (loss of cladinose) than that of one the precursor ion (m/z 749), whereas the ion at m/z 434 was subsequently 157 Da lower (loss of desosamine) than the former ion. Based on these data, they were identified as (*Z*)- and (*E*)-ERY-oxime, respectively. For metabolite M5, the above described (Z) and (E) isomers distribution was also observed at 1.65 and 1.76 min (Figure 23a).
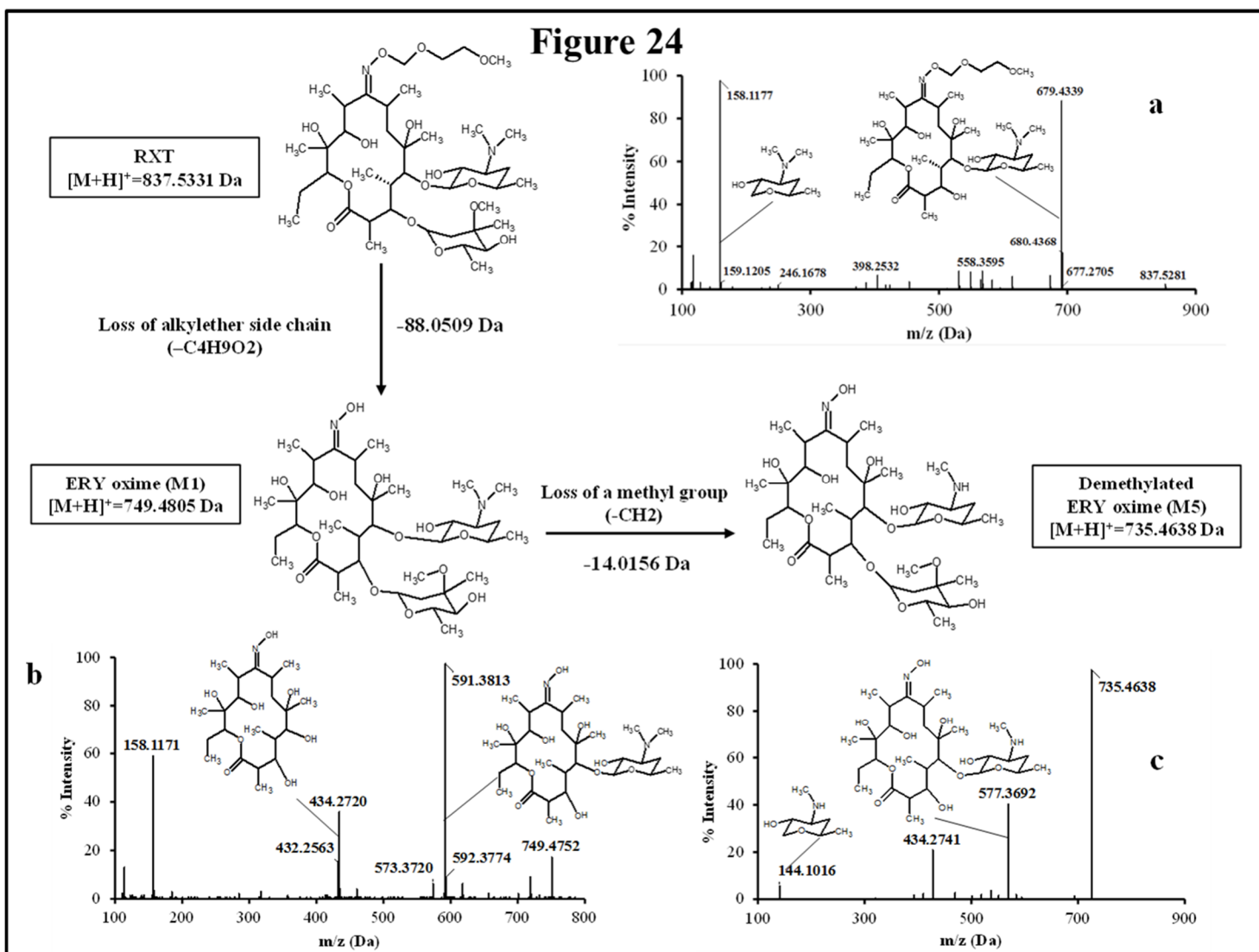
Figure 24. Proposed biotransformation route from RXT to metabolites to ERY oxime (M1) and Demethylated ERY oxime in HLM incubations.

The loss of 88 Da from RXT at $[M+H]^+=837.5331$ to M1 at $[M+H]^+=749.4805$ Da is fully compatible with the loss of the alkylether side chain. The fragment ion analysis of MS/MS spectrum from RXT **(a)** and M1 **(b)** revealed an analog loss of 88 Da from m/z =679 Da in RXT to m/z=591 Da in M1, confirming the site of alkylether chain at the lactone ring. The ion at m/z 591 was 158 Da lower (loss of cladinose) than the precursor ion (m/z 749), whereas the ion at m/z 434 was subsequently 157 Da lower (loss of desosamine) than the former ion. Based on these data, M1 was identified as ERY-oxime. The difference of 14 Da between M1 at $[M+H]^+=749.4805$ Da and M5 at $[M+H]^+=735.4638$ Da indicated the loss of a methyl group in the biotransformation. The MS/MS spectra of m/z 735 Da **(c)** gave fragment ions at m/z 577, 434 and 144 Da. The ions at m/z 434 Da indicated that the lactone ring was unaltered. The loss of the cladinose moiety produced the peak at m/z 577 Da, suggesting that the demethylation took place at the desosamine wich was confirmed by the peak at m/z 144 Da. Based on these data M5 was identified as demethylated ERY oxime.

Their protonated molecular ions (m/z 735) were 102 Da lower than those of the parent drug, indicating a cleavage of the alkylether side chain (88 Da), followed by the loss of a methyl group. The MS/MS spectra of m/z 735 gave ions at m/z 577, 434 and 144 (Figure 24c). The diagnostic ions at m/z 434 indicated that the 14-member lactone ring nucleus was unaltered. The loss of the cladinose moiety produced the peak at m/z 577, suggesting that the demethylation took place at the desosamine which was confirmed by the peak at m/z 144 (Figure 24c). Based on these data, these peaks were identified as *N*-monodemethylated derivatives of (*Z*)- and (*E*)-ERY-oxime, respectively. The stereochemical aspects of RXT and its metabolites have been extensively described in previous works using LC-MS in combination with NMR and our results are consistent with them [126]. Therefore, 2 major RXT metabolites (M1-M5) and their corresponding (Z)- isomers were isolated from the rest of the components of microsomal incubations in a semi-preparative HPLC fraction which yielded a dry weight of 1 mg. Since our main objective was to clarify the implication of RXT metabolites in inactivation of NO production and not activity ascription, we considered that isolation of single metabolites was not critical, the separation of the parent compound (RXT) and the main matrix components being much more important. Regarding the relative composition we can conclude from XICs that metabolites M1and M5 represent 78% (68 and 10% for (E) and (Z)-isomers respectively) and 15% (14 and 1% for (E) and (Z)-isomers, respectively) of the total dry amount, respectively. It is very interesting to note that the (E)-isomer of RXT was reported to be the more potent of the two geometric forms in antibacterial tests and consequently, RXT in clinical use exclusively contains this isomer [126]. Hence, we can assume that the therapeutic effects observed are due to the (E) isomers of either RXT or its metabolites.

5.1.6 Biological evaluation of isolated RXT metabolites

Considering the previously reported RXT IC_{50} value (5 µg/mL) in NO production using primary cultures of alveolar rat macrophages, we dissolved the dry amount (1mg) of RXT metabolites (M1, M5 and the corresponding geometric isomers) in 0.133 mL of pure DMSO [150, 151]. After two-fold serial dilution in DMSO, the metabolite mixture was 1/5 diluted in water in order to minimize the DMSO content, and it was finally tested (max dose 35 µg/mL) in triplicate using the LPS stimulated RAW 274.6 macrophage model to evaluate its ability to inhibit NO production. The mixture of RXT metabolites had the ability to inhibit NO production to 50% at a concentration of 31.6 µg/mL (Figure 25) while inactivation of NO production was not observed for RXT from 0.488 to 250 µM (Figure 20b).

Figure 25. Dose-dependent effects of RXT metabolites (M1 & M5) on the release of NO from RAW 264.7 mouse macrophages stimulated with LPS.
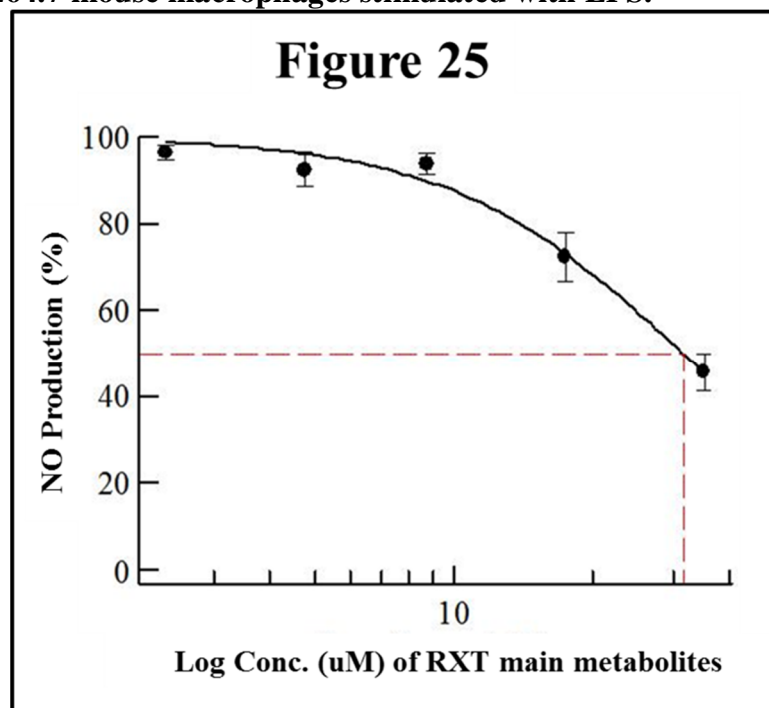
Data are means ± SEM; n = 3 for each point

Considering relative composition of the RXT metabolite mixture and the isomer activity ascription previously discussed, it is possible to infer an IC_{50} values of 23.07 and 4.74 μg/mL for M1 and M5, respectively, for inactivation of NO production. These values are in line with the previously reported for RXT, IC_{50} value (5 μg/mL) in NO production using primary cultures of alveolar rat macrophages.

5.1.7   Discussion about the involvement of CYP450 in NO production

Based on these results we can assert that the metabolites of RXT (M1&M5) demonstrated significant activity as inhibitors of NO production, affording better activity than the parent compound in LPS stimulated RAW 274.6 macrophage cell lines. It is therefore apparent that CYP450 metabolites may represent an attractive innovative way to search for new structures with enhanced immunomodulatory activity.

As a general mechanism of in vivo inhibition, we propose two compatible approaches. First, as described, alveolar macrophages represent clear evidence of co-expression of these enzymes (CYP450 and NOS), and this can be considered to be common to other cell types in primary sites of exposure to chemical toxicants such as hepatic macrophages which present an expression pattern of cytochromes P450 specifically adapted for their major role in the protection of the organism [115, 152, 153]. Therefore, it makes sense to expect that compound biotransformation and NOS inhibition might take place in the same cell. Second, hepatic metabolites might be cleared to plasma and distributed systemicaly to immune system cells and epithelial tissues where it would inhibit NOS activity.

5.2 Development and validation of a HTS platform for evaluation of immunomodulatory activity

5.2.1 Optimization of immunomodulatory activity in vitro assays in a 96-well format

The objective was to optimize the experimental model of NO production in RAW 264.7 mouse macrophages in response to LPS stimulation for HTS in a 96-well format. The influence of cell density, LPS concentration, LPS stimulation duration and culture medium volume on NO production was investigated. As a result, the macrophage density and the LPS concentration were identified as the main factors affecting LPS-stimulated NO production in mouse macrophages. The density of macrophages produced an optimal effect on NO production at 1×10^5 cells/mL in a volume of 200 µL in each well (20×10^3 cells/well) of a 96-well plate (Figure 9A). At an LPS concentration below 200 ng/mL, NO production increased proportionally with the increment of LPS concentration (P<0.001), but the NO production did not perceptibly increase at LPS concentrations beyond 200 ng/mL (Figure 9B). Moreover NO production did not significantly increase with the prolongation of LPS stimulation (Figure 9C). The NO content in the culture supernatant was associated with the volume of the medium, and the highest level occurred in a system volume of 200 µL (data not shown). In summary, optimal results were obtained with a macrophage density of 1×10^5 cells/ml (20×10^3 cells per well), an LPS concentration of 150 ng/mL, an LPS stimulation duration of 24 h, and a culture medium volume of 200 µL. The feasibility of the model was also confirmed with specific anti-inflammatory drugs. Reference inhibitors of NO production such as dexamethasone (IC_{50}=0.09 µM), cortisol (IC_{50}=0.17µM) and cyclosporine A (IC_{50}=1.16 µM), all significantly inhibited LPS-stimulated production of NO in RAW 264.7 cell line [154–156].

Similarly, the influence of cell density, IL-1β concentration, IL-1β stimulation duration and culture medium volume on IL-8 production was investigated in the Caco-2 in vitro model. Cell

density and IL-1β concentration were identified as the main factors affecting IL-8 production in Caco-2 cells. Optimal results can be obtained with a cell density of 1×10^5 cells/mL (20×10^3 cells per well), IL-1β concentration of 50 pg/mL, IL-1β stimulation duration of 24 h, and a culture medium volume of 200 μL (Fig. 26D, E & F).
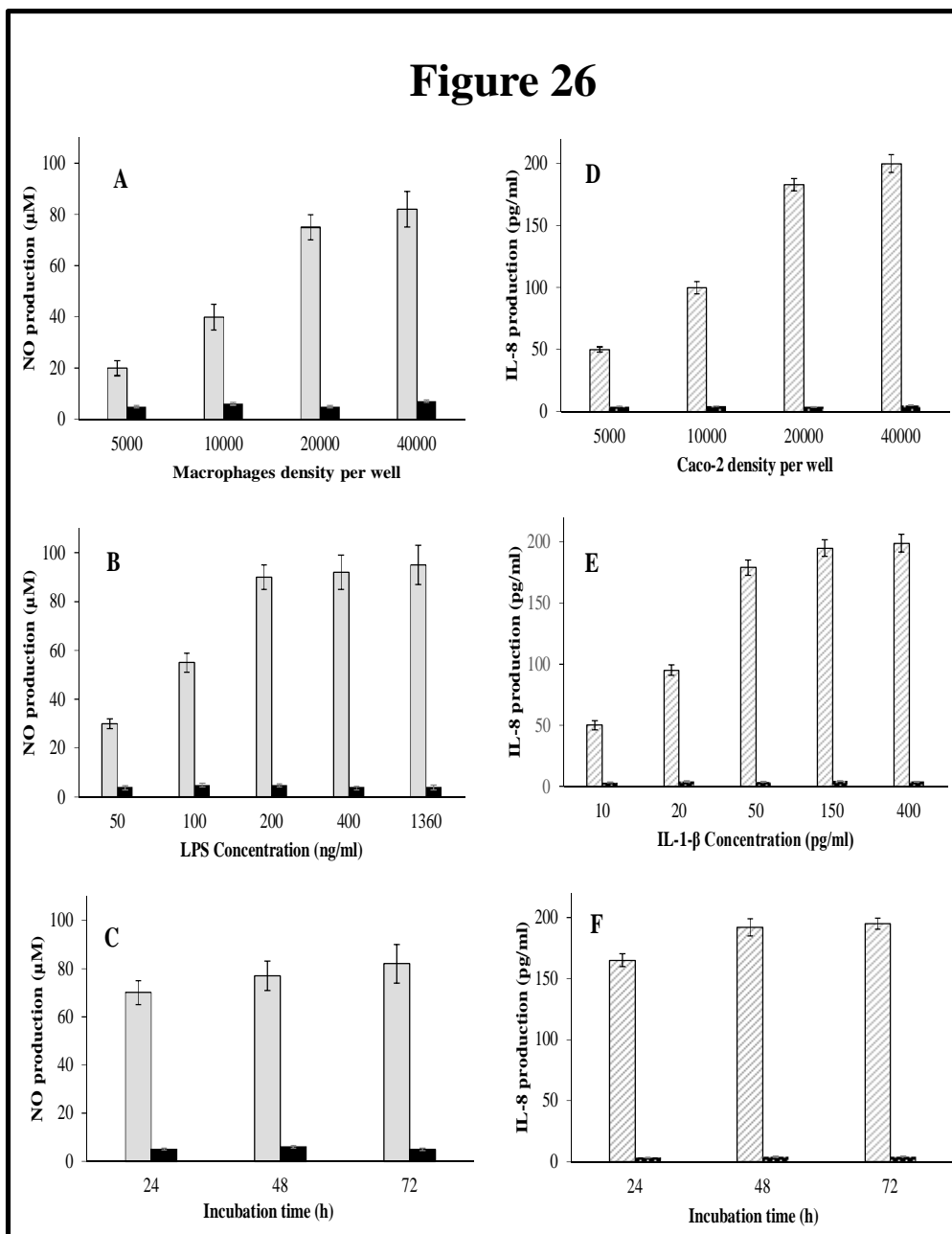
Figure 26. Assay optimization.
(Grey solid bars: LPS stimulated RAW 264.7 cells. Black solid bars: Non-LPS stimulated RAW 264.7 cells. Grey striped bars: IL-1β stimulated Caco-2 cells. White dotted black bars: Non-IL-1β stimulated Caco-2 cells). (A) Effect of macrophage density on NO production (Mean ± SD, n=5). (B) Effect of LPS concentration on NO production (Mean ± SD, n=5). (C) Effect of LPS stimulation duration on NO production (Mean ± SD, n=5). (D) Effect of Caco-2 density on IL-8 production (Mean ± SD, n=5). (E) Effect of IL-1β concentration on IL-8 production (Mean ± SD, n=5). (F) Effect of IL-1β stimulation on IL-8 production (Mean ± SD, n=5).

To determine the optimal extract concentration for obtaining a reasonable hit rate, different extract dilutions were tested for each in vitro model. Other important factors considered when establishing the optimum extract concentrations were that (a) the crude extracts to be tested were prepared in 20% DMSO and that cytotoxic concentrations of this solvent should be avoided; and (b) a hit rate of about 1–5% is desirable, a hit being defined as an extract that, at a given dilution, exhibits an inhibition of NO production ≥80%. Using the stated guidelines, dilutions of 1/40 (from $2 \times$ WBE) were chosen for both assays. The quality and reproducibility of whole cell–based assays were ascertained by RZ' factor calculations [133]. The mean RZ' factors obtained for IL-8 regulation in IL-1β stimulated Caco-2 cells, and NO assays, were 0.83 and 0.87, respectively, indicating that the assays were appropriate for HTS format (Figure. 27A).
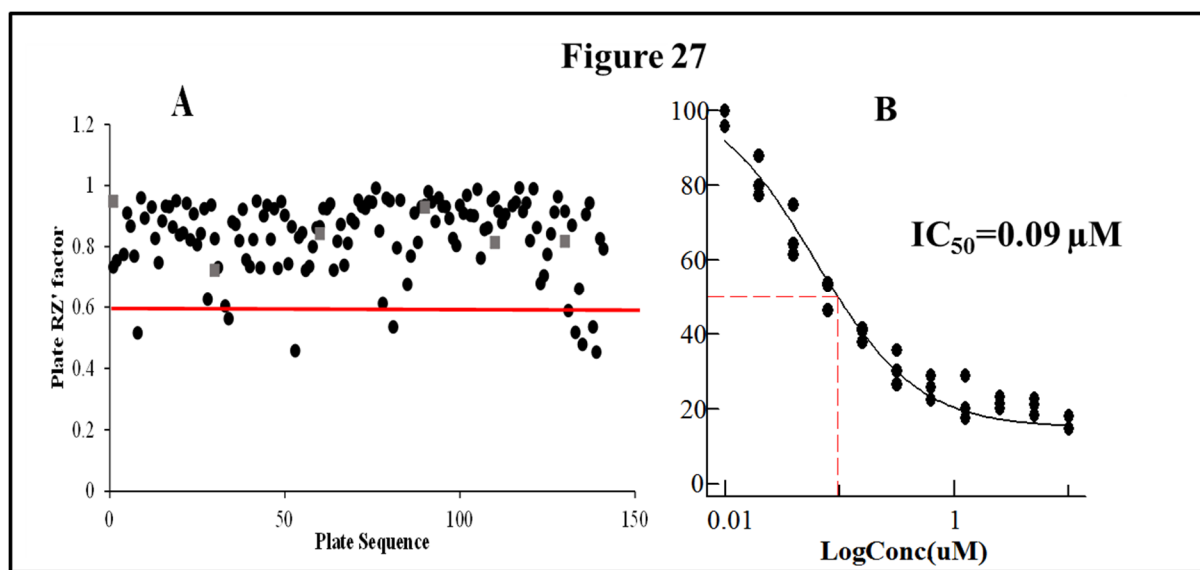
Figure 27. Quality control (QC) in high throughput screening.
To assess the quality of screening data in the screening campaign, each 96-well plate contained a number of control wells (4 positive and 4 negative control wells) which were used to calculate of QC parameters (RZ' factor and IC_{50} values of pharmacological standards). **(A)** RZ' factor for NO and IL-8 assays are displayed in black circles and gray squares respectively. **(B)** Dose response curve of reference inhibitor, dexamethasone in NO assay (data are triplicates for each concentration point).

Although an assay with an RZ' factor above 0.4 is generally considered appropriately robust for compound screening, we preferred to work with an RZ' factor ≥ 0.6 [157]. Plates that generated an RZ' factor <0.6 were rescreened. Additionally, the dose response curves of pharmacological standards such as dexamethasone (Figure 27B), among others, were periodically monitored to assess the variance in the assay. Assay plates were rescreened if these IC_{50} values fell outside predefined limits ($\pm$ 3-fold IC_{50} value) [158].

5.2.2   Screening Campaigns and Hit Identification

From the primary screening of 5,976 non-cytotoxic microbial extracts from the MEDINA microbial extract collection (general workflow and screening process shown in Figure 18 and Table 4, respectively), 79 extracts (1.32%) were initially identified as hits. We re-assessed the activities of the selected extracts in triplicate by cherry-picking, and 34 extracts were confirmed as NO inhibition hits. Next, we used dose response experiments to investigate the extract potency in order to select only those exhibiting at least 70% of NO inhibition at the initial extract dilution (Figure 28A). Using this criterion, 14 inhibitor extracts were selected as hits for LC-MS de-replication. Results showed that none of them obtained a positive identification in the spectral metabolite data base. Within these extracts, those showing steeper dose–response curve slopes (12 extracts) were selected for confirmation of immunomodulatory activity in the secondary screening assay. In these results 4 extracts out of 12 showed inhibition of IL-8 production $\geq 60\%$ at the initial extract dilution (Figure 28B) and cell viability $\geq 75\%$ and they were selected for medium scale up re-growths.

Table 4. Number of Extracts Identified as Hits at Different Stages of the Screening Process.

	Number of Active Extracts Selected at Each Stage (%)[a]
Primary high-throughput screening	79 (1.3)
Cherry-picking for confirmation	34 (0.6)
Dose–response curves for IC$_{50}$ calculation	14 (0.2)
LC-MS de-replication	14 (0.2)
Secondary screening	12 (0.2)
Prioritized for re-growths in 100 mL volume	4 (0.07)
Activity confirmation after 100 mL re-growths	**2 (0.035)**
Bioassay-guided fractionation	**2 (0.035)**
LC-HRMS & NMR molecular identification	**1(0.017)**
Large scale-up growths & bioassay-guided purification	**1(0.017)**

Summary of deconvolution workflow: From the primary screening of 5,976 microbial extracts (Fig. 18A), 79 extracts were initially identified as hits (inhibition of NO production ≥80% and cell viability ≥75%) and 34 extracts out of these 79 confirmed these activity values in triplicate by cherry-picking (Fig 18B). Next, these 34 confirmed extracts were investigated in dose response experiments for potency determination in NO assay (Fig. 18C). As a result, 14 extracts exhibited at least 70% NO inhibition at the initial extract dilution (Fig. 28A) and they were subjected to LC-MS de-replication (Fig. 18D). As a result, none of them obtained a positive identification in the spectral metabolite data base. Within these extracts, those showing steeper dose–response curve slopes (12 extracts) were selected for confirmation of immunomodulatory activity in the secondary screening assay (Fig. 18E). As a result 4 extracts out of 12 met the selection criteria (inhibition of IL-8 production ≥60% and cell viability ≥75% at the initial extract dilution, Fig. 28B) for prioritization to medium scale up re-growth. The specific immunomodulatory activities were confirmed in 2 of the re-growths (Fig.18F) and they were consequently subjected to bioassay-guided fractionation (Fig. 18G). The corresponding active fractions were analyzed by LC-HRMS & NMR (Fig. 18H). As a result, 2 previously described epimer compounds were identified from one of the extracts (the other extract is currently under study for the identification of novel hit components). At this point, 2.5 mg of this epimer mixture were purified from 1L fermentation (Fig. 18I).

[a] The number of actives selected at each stage expressed as a percentage of the total number of extracts screened (5,976)
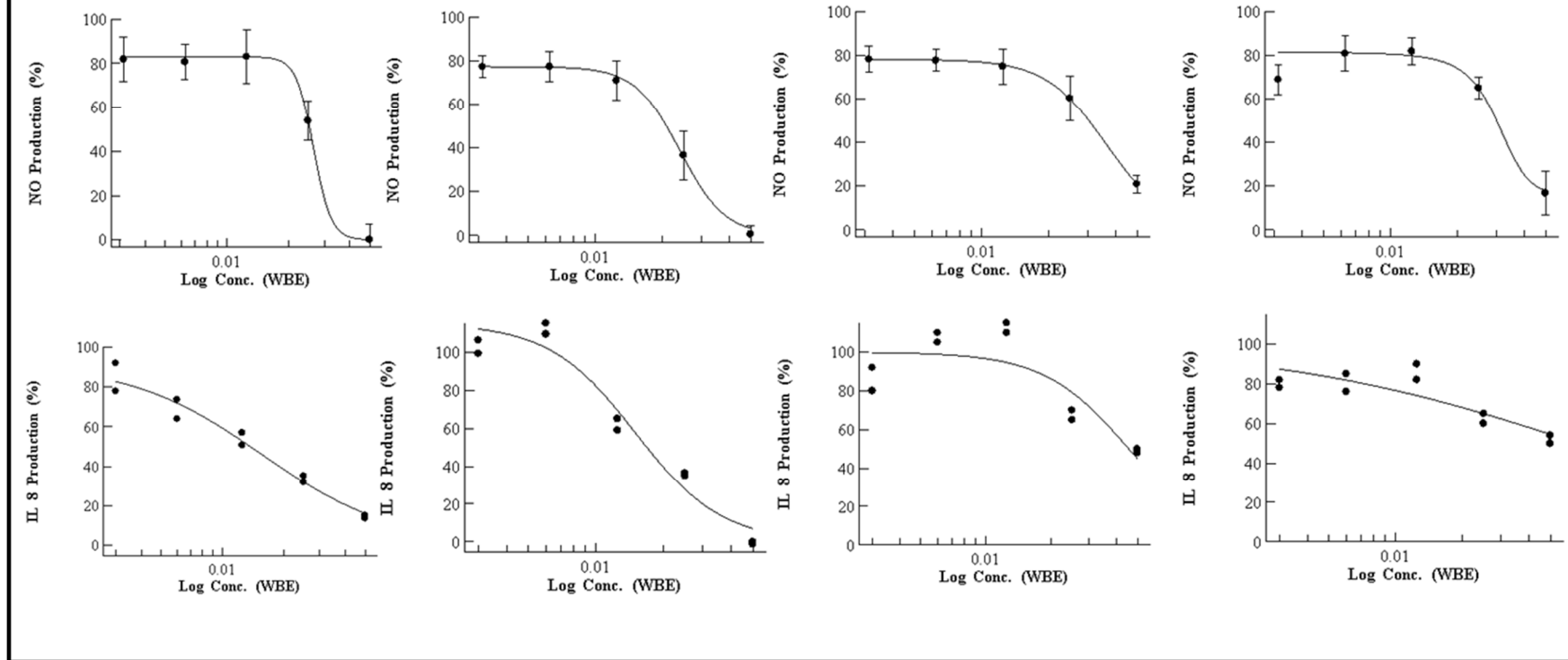
Figure 28. Dose response experiments for extract screening.
(A) Examples of dose-response curves in RAW 264.7/NO production assay of extracts that were identified as active and further selected for secondary screening in Caco-2/IL-8 production assay (Data are means ± SD; n = 3 for each concentration point. **(B)** Examples of dose-response curves identified as active in secondary screening and further selected for LC-MS de-replication and medium scale up growths for bioassay-guided fractionation (data are duplicates for each concentration point).

5.2.3 Early LC-MS De-replication

A database search performed using our in-house application, which matches UV-LC-MS data of the metabolites in the active extracts to UV-LC-MS data of known metabolites stored in our proprietary database obtained using the exact same LC-MS conditions, did not identify any metabolites in the 14 active extracts mentioned, and therefore those extracts were classified as potentially not containing known active components. As proof of concept to assess the ability of this HTS platform to effectively retrieve already known immunomodulatory compounds from microbial fermentations, we also subjected the remaining 20 active extracts from the primary screening which did not meet the de-replication selection criteria described above (extracts that had lower than 70% inhibition at the initial extract dilution in the dose response experiment) to LC-MS de-replication. As a result we identified profiles associated with known secondary metabolites, such as diketocoriolin B, a secondary metabolite of fungi (*Coriolus consors*) with immuno-stimulant activity described or eremoxylarin A, a secondary metabolite of xylariaceous endophytic fungus strain YUA-026 with calcineurin inhibitor activity [159].

5.2.4 Large-Scale up Growths for Bioassay-Guided Fractionation

At this stage, the 4 previously selected active extracts identified as potentially not containing known active components were prioritized and the producing strains were regrown in 100 mL volumes. The specific immunomodulatory activities were confirmed in the re-growths for 2 of them (Figure 28, extracts 1 and 2) and consequently they were submitted to fractionation guided by bioassays. Simultaneously, we ran liquid chromatography high resolution mass spectrometry (LC-HRMS) and NMR analyses of the active semi-preparative HPLC fractions of each of the 2 active extracts to assess the

novelty of the active components. As a result, 2 previously described epimer compounds (1:3) were identified (TAN-2483A and TAN-2483B) in a highly purified fraction (concentration 245 µg/mL) from extract 1 (CF-097474; Figure.29)[160]. These compounds are members of the gamma-lactone family and they were previously isolated by the Takeda Chemical Industries group[160, 161] from the filamentous fungus NF 2329,3 but no immunomodulatory activity has been reported for this compound so far. Therefore, it was tested for immunomodulatory activity. Determination of IC_{50} value in NO production showed the compound to be active with an IC_{50} value of 2.26 µM (Figure. 31A). Additionally, it showed strong inhibition of IL-8 production (100%) at 29.1 µM. At this point, 2.5 mg of this epimer mixture was purified from 1L fermentation of *Seimatosporium* (CF-097474) and will be assessed for immunomodulatory activity in an animal inflammation model. Regarding extract 2, it is currently under study for the identification of novel hit components.

Figure 29. Ultraviolet (210 nm) chromatogram of HPLC fractionation for active extract containing the epimer mixture (TAN-2483A & TAN2483B).
A highly purified fraction of these compounds was collected at 13 minutes, corresponding to the most intense peak.

Figure 29
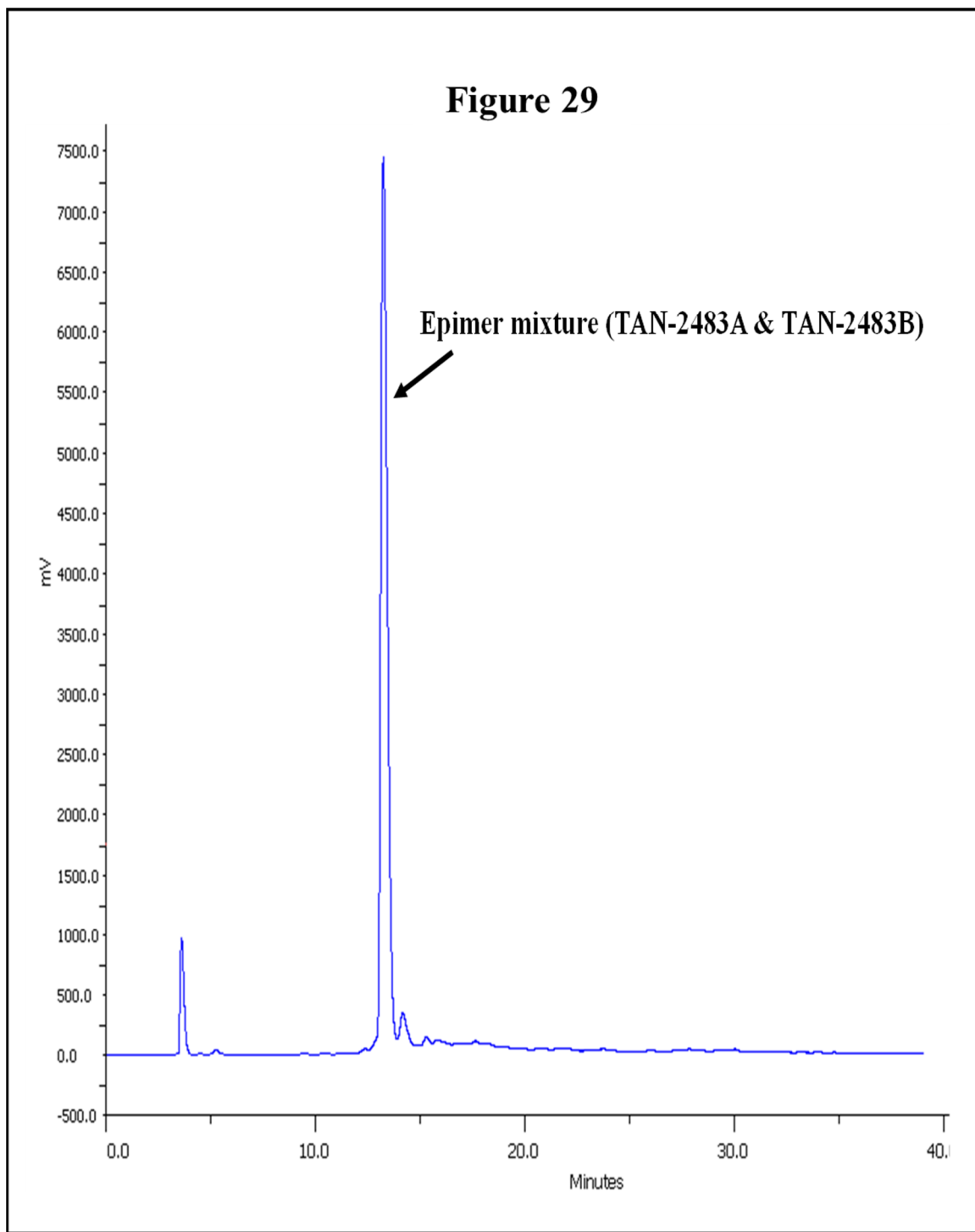
5.2.5 Evaluation of Antimicrobial activity

Considering the long and successful track record of microbial fermentations yielding new antibiotic compounds, the highly purified extract fraction containing TAN-2483A and TAN-2483B was evaluated for antimicrobial properties [162]. As shown in Figure 30B, this fraction was able to strongly inhibit the growth of Gram negative *Acinetobacter baumannii* CL5973 (100%) and *E. coli* MB5746 (100%) while moderate inhibition (37%) was observed for *Escherichia coli* MB2884 and no effect was observed against *Meticillin-resistant Staphylococcus aureus* MB5393 or *Candida albicans* MY1055 at this concentration (24 µg/mL).
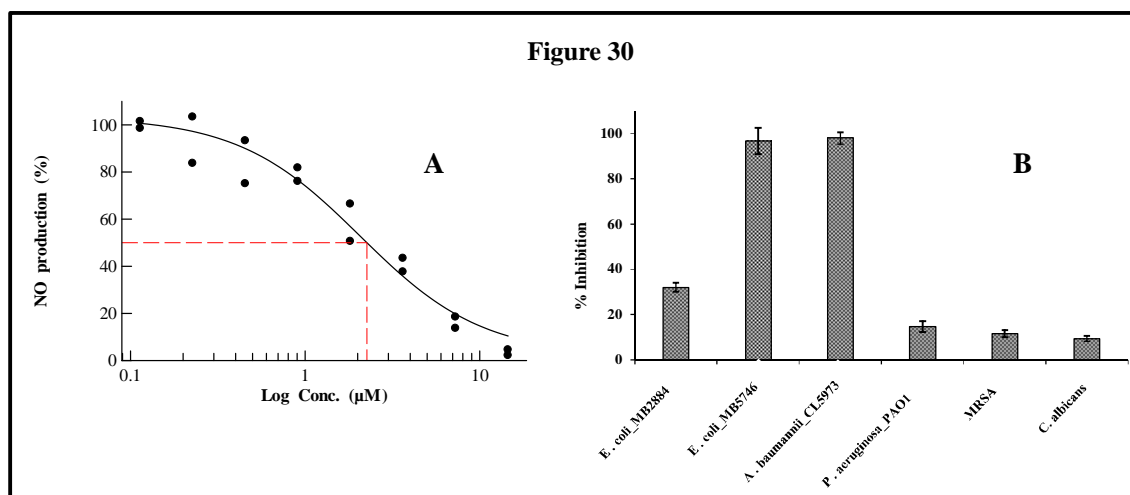
Figure 30. Bioactivity results of HPLC fraction containing the epimer mixture (TAN-2483A & TAN2483B).
(A) Dose-response curve (from 14.5 µM to 0.1 µM) in RAW 264.7/NO production assay for IC$_{50}$ calculation (data are duplicates for each concentration point) **(B)** Antimicrobial activities at 24 µg/ml (Data are means ± SEM; n = 3 of each microorganism incubation).

5.2.6 Discussion

It has long been reported that neurodegenerative diseases (NDD), including Alzheimer's disease, are characterized by redox imbalance, glial cell activation, neuro-inflammation and ultimately neuronal death [163]. In this context, NF-κB plays an important role in the pathogenesis of oxidative stress-associated neurodegenerative diseases, since it is one of

the most important transcriptional factors of pro-inflammatory gene expression. NF-κB facilitates the synthesis of pro-inflammatory cytokines, such as TNFα, IL-1β, IL-6, and IL-8, as well as of inducible enzymes, such as inducible iNOS which produces large amounts of NO, all of which can contribute to neuro-degeneration. The suppression of the production of these pro-inflammatory mediators can therefore offer protection from neuronal damage in neurodegenerative conditions by interfering with the inflammatory cascade at different levels (mainly enzyme inhibition and down-regulation of gene transcription), as previously demonstrated on animal models [164]. For this reason, the measurements of NO or IL-8 in cultured cells is a popular assay for identification of anti-inflammatory compounds of pharmacological interest. However, most applications previously described are devoted to a 24-well plate format or manual liquid dispensing which, for whole cell assay based HTS campaigns, is costly in terms of time and economic resources. In recent years, advances in spectrophotometry-based detection techniques and automation technologies have made it feasible to adapt these assays to the 96-well microplate miniaturized format, in which assay volumes can be decreased and plate throughput increased several fold. Moreover, this approach to microbial fermentations enables access to the unfathomable depths of chemical diversity in natural products, which consists of as many diverse chemotypes as there are species and strains in this realm. Useful information may be drawn from this experience. First, the general workflow used (Figure 18) ensures that only extracts that have been tested and proven, through rigorous methodology, to consistently contain active and potentially novel metabolites with immunomodulatory activity are selected for further development. Second, our efficiently integrated LC-MS de-replication system also enables us to pick up on active extracts containing already known compounds for which the immunomodulatory activity

has not been previously reported. In this regard, the results confirming the immunomodulatory activity of the TAN-2483A and TAN-2483B epimer mixture (3:1) further validate the strategy used in the present screening approach. These known bioactive compounds have not been previously reported to exhibit immunomodulatory activity. However, TAN-2483A has displayed strong inhibitory action in Src kinase, a human protein kinase that plays a pivotal role in macrophage-mediated inflammatory responses [165]. In fact, a variety of inflammatory diseases are closely related to macrophage activation. The critical role of Src in macrophage activation has prompted researchers to consider that the inhibition of Src activity may be a useful therapeutic strategy for macrophage-mediated diseases; specifically, Src has been described as a suitable therapeutic target for the treatment of NDD involving the activation of pathological microglia [166]. Taking into consideration other works highlighting the anti-inflammatory potential of natural products inhibitors of Src activity [167], we expect that novel and safe compounds exhibiting strong immuno-suppressive and anti-inflammatory properties will be discovered and could contribute to the development of innovative therapies for the treatment of macrophage-mediated diseases. Additionally, it has been demonstrated that certain antibiotics have potential as neuro-therapeutics for treating neurological diseases such as amyotrophic lateral sclerosis, adult motor neuron disease, and ischemic injury [168]. In multiple sclerosis—the archetypal inflammatory response in the central nervous system—T cells and macrophages invade the brain and damage the myelin and neurons. These macrophages are primed by components of neuropathology but might be further activated by systemic infection, which in turn has pronounced effects on inflammation in the brain and perhaps on neurological function. There is emerging evidence to support the idea that non-specific systemic infection or

inflammation in people with existing inflammation in the brain contributes to the disease progression rate through further activation of these already primed macrophages [169]. Therefore, the use of a compound with both immunomodulatory and antibacterial properties could be very useful in the treatment of inflammation in NDD. The results from antimicrobial in vitro activity of the purified epimer mixture (TAN-2483A and TAN-2483B) underline the ability and the specificity of these compounds against gram negative bacteria. This is important when set against the difficulty in inhibiting these kinds of pathogens, and suggests the potential of microbial extracts as a source of compounds with dual activity. Clearly, further investigations will be needed to determine the modes of action and establish the association of its antibacterial and immunomodulatory properties. Furthermore, we can confidently infer from the LC-MS de-replication data that the screening platform can effectively determine known active immunomodulatory compounds (diketocoriolin B and eremoxylarin A) from crude extracts, thus proving that we have a working system that can be used to de-replicate extracts which contain compounds with immunomodulatory activities. Lastly, the disadvantage of this de-replication step is that potentially active metabolites that may be present at undetectable levels in these crude extracts may be overshadowed by more abundant cytotoxic metabolites and consequently missed. It is our hope that, through this work, we will generate more interest in natural products as a source of novel chemotypes to meet global medical challenges.

5.3 Effect of compound low aqueous solubility on CYP450 inhibition assays

This section of the work was undertaken in order assess how the compound solubility might influence its interaction with the target based on the complexity of the in vitro model. To this aim, we selected a broad number of compounds comprising drug discovery compounds (with optimized physicochemical properties) and commercial compounds, and tested them in two CYP450 inhibition models with differential complexity. The drug discovery compound set was composed of 42 molecules from the GSK3 drug discovery research program of the IQM-CSIC. The commercial compound set comprised 20 commercial inhibitors with activity over the three major CYP450 isoforms involved in drug metabolism (CYP3A4, CYP2C9 and CYP2D6).

Each compound set was assessed for their CYP450 inhibitory potential using fluorogenic substrates together with hrCYP isoforms, as well as in the standard HLM+LC-MS CYP450 inhibition assays. In addition, the aqueous KS of each compound was determined using a turbidimetric solubility assay. The complete results for both compound sets are summarized in Tables 5 and 6.

5.3.1 Distribution of compounds according to their solubility

According to the KS classification bands established by Rogge and Taft (2010) [134], the data from the turbidimetric solubility assay revealed that 50% of the commercial compounds showed an acceptable KS (>50 µM) in assay buffer, whereas only 9.5% of the drug discovery compounds appeared in this solubility band. The percentage of commercial compounds classified within the marginal KS band (12-50 µM) was 30%, whereas this percentage increased to 43% for drug discovery compounds. Compounds

showing unacceptable KS (12-3 µM) represented 20% and 47.7% of commercial and drug discovery compounds, respectively.

In contrast, data from calculated logP values (cLogP) did not reveal remarkable differences between the two compound sets. Most compounds (69% for drug discovery compounds and 50% for commercial compounds) displayed a cLogP value between 3 and 5. The distribution of compounds with a cLogP value higher than 5 was very similar for both compound sets (17% for drug discovery compounds and 15% for commercial compounds). Larger differences were observed for compounds displaying cLogP below 3 (14% for drug discovery compounds and 35% for commercial compounds).

5.3.2 Correlation Between CYP450 Inhibition Assay Data

In general terms, we observed a clear tendency of both compound sets to yield lower IC_{50} values in the flourometric based methodologies for the three CYP450 isoforms, as compared to the HLM+LC-MS based assays (Figure 31, Tables 5 and 6). Only three compounds (IQM 11, IQM 12, IQM 13) displayed much lower IC_{50} values in the CYP3A4 HLM/LC-MS assay than in the CYP3A4 fluorometric assay. According to the linear correlation analysis, performed with the compounds with IC_{50} values bellow the maximum dose tested in both assay formats (Figure 31), the commercial compounds showed higher correlation coefficients in the three isoforms (r = 0.81 – 0.98, N= 8 - 13) than drug discovery compounds (r = 0.18 – 0.68, N = 12 – 30). For both sets of compounds, CYP2C9 displayed the weakest correlation (Tables 5 and 6, Figure 31).

Table 5. Summary of IC$_{50}$ values and KS obtained for drug discovery compounds

Isoform	CYP3A4			CYP2C9			CYP2D6						
Enzyme Source	hrCYP	HLM		hrCYP	HLM		hrCYP	HLM					
Substrate	BFC	Testosterone		MFC	Diclofenac		AMMC	Dextromethorphan		Kinetic Solubility Limits			
Detection	Fluor	LC/MS		Fluor	LC/MS		Fluor	LC/MS		Lower	Upper	Solubility	
		IC$_{50}$ (µM)	Ratio		IC$_{50}$ (µM)	Ratio		IC$_{50}$ (µM)	Ratio	Bound (µM)	Bound (µM)	Category	cLogP(a)
IQM 1	3.66	5.14	1	2.54	5.30	2	7.35	13.1	2	>100	>100	Acceptable	2.76
IQM 2	6.14	13.1	2	4.5	15.7	3	16.1	22.5	1	>100	>100	Acceptable	2.37
IQM 3	<0.5	<0.14	Match	4.2	13.2	3	8.42	14.9	1	50	100	Acceptable	3.28
IQM 4	6.34	14.2	2	6.39	29.3	5	19.3	20.4	1	50	100	Acceptable	2.17
IQM 5	17.9	24.3	1	1.56	18.3	12	15.6	49.1	3	25	50	Marginal	4.79
IQM 6	>88	>88	Match	3.43	>88	>26	>88	>88	Match	25	50	Marginal	4.11
IQM 7	5.09	7.72	2	1.99	17.5	9	>88	>88	Match	25	50	Marginal	3.45
IQM 8	0.68	0.171	Match	2.04	15.6	8	>88	>88	Match	25	50	Marginal	3.45
IQM 9	4.6	15.3	3	4.3	6.34	1	3.52	3.84	1	25	50	Marginal	3.62
IQM 10	>88	>88	Match	>88	>88	Match	>88	>88	Match	25	50	Marginal	3.76
IQM 11	>88	0.22	< 0.002	2.21	10.1	5	4.29	>88	>20	25	50	Marginal	3.86
IQM 12	>88	13.5	<0.15	2.78	39.3	14	>88	>88	Match	12	25	Marginal	3.36
IQM 13	>88	23.3	<0.27	0.68	9.11	13	>88	>88	Match	12	25	Marginal	3.04
IQM 14	4.07	>88	>22	2.77	6.12	2	10.9	>88	>88	12	25	Marginal	4.13
IQM 15	3.01	13.4	4	4.51	20.7	5	>88	>88	Match	12	25	Marginal	3.45
IQM 16	2.84	3.56	1	11.8	12.2	1	>88	>88	Match	12	25	Marginal	3.98
IQM 17	22.4	>88	> 4	2.55	3.54	1	5.59	>88	>15	12	25	Marginal	5.35
IQM 18	14.9	19.9	1	1.9	8.08	4	0.831	5.76	7	12	25	Marginal	5.65
IQM 19	13.3	39.1	3	3.37	8.78	3	14.5	24.3	2	12	25	Marginal	4.79
IQM 20	53.5	>88	Match	13.4	88.1	7	>88	>88	Match	12	25	Marginal	5.04
IQM 21	>88	>88	Match	>88	>88	Match	>88	>88	Match	12	25	Marginal	5.02
IQM 22	5.80	15.6	3	6.24	17.7	3	16.5	28.7	2	12	25	Marginal	3.63
IQM 23	0.18	9.39	50	3.02	24.8	10	2.79	25.4	9	6	12	Unacceptable	6.41
IQM 24	6.30	26.9	4	2.61	54.5	21	19.1	74.1	4	6	12	Unacceptable	4.13
IQM 25	31.2	>88	Match	3.33	88.0	26	41.9	>88	Match	6	12	Unacceptable	4.66
IQM 26	8.33	71.4	9	1.97	39.3	20	>88	>88	Match	6	12	Unacceptable	3.98
IQM 27	1.80	>88	>49	2.28	11.1	5	57.8	>88	Match	6	12	Unacceptable	4.11
IQM 28	>88	>88	Match	4.05	>88	>21	>88	>88	Match	6	12	Unacceptable	4.63
IQM 29	21.1	>88	>4	2.00	16.1	8	>88	>88	Match	6	12	Unacceptable	5.85
IQM 30	16.8	74.1	4	2.73	23.9	12	>88	>88	Match	6	12	Unacceptable	3.99
IQM 31	2.45	11.6	5	0.91	7.97	10	>88	>88	Match	6	12	Unacceptable	3.67
IQM 32	12.5	>88	>7	4.13	20.1	5	9.25	58.5	6	6	12	Unacceptable	4.13
IQM 33	>88	>88	Match	>88	>88	Match	>88	>88	Match	6	12	Unacceptable	2.69

Table 5. Summary of IC$_{50}$ values and KS obtained for drug discovery compounds (continuation)

Isoform	CYP3A4			CYP2C9			CYP2D6						
Enzyme Source	hrCYP	HLM		hrCYP	HLM		hrCYP	HLM					
Substrate	BFC	Testosterone		MFC	Diclofenac		AMMC	Dextromethorphan		Kinetic Solubility Limits			
Detection	Fluor	LC/MS		Fluor	LC/MS		Fluor	LC/MS		Lower	Upper	Solubility	
		IC$_{50}$ (µM)	Ratio		IC$_{50}$ (µM)	Ratio		IC$_{50}$ (µM)	Ratio	Bound (µM)	Bound (µM)	Category	cLogP(a)
IQM 34	8.81	32.34	4	8.91	41	5	>88	>88	Match	6	12	Unacceptable	3.92
IQM 35	>88	>88	Match	4.88	20	4	>88	>88	Match	6	12	Unacceptable	3.29
IQM 36	30.1	>88	Match	50.7	>88	Match	72	>88	Match	6	12	Unacceptable	1.02
IQM 37	>88	>88	Match	>88	>88	Match	>88	>88	Match	3.12	6.25	Unacceptable	4.79
IQM 38	0.681	>88	>129	21.1	>88	4	>88	>88	Match	3.12	6.25	Unacceptable	3.98
IQM 39	>88	>88	Match	5.18	7.10	1	>88	>88	Match	3.12	6.25	Unacceptable	4.66
IQM 40	>88	>88	Match	>88	>88	Match	>88	>88	Match	3.12	6.25	Unacceptable	4.01
IQM 41	19.9	>88	>4	6.35	8.64	2	>88	>88	Match	3.12	6.25	Unacceptable	5.21
IQM 42	44.1	>88	Match	5.61	>88	>16	>88	>88	Match	3.12	6.25	Unacceptable	1.61
Number of Matches			25			17			35				
Percentage of Matches			60			40			83				
r			0.652			0.181			0.677				
p value			0.003			0.338			0.016				
N			42			42			42				

Summary of global (b) assays correlation and kinetic solubility relationship for drug discovery compounds

Solubility Category	Acceptable	Marginal	Unacceptable	Total matching
Kinetic Solubility Range (µM)	100-50	50-12	12-3	
# Compounds Tested	4	18	20	42
# Compounds Matching in both CYP3A4 assays (N=42)	4 (100%)	11 (61%)	10 (50%)	25 (60%)
# Compounds Matching in both CYP2C9 assays (N=42)	3 (75%)	7 (39%)	6 (30%)	16 (40%)
# Compounds Matching in both CYP2D6 assays (N=42)	4 (100%)	14 (77%)	17 (85%)	35 (83%)

rCYP = recombinantly expressed CYPs; HLM = human liver microsomes;
(a)   Calculated LogP
(b)   Data from compounds with nonqualified and qualified IC50 values
IC$_{50}$ values are means of n=3. Standard deviation (STDVE) values are not show. However in any single case the relative STDEV displayed values lower than 15%

Table 6. Summary of IC$_{50}$ values and KS obtained for drug discovery compounds

Isoform	CYP3A4			CYP2C9			CYP2D6						
Enzyme Source	hrCYP	HLM		hrCYP	HLM		hrCYP	HLM					
Substrate	BFC	Testosterone		MFC	Diclofenac		AMMC	Dextromethorphan		Kinetic Solubility Limits			
Detection Method	Fluor	LC/MS		Fluor	LC/MS		Fluor	LC/MS		Lower	Upper	Solubility	
	IC$_{50}$ (µM)		Ratio	IC$_{50}$ (µM)		Ratio	IC$_{50}$ (µM)		Ratio	Bound (µM)	Bound (µM)	Category	cLogP(a)
Cimetidine	—	—	—	16.34	>88	—	7.35	—	—	>100	>100	Acceptable	0.071
5 Hydroxytriptamine	—	—	—	—	—	42.1	16.1	>88	Match	>100	>100	Acceptable	0.212
Erythromycin	6.70	>88	>13	—	—	—	8.42	—	—	>100	>100	Acceptable	2.02
Fluvoxamine	—	—	—	2.99	23.1	3.29	19.3	7.63	2	>100	>100	Acceptable	3.11
Gemfibrozil	—	—	—	5.41	14.2	—	15.6	—	—	>100	>100	Acceptable	4.39
Imipramine	—	—	—	—	—	3.49	>88	8.91	3	>100	>100	Acceptable	4.8
Omeprazole	19.7	59.9	3	—	—	>88	>88	>88	Match	>100	>100	Acceptable	0.0695
Quinidine	32.1	>88	Match	—	—	0.0131	>88	0.00811	1	>100	>100	Acceptable	3.44
Sulfaphenazole	—	—	—	0.112	0.151	—	3.52	—	—	>100	>100	Acceptable	1.52
Verapamil	2.51	10.6	4	—	—	43.8	>88	40.2	1	>100	>100	Acceptable	3.91
Nifedipine	13.0	14.4	1	>12	>12	>88	4.29	>88	Match	25	50	Marginal	2.13
Mianserine	—	—	—	—	—	2.54	>88	4.07	2	25	50	Marginal	3.62
Propranolol	—	—	—	—	—	1.42	>88	3.47	2	25	50	Marginal	2.97
Bromoergocriptina	0.221	0.741	3	—	—	—	10.9	—	—	12	25	Marginal	3.61
Haloperidol	—	—	—	—	—	0.77	>88	2.05	3	12	25	Marginal	4.25
Ethynilestradiol	5.50	2.31	2	2.38	10.9	—	>88	—	—	12	25	Marginal	3.66
Ketoconazole	0.0337	0.0198	1	3.30	13.3	15.8	5.59	20.5	1	6	12	Unacceptable	3.67
Miconazole	0.0213	0.0221	2	0.315	0.52	1.47	0.831	4.64	3	3	6	Unacceptable	5.72
Nicardipine	0.190	1.12	6	0.121	4.88	3.02	14.5	7.56	3	3	6	Unacceptable	5.00
Clotrimazole	0.0987	0.0121	1	0.124	1.16	9.96	>88	12.5	1	3	6	Unacceptable	5.47
Number of Matches		9			4			14					
Percentage of Matches		82			40			100					
r		0.956			0.814			0.983					
p value		0.0001			0.014			0.0001					
N		11			10			14					

Summary of global (b) assays correlation and kinetic solubility relationship for commercial compounds

Solubility Category	Acceptable	Marginal	Unacceptable
Kinetic Solubility Range (µM)	100-50	50-12	12-3
# Compounds Tested CYP3A4/CYP2C9/CYP2D6	4/4/6	3/2/4	4/4/4
# Compounds Matching in both CYP3A4 assays (N=11)	2 (50%)	3 (100%)	3 (75%)
# Compounds Matching in both CYP2C9 assays (N=10)	2 (50%)	1 (50%)	1 (25%)
# Compounds Matching in both CYP2D6 assays (N=14)	6 (100%)	4 (100%)	4 (100%)

rCYP = recombinantly expressed CYPs; HLM = human liver microsomes;

(a) Calculated LogP

(b) Data from compounds with nonqualified and qualified IC$_{50}$ values

IC$_{50}$ values are means of n=3. Standard deviation (STDVE) values are not show. However in any single case the relative STDEV displayed values lower than 15%
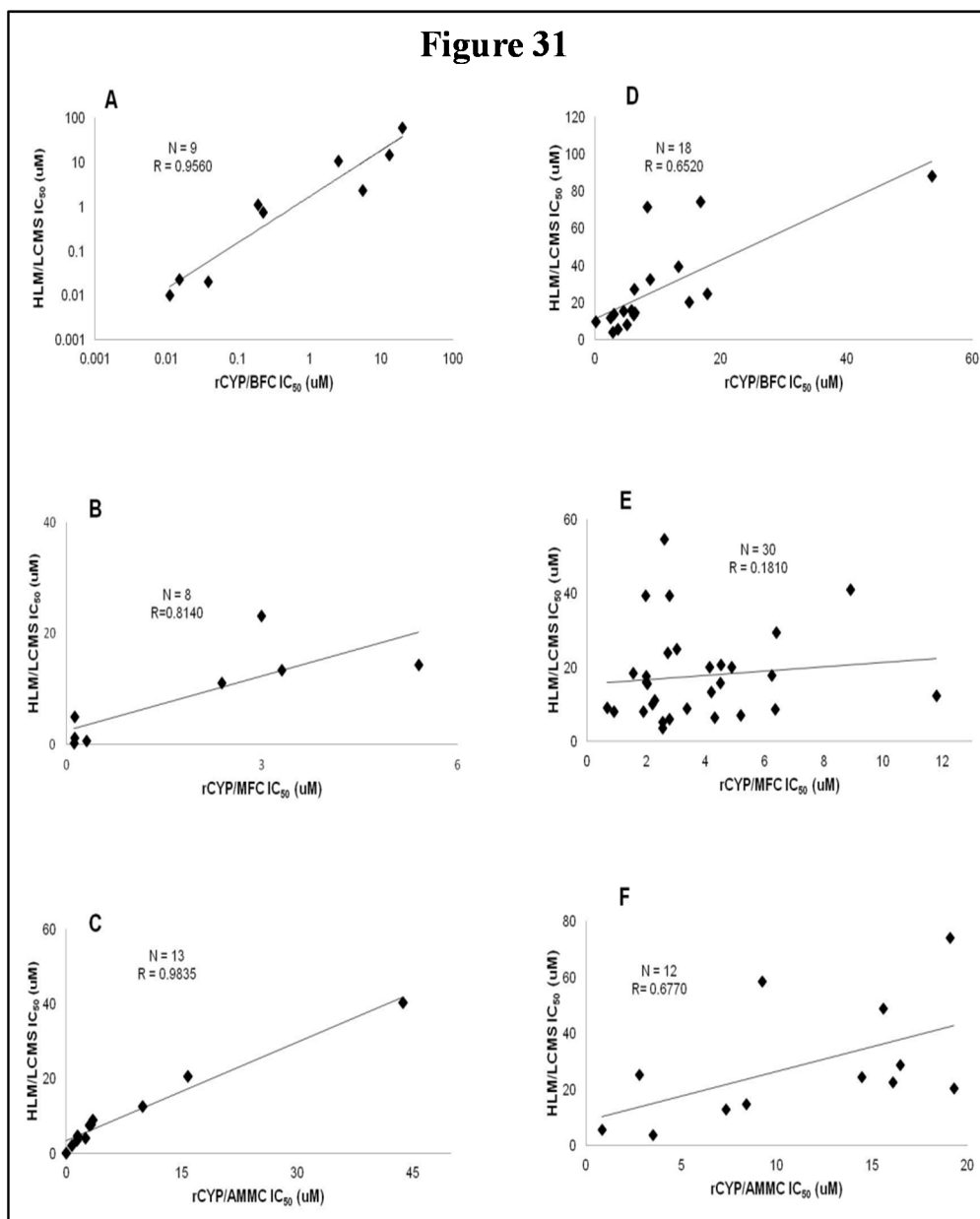
Figure 31

Figure 31. Correlation between hrCYP fluorometric and HLM/LC-MS assays. Nonqualified IC_{50} values obtained in hrCYP fluorometric assays are represented versus the values obtained in HLM/LC-MS for the same compounds, in order to calculate the coefficient of linear correlation(IC_{50} values are means of n=3. Standard deviation (STDVE) values are not show. However in any single case the relative STDEV displayed values lower than 15%). (A) CYP3A4 BFC versus Testosterone for commercial compounds; (B) CYP2C9 MFC versus Diclofenac for commercial compounds; (C) CYP2D6 AMMC versus Dextromethorphan for commercial compounds; (D) CYP3A4 BFC versus Testoterone for drug discovery compounds; (E) CYP2C9 MFC versus Diclofenac for drug discovery compounds; (F) CYP2D6 AMMC versus Dextromethorphan for drug discovery compounds.

5.3.3 Correlation of the CYP450 Inhibitory Potential Category Between Assays

In drug discovery programs, compounds are often categorized in three groups according to their activity as CYP450 inhibitors [2]: Potent inhibitors ($IC_{50}<1$ µM), moderate (IC_{50} between 1 and 10 µM) and weak inhibitors ($IC_{50}>10$ µM). In order to analyze in more detail the extent of the match between the fluorometric and LC/MS based methods, we applied the following criteria: one compound was considered as matching, or giving comparable results in both methodologies, if it was categorized in the same classification band in both assays, or displayed an IC_{50} ratio between both methodologies of 3-fold or lower. For this analysis, we considered all of the compounds tested in both the drug discovery compound set and the commercial compound set. According to these criteria, we observed that for the drug discovery set in CYP3A4, 25 out of 42 compounds (60%) showed comparable results in both assay methodologies. For the same set of compounds, 17 out of 42 compounds (40%) in the CYP2C9 assay, and 35 out of 42 compounds (83%) in the CYP2D6 assay, complied with this condition. For the commercial compound set, this concordance was observed for 9 out of 11 compounds (82%) in the CYP3A4 assays, 4 out of 10 compounds (40%) in the CYP2C9 assay, and 14 out of 14 compounds (100%) in the CYP2D6 assay.

5.3.4 Relationship between solubility and correlation of CYP450 inhibition assay data

In this analysis, we used all of the compounds tested in both compound sets, and compared the results from the different assay types for the compounds grouped within each category of KS. Thus, considering the compounds classified in the acceptable solubility range (>50 µM), all the drug discovery compounds (4 out of 4) tested in the CYP3A4 assays showed matching results between the two assay methods. The same

results were obtained from the CYP2D6 assay. For the CYP2C9 assay, 3 out of 4 compounds (75%) matched (Table 5). In the commercial compound set, 2 out of 4 compounds (50%) matched for CYP3A4 and CYP2C9 assay, while for CYP2D6 assay, all 4 compounds tested matched results (Table 6).

In the marginal solubility band (50 µM to 12 µM), the number of drug discovery compounds correlated between the two assay types decreased significantly for the three isoforms. For CYP3A4, 11 out of 18 compounds (61%) matched, for CYP2C9, 7 out of 18 compounds (39%) matched, and in CYP2D6, 14 out of 18 compounds matched (77%) (Table 5). The commercial compounds tested in the same solubility range yielded a matching rate of 3 compounds out of 3 for CYP3A4, 4 compounds out of 4 for CYP2D6, and 1 compound out of 2 for CYP2C9 (Table 5).

For the compounds within the unacceptable solubility band, the drug discovery compound matching rate was even lower for CYP3A4 and CYP2C9, with 10 out of 20 compounds (50%) and 6 out of 20 compounds (30%), respectively. However, in the CYP2D6 assay, 17 out of 20 compounds (85%) displayed a matching rate very similar to the previous solubility band (Table 5). The commercial compounds classified in this band showed a matching rate of 3 compounds out of 4 in the CYP3A4 assay, 1 compound out of 4 in CYP2C9, and 4 compounds out of 4 in CYP2D6 (Table 6).

5.3.5 Restricted Compound Analysis

The effect of compound aqueous solubility on the correlation of CYP450 assay data was also evaluated by classifying compounds in two groups according to the ratio of their IC_{50} in the two types of CYP450 assays: Below 3-fold or above 3-fold (Table 7).Thus, those compounds showing an undefined IC_{50} value (e.g. >88) in both CYP450

inhibition assays were not considered in order to reduce the extent of uncertainty. In terms of solubility, compounds were grouped according to classification bands mentioned before.

Within the drug discovery compound set, none of the 3 compounds in the acceptable solubility classification band (>50 µM) showed an IC_{50} values ratio higher than 3-fold in the CYP3A4 assays. Identical results were obtained in the CYP2D6 assay for the 4 compounds in this solubility band, and just one compound out of the 4 with acceptable KS displayed

Table 7. Summary of restricted[(a)] assay correlation and solubility relationship for commercial compounds.

Kinetic Solubility band	Acceptable		Marginal		Unacceptable	
Upper bound- Lower bound (uM)	>100 -50		50-25		12-3	
IC_{50} Ratio	1-3	>3	1-3	>3	1-3	>3
CYP3A4 # Compounds (N=11)	2	2	3	N.A.	3	1
CYP2C9 # Compounds (N=9)	2	2	1	N.A.	1	3
CYP2D6 # Compounds (N=11)	4	N.A.	3	N.A.	4	N.A.

(a) Data from compounds with nonqualified IC_{50} value.

an IC_{50} ratio higher than 3-fold for CYP2C9 (Table 4). In the marginal band of aqueous solubility (50-12 µM), the IC_{50} ratio distribution was slightly different. For CYP3A4, 6 compounds out of 14 yielded an IC_{50} ratio that was higher than 3-fold, whereas for CYP2C9 this proportion was 10 out of 16 compounds. For CYP2D6, 4 compounds out of 8 showed an IC_{50} ratio higher than 3-fold (Table 5). For the compounds with low aqueous solubility (12-3 µM), most of the compounds showed an IC_{50} ratio higher than 3-fold for the three CYP450 isoforms (all the compounds for CYP3A4 (N=11) and CYP2D6 (N=3), and 12 out of 14 compounds for CYP2C9). In relative terms, there is a clear bias, in the set of drug discovery compounds with IC_{50} ratios higher than 3-fold, towards lower aqueous solubility bands. As for the commercial compound set (N=11

for CYP3A4, N=9 for CYP2C9 and N=11 CYP2D6), 2 out of the 4 compounds in the acceptable solubility classification band displayed an IC_{50} ratio higher than 3-fold in the CYP3A4 and CYP2C9 assays. All the compounds with acceptable solubility displayed an IC_{50} ratio below 3-fold for CYP2D6. In the marginal band of aqueous solubility (50-12 µM), none of the compounds grouped in this band (N=3 for CYP3A4, N=1 for CYP2C9, N=3 for CYP2D6) showed an IC_{50} ratio higher than 3-fold. In the unacceptable band of aqueous solubility (12-3 µM), only 1 compound out of 4 showed an IC_{50} ratio higher than 3-fold in the CYP3A4 assays. The exact opposite behavior was observed for these 4 compounds for in the CYP2C9 assay (3 out of 4 with IC_{50} ratios higher than 3-fold), whereas for CYP2D6, all these compounds displayed IC_{50} ratios below 3-fold.

In terms of their IC_{50} ratios, the commercial compounds were distributed over the three solubility bands and showed no clear trend (Figure 32).
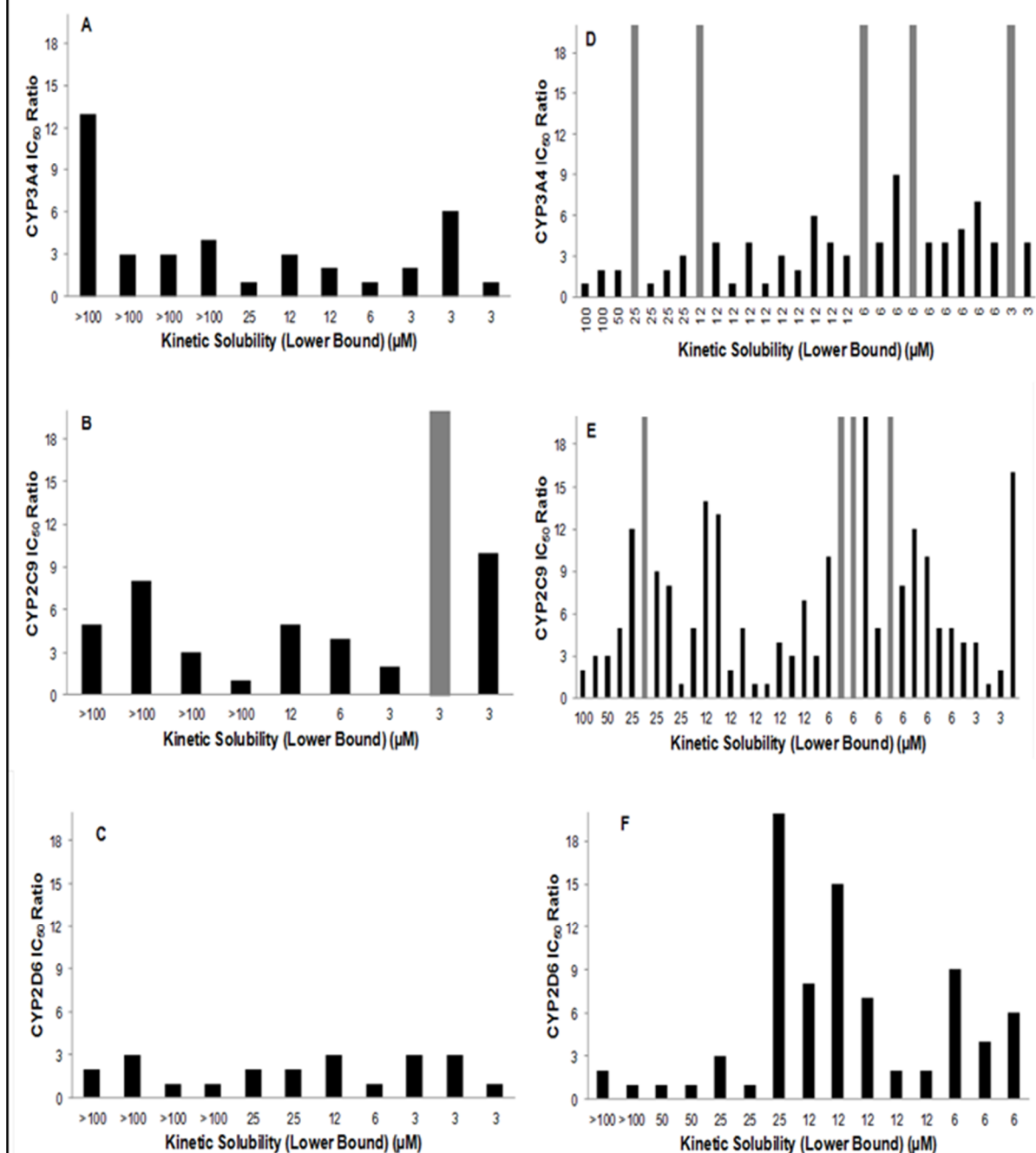
Figure 32. Distribution of IC$_{50}$ ratios between CYP450 assay types in terms of compound KS.

Each bar represents the IC$_{50}$ ratio between the 2 CYP450 assays, for each compound, sorted by their kinetic solubility. Dark gray columns indicate higher IC$_{50}$ ratios than the maximum values in the y axis. (A) Commercial compounds in CYP3A4 assays, (B) Commercial compounds in CYP2C9 assays, (C) Commercial compounds in CYP2D6 assays, (D) Drug discovery compounds in CYP3A4 assays, (E) Drug discovery compounds in CYP2C9 assays, (F) Drug discovery compounds in CYP2D6 assays.

5.3.6 Discussion

Our results with commercial compounds and data from Crespi and collaborators [170] support the notion that CYP450 fluorometric assays can rapidly determine a compound's potential to inhibit CYP450 in a drug discovery setting, based on their good correlation with the standard HLM+LC-MS assays. However, data from our drug discovery compound set showed disparities between hrCYP fluorometric and HLM+LC-MS based assays for a significant number of compounds. Therefore, the results from fluorometric inhibition assays are sometimes insufficient for determining structure-activity relationships (SAR) predicting drug-drug interactions mediated by CYP450 inhibition. This general observation is consistent with other studies [85, 171, 172]. The main causes for such differences have been reviewed [85, 171], and key experimental differences, e.g., the choice of the probe substrate, enzyme source and enzyme concentration, might partially explain disparities. However, the role of physicochemical properties, e.g. compound aqueous solubility, has not been properly studied to date. Compound solubility is a well-known source of variability for in vitro compound profiling tests. Poorly soluble compounds may precipitate or bind nonspecifically to other components of the incubation mix during in vitro assays, lowering expected concentrations of free compound. In a CYP450 inhibition assay, poorly soluble compounds might artificially behave as weak- or non-inhibitors, which could miss potential drug–drug interactions [173, 174]. Turbidimetric solubility assay results indicated that the compound distribution according to their KS clearly differed between drug discovery compounds and commercial compounds, especially between the acceptable and unacceptable solubility bands. Obviously, drug discovery compounds were still unoptimized for aqueous solubility, because barely 10% were

classified within the acceptable solubility range, whereas half of the commercial compounds fall into this category. At the other extreme, in the unacceptable solubility range, nearly half of the drug discovery compounds were found to fall in this category, more than twice the proportion of commercial compounds.

Computer applications can estimate a compound's cLogP value, an estimate of its lipophilicity [175]. Interestingly, no major differences in cLogP values were observed between drug discovery and commercial compound sets. In both cases, the calculated cLogP values ranged between 3 and 5. The distribution of compounds with a high cLogP value (>5) was also very similar in both sets. Thus, no clear relationship was observed between the cLogP values, and the lack of correlation in the CYP450 assays.

Although an inverse relation between lipophilicity and solubility is expected, factors such as high / low melting points or pKa influence the rule, making it possible to have water soluble compounds with high cLogP values and low cLogP compounds with a high melting point, and thus very low water solubility. cLogP values are not directly correlated with solubility limits; they merely indicate whether compounds are more or less soluble in water vs. organic solvent [176]. Two compounds may both have cLogP values of -1, indicating that they are more soluble in aqueous than in organic solvents, but they may differ in solubility in aqueous buffers.

As stated previously [177], our drug discovery compounds trended towards molecules with low KS. This effect has been previously described as molecular obesity. Higher lipophilicity has consequences during the quest for potency and it affects various factors leading to the attrition of compounds during drug development. The phenomenon of

"molecular obesity" affects development risks and could contribute substantially to the limited productivity of drug discovery programs [110].

Low water solubility may contribute to the poor correlation observed for drug discovery compounds in the CYP450 assays. The excess of lipids in HLM incubations (compared to the hrCYP assays), even at low total protein concentrations, can increase nonspecific binding to the lipid membranes for compounds with low aqueous solubility, resulting in an apparent increase in the IC_{50} value [95]. Other investigators demonstrated that lipophilic agents exhibiting moderate-to-extensive nonspecific binding were less inhibitory as the concentration of inactive microsomal protein increased [178]. Hence, compounds displaying lower limits of KS could conceivably yield higher IC_{50} values in the HLM/LC-MS in vitro system.

During experiments with drug discovery compounds, we observed a decrease in the number of compounds matching or achieving IC_{50} ratios within the 3-fold threshold, as the KS range decreased. These observations indicated that the drug discovery compounds with very low KS tended to yield higher IC_{50} values (at least 3-fold) in the HLM/LC-MS and consequently were more prone to being classified in different inhibitory potential categories. Conversely, drug discovery compounds with high KS limits tended to yield more similar IC_{50} values (IC_{50} ratios of between 1 and 3) and therefore it is reasonable for them to be classified the same for drug–drug interaction purposes.

No clear trend was observed in IC_{50} value shifts between the two assays systems for drug discovery compounds classified in the marginal KS band. Interestingly, we observed (Table 5) that some compounds yielded similar IC_{50} values in one particular

isoform whereas large differences were seen in other isoforms (e.g., IQM 5, IQM 8, IQM 17, IQM 18). These data suggest that factors other than compound aqueous solubility, e.g., probe substrate specificity [17–21], presence of non-target enzymes in HLM, multiple CYP450 metabolism, or accumulation of potent inhibitory metabolites [22], could cause these differences.

Enzyme concentration can also affect the final outcome of CYP450 inhibition assays [23, 24]. However, under a low microsomal protein concentration (0.25 mg/ml), molecules such as ketoconazole and clotrimazole with proven extensive unspecific binding, displayed very similar IC_{50} values [11]. In our experiments, the concentrations of each isoenzyme in the assay and total protein content were adjusted when possible to reach comparable concentrations in both in vitro models and to minimize unspecific binding (Table 1). In fact, the IC_{50} values for ketoconazole, sulfaphenazole and quinidine, selective inhibitors of CYP3A4, CYP2C9 and CYP2D6 respectively, were very similar in both in vitro models (Table 6) and also coincided with the results obtained in inhibition experiments carried out by other investigators [23] with much lower total protein concentration. Therefore, when using low enough total protein concentrations (e.g.0.25 mg/ml) in the incubations, this factor seems to contribute less to the IC_{50} variation. According to these results, a difference of 3-fold or less in the IC_{50} value could be expected as a result of the different protein concentrations.

According to other investigators [25], we found in previous studies that DMSO inhibited CYP3A4 activity even at low concentrations (0.35%). To assess this issue, we performed in previous works [26, 27] extensive IC_{50} comparisons of drug discovery compounds and commercial compounds using different organic solvent contents and

we did not find significant differences when keeping the DMSO level at 0.35%. Although it is still possible that organic solvents could have a differential effect depending on the enzyme source studied, it does not seem to be the main driver contributing to the lack of correlation between hrCYP and HLM.

It is also relevant to point out that when drug discovery compounds with unacceptable KS from the linear correlation analysis were excluded, the correlation coefficients increased (r=0.882 for CYP3A4, r=0.369 for CYP2C9 and r=0.824 for CYP2D6), reaching similar values to those observed for commercial compounds except CYP2C9 isoform, which still displayed a low correlation coefficient. The same poor correlation was observed when comparing different drug inhibition for diclofenac and MFC [172].

For commercial compounds, the relationship between assay data correlation and aqueous solubility was not as clear. In the acceptable solubility band, both methods should yield similar IC_{50} values. However, for CYP3A4 and CYPC9 isoforms, 2 compounds out of 4 yielded IC_{50} ratios higher than 3-fold. The behavior of some of these compounds as CYP450 inhibitors has been previously reported. Thus, [179] the assay showed that large molecules. e.g., erythromycin, can occupy the CYP3A4 active site, differentially affecting metabolic activity toward testosterone and BFC. Compounds, e.g., fluoxetin and verapamil, that are metabolized by multiple CYP450 isoforms [180–183] in HLM incubations during the course of IC_{50} measurements may be prone to underestimation of inhibitor potential in microsomal system, relative to measurements made simply with hrCYP, because of lower effective assay concentrations of parent drug. Others [184] have demonstrated that main verapamil metabolites are irreversible inhibitors of hrCYP3A4 and CYP3A activity in HLM,

which are further breakdown via CYP3A5 and CYP2C8 [183]. This fact may also contribute to the higher IC_{50} values observed for verapamil during HLM incubations.

On the contrary, for the commercial compounds within the unacceptable solubility range, no significant IC_{50} value variations for the CYP3A4 and CYP2D6 isoforms were observed. As previously shown [185], when protein concentration is low enough, very strong inhibitors of CYP3A4, such as ketoconazole, miconazole or clotrimazole, displayed very similar IC_{50} values regardless of the probe substrate or KS. Although some compound properties,.e.g., pKa or compound formulation, might partially explain these results, low KS seems not to produce a lack of correlation for commercial compounds.

5.4 Development and validation of a novel in vitro approach for simultaneous evaluation of CYP3A4 inhibition and kinetic aqueous solubility

In order to assess the usefulness of this NIVA-CYPI-KS, 10 commercial compounds with previously described IC_{50} values (from very potent inhibitors such as ketoconazole to moderate-weak inhibitors such as cimetidine) and water solubility (from highly soluble compounds such as erythromycin to poorly soluble compounds such as ketoconazole), were selected for parallel evaluation in NIVA-CYPI-KS, CSIVM-CYPI and CSIVM-KS assays. Consequently 12 microtiter 96 well plates containing 3 replicates of each compound were assayed in each methodology under study.

5.4.1 Analysis of the CYP450 inhibition assays

The assay performance for CYP34A4 inhibition experiments was assessed using robust statistic parameter, Z' factor (Z') [133], which displayed values of 0.76 for CSIVM-CYPI

and 0.87 for NIVA-CYPI-KS. These results allowed establishing that the evaluation of CYP3A4 inhibition was carried out at optimal sensibility and reproducibility, either for NIVA-CYPI-KS or for CSIVM-CYPI separately (Table 7). These findings were confirmed in the analysis of the dose response curves generated for the selected molecules in each in vitro model. Especially in the case of ketoconazole, an antifungal drug and also a well-known potent CYP3A4 inhibitor in humans which is widely used in vitro as a selective CYP3A4 inhibitor at low concentrations (Figure 19E), the results obtained were very similar regardless of the methodology and were in line with data from earlier investigations [186] (Table 7). The rest of the molecules under evaluation for CYP3A4 inhibition also rendered very similar IC_{50} values as reflected in the linear regression analysis, which yielded an r^2 value of 0.9622 (Figure 33). In all cases the differences observed were lower than 3-fold regardless of the methodology and what is more important, none of the molecules considered were misclassified in terms of inhibitor category according to the information from related literature (Table 7).
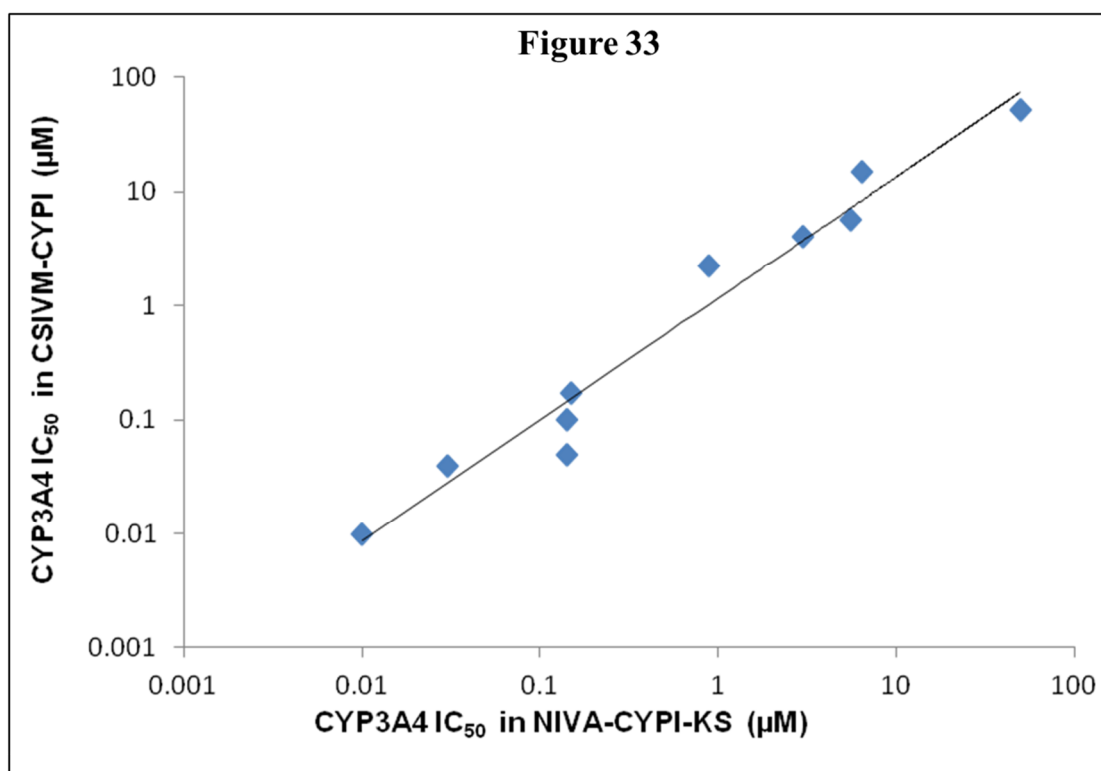
Figure 33. Comparison of CYP3A4 IC$_{50}$ values obtained for commercial compounds in CSIVM-CYPI and NIVA-CYPI-KS. IC$_{50}$ values are means of n=3. Standard deviation (STDVE) values are not show. However in any single case the relative STDEV displayed values lower than 15%

These results perfectly match our expectations, since the main experimental differences between NIVA-CYPI-KS and CSIVM-CYPI are the reagent stock concentrations, the reagent dispensing volumes and the reagents addition order, whilst other experimental conditions remained the same. In contrast, with CSIVM-CYPI, where serial dilutions of test compounds in organic solvents are dispensed into a buffered pre warmed solution containing NADPH regenerating system and representing half the final incubation volume, for NIVA-CYPI-KS, test compound dilutions in organic solvent are dispensed into a buffered solution representing 90% of the final incubation volume, and the initiation of reaction is achieved by adding of separate solutions of enzyme/substrate and the NADP regenerating system. This order of addition enables us to assess the compound solubility just before triggering the enzymatic reaction very close to the final assay

concentration. Although this dispensing procedure means one more pipetting step in comparison with commonly practiced CYP450 inhibition procedures, it does not really represent an increase in the final turnaround time, reproducibility or accuracy of the global assay performance for an eight channel reagent dispenser such as Thermo Mutidrop Combi. The concentration of enzyme / substrate and NADP regeneration system solutions required in NIVA-CYPI-KS should have very little effect on IC_{50} values since final reagent concentrations remain the same. Therefore, we can assume that the small IC_{50} variation observed between methodologies (<3-fold) might be due to minor changes in the assay conditions (including incubation temperature, minute changes in the pH of a buffer, etc, …) which matches perfectly with the inter-day variation typically observed in a biological assay [187].

Neither the commercial compounds nor the lead compounds used in this study displayed fluorescent or quenching interference.

5.4.2 Analysis of the solubility assays

Analogously, the analysis of solubility limits obtained in each methodology revealed very similar data in both cases (NIVA-CYPI-KS vs. CSIVM-KS), all the compounds being classified in the same solubility categories in both methods and coinciding with the results retrieved from related literature (Table 7). The main differential factors between the procedures to determine KS discussed in this study are final test compound concentration and final content of DMSO. Other critical conditions such as buffer system and incubation time were maintained the same in both procedures and therefore their contribution to inter assay variability must be minimal. The ratio between the final concentration of test compound in the NIVA-CYPI-KS and the CSIVM-KS has been determined as 1.1 and consequently the factor's effect on the final results is expected to be very low.

Table 7. Summary of IC$_{50}$ values and solubility limits obtained for commercial compounds using NIVA-CYPI-KS vs. CSIVM-CYPI / CSIVM-KS

Compound ID	NIVA-CYPI-KS						CSIVM-CYPI / CSIVM-KS						Literature		
	CYP3A4 IC$_{50}$ (µM)	CL 95%	Inhibitor category	S.R. (µM) L.B.	U.B.	Solubility category	CYP3A4 IC$_{50}$ (µM)	CL 95%	Inhibitor category	S.R. (µM) L.B.	U.B.	Solubility category	CYP3A4 IC$_{50}$ (µM)	Solub.* (µM)	Ref.
Cimetidine	49.86	42-60	W	>86	>86	A	51.81	43.10-61.00	W	>100	>100	A	1000	>86	◊a / ∎
Roxithromycin	6.40	5.70-7.20	M	>86	>86	A	15.03	13.23-17.11	W	>100	>100	A	N.D.A	N.D.A.	- /-
Ethinylestradiol	5.51	5.01-6.06	M	43.00	86.00	Mar	5.60	4.61-7.01	M	12.5	50	Mar	1.4	38.1	15b / ♦
Erythromycin	3.01	2.7-3.7	M	>86	>86	A	4.10	3.41-6.00	M	>100	>100	A	4.6	>86	15b / □
Nifedipine	2.80	2.1-3.7	M	21.50	43.00	Mar	1.90	1.61-2.02	M	25	50	Mar	8.4	16	15b / ○
Verapamil	0.90	0.70-1.50	M	>86	>86	A	2.30	2.2-3	M	>100	>100	A	0.36	>86	15b / 20
Clotrimazole	1.40E-02	(1.30-1.50)E-02	S	2.59	10.35	U	1.00E-02	(0.80-1.2)E-02	S	3.13	6.25	U	0.002	1.42-14.5	15b / ●
Ketoconazole	0.33E0-1	(0.30-0.36)E-02	S	>1.06	>1.06	U	0.04	0.03-0.05	S	6.25	12.5	U	0.005	2	15b/ ▲
Miconazole	0.14	0.12-0.17	S	8.62	34.00	U	0.13	0.10-0.16	S	3.13	12.5	U	0.06	poor	15b/ △
Nicardipine	0.14	0.13-0.16	S	2.15	8.60	U	0.10	0.09-0.11	S	3.13	12.5	U	0.71	4.6	∎c / □
Bromocryptine	0.15	0.12-0.18	S	0.33	1.34	U	0.17	0.15-0.20	S	3.13	12.5	U	0.6 – 1.7	0.2	▼d / Δ
Pyrene	N.D.A	N.D.A	N.D.A	6.25	12.50	U	N.D.A	N.D.A	N.D.A	3.13	12.5	U	N.A.D.	0.02	- /18
Z' factor	0.76						0.87								

NIVA-CYPI-KS= Novel in vitro approach for simultaneous CYP450-inhibition and turbidimetric solubility evaluation; CSIVM-CYPI= Conventional separate in vitro model for CYP450-inhibition evaluation; CSIVM-KS= Conventional separate in vitro model for KS evaluation; S.R.= Solubility Range; L.B.= Lower Bound; U.B.= Upper Bound; N.D.A. =No data available; M= Medium; W= Weak; S= Strong; A= Acceptable; U= Unacceptable; Mar = Marginal; CL95% ascertains the concentration interval in which the true IC$_{50}$ value resides with 95% probability (CL=confidence limit); a= Reference based on human liver microsomes and erythromycin as substrate; b= Reference based on recombinant CYP3A4 enzymes and BFC as substrate; c= Reference based on recombinant CYP3A4 enzymes and DBF as substrate; d= Reference based on human liver microsomes and testosterone as substrate; *= All data from solubility references are based on thermodynamic experiments; (◊)Riley, R. J.; Parker, A. J.; Trigg, S.et al. Development of a generalized, quantitative physicochemical model of CYP3A4 inhibition for use in early drug discovery Pharm Res 2001, 18, 652-5. ; (∎) McFarland, J. W.; Avdeef, A.; Berger, C. M.;et al. Estimating the water solubilities of crystalline compounds from their chemical structures alone J Chem Inf Comput Sci 2001, 41, 1355-9.; (♦) Yalkowsky, S. H.; Dannenfelser, R. H.; College of Pharmacy, University of Arizona: 1992.; (□) Law, V.; Knox, C.; Djoumbou, Y. et al. DrugBank 4.0: shedding new light on drug metabolism Nucleic Acids Res, 42, D1091-7. ; (○) Yang, W.; de Villiers, M. M. The solubilization of the poorly water soluble drug nifedipine by water soluble 4-sulphonic calix[n]arenes European Journal of Pharmaceutics and Biopharmaceutics 2004, 58, 629-636. ; (●) Buchanan, C. M., N.L. Buchanan, K.J. Edgar, and M.G. Ramsey Solubility and dissolution studies of antifungal drug: hydroxyl-ß-cyclodextrin complexes Cellulose 2007, 35-47.; (▲) Helming Tan; David Semin; Cheetham, M. W. a. J. An Automated Screening Assay for Determination of Aqueous Equilibrium Solubility EnablingSPR Study During Drug Lead Optimization Journal of Laboratory Automation 2005, 10, 364. ; (△) Douroumis, D.; Fahr, A.; ebrary Inc. Drug delivery strategies for poorly water-soluble drugs; John Wiley & Sons: Chichester, West Sussex.; (∎) Bell, L.; Bickford, S.; Nguyen, P. H.;et al. Evaluation of fluorescence- and mass spectrometry-based CYP450 inhibition assays for use in drug discovery, J Biomol Screen 2008, 13, 343-53. ; Di Marco, A.; (▼) Marcucci, I.; Verdirame, M. et al. Development and validation of a high-throughput radiometric CYP3A4/5 inhibition assay using tritiated testosterone, Drug Metab Dispos, 2005, 33, 349-58.; (Δ) Cummings, J. The Chemical Database Reference Reviews 2004, 18, 32-33.

Conversely, the lower content of DMSO required in NIVA-CYPI-KS in order to minimize its inhibitory effect in CYP3A4 activity might lead to worse prevention of precipitation since DMSO role is as co-solvent has been previously described [188]. This solubility enhancement by DMSO, which can be dramatic, is highly compound specific and hardly predictable [189, 190]. However when DMSO concentration is kept to an absolute minimum ($\leq 1\%$), the potential co-solvent effects are reduced achieving better correlations with thermodynamic methods [111] (kinetic assessment typically evaluates the solubility of a compound already fully dissolved in an organic solvent. It does not allow for equilibrium to be reached between dissolved compound and solid compound. Thermodynamic assessment evaluates the solubility of solid crystalline material in aqueous solvent as a saturated solution in equilibrium. Due to the presence of DMSO, it is expected that the solubility obtained from kinetic methods generally yields results which are higher than the solubility determined by thermodynamic methods.   The relevance of thermodynamic solubility is less useful in drug discovery as it is not common for early in vitro screens to start with solid material. The importance of thermodynamic assessment is greater in late discovery / early development where it is used to confirm earlier KS results, to rule out potential artifacts and to generate high quality solubility data using crystalline materia. Taking into consideration this general rule a moderate deviation towards higher solubility limits might be expected in lipophilic compounds from CSIVM-KS where DMSO contents represents 1% of final volume in contrast with NIVA-CYPI-KS (0.35 % final content of DMSO). Pyrene, a polycyclic aromatic compound with very low water solubility [191] was used to assess the effect of DMSO content in turbidimetric solubility measurements (Figure 19F). As shown in Table 7, the

lowest concentration of pyrene displaying absorbance with intensity above the background signal (upper solubility bound) was 12.5 µM for the two methodologies under study. Additionally, the raw absorbance values of pyrene at 12.5 µM and the background controls (buffer / DMSO:AcN for NIVA-CYPI-KS and buffer / DMSO for CSIVM-KS) were very similar in both determinations. Hence, from the upper solubility limits determined for the rest of compounds, we can assume that the different contents of DMSO used in this work have very little effect on the solvation of compounds.

Replacement of DMSO by other co-solvents, such as AcN with lower UV absorption in the low UV range, causes similar problems in terms of enhancing solubility[111]. Thus, while keeping the total amount of organic solvent at 1%, no significant differences should be expected between methodologies for most compounds. Therefore, the effect of organic solvents should not be overemphasized since, even for DMSO concentrations as high as 5%, this effect produces an increase in solubility which is below 1 order of magnitude. We only observed a major difference in the upper solubility limit for bromocryptine. In this case, the compound displayed a 10-fold higher solubility limit in the presence of DMSO at 1%. Bromocriptine is an ergloid-based drug similar to ergotamine and ergonovine, which have been previously described as extremely lipophilic and soluble in DMSO (50 mg/ml) [192, 193]. Thus, bromocriptine might be more sensitive to the higher content of DMSO, enabling an increase in the solubility limits. According to the upper solubility determined for pyrene using NIVA-CYPI-KS (12.5 µM) and considering the reported aqueous solubility by thermodynamic methods for pyrene (0.02 µM), we can assume a detection limit for turbidimetric measurements in NIVA-CYPI-KS in the range of 1 to 10 µM, depending on the compound, which is perfectly in line with previously published reports and is appropriate for solubility screening since it covers the required

concentration levels in the assays used in early discovery [111]. Even though the dilution pattern considered for commercial compounds in either CSIVM-KS or NIVA-CYPI-KS was 1/2 in most cases, for some compounds, the replicates at some concentration levels were scattered either just below or just above the background threshold. This occurred for concentration values very close to the solubility limit. In such situations, the algorithm calculation was configured to set the upper and lower bounds at concentrations where absorbance values were clearly above or below the background threshold. Although this approach might enhance the solubility range between the upper and lower bounds making the classification in solubility categories difficult, it delivers more reproducible data. The close examination of absorbance values in the upper and lower solubility bounds enables predicting the solubility limit and therefore classifying it correct correctly.

5.4.3 Discussion

From these results we can conclude that NIVA-CYPI-KS enables us to monitor aqueous solubility and CYP3A4 inhibition using a unique experiment performance without compromising data quality. This NIVA-CYPI-KS offers many advantages due to conducting two assays in a single experiment, as compared to previously published separate methods for the evaluation of CP450 activity and aqueous solubility, such as a significant decrease in the amount of reagents, test compounds, materials necessary for experiments and in turnaround time. Additionally, this NIVA-CYPI-KS is also readily compatible with automation since experiments have been done successfully in 96-well plates using liquid handlers, an automated workstation, and autosamplers. In terms of data management, the data acquisition for solubility and CYP3A4 inhibition, achieved within a short time frame using NIVA-CYPI-KS, allows the effective analysis and interpretation of CYP3A4 inhibition data taking into account the real compound situation in the assay

solution. Solubility of drug candidates is very important because it affects gastrointestinal absorption of oral drugs. High potency and permeability can somewhat overcome solubility issues, but at the expense of increased cost and delays, and no guarantee of success. Low solubility can lead to a number of problems downstream (poor oral bioavailability, lack of efficacy, abnormal PK profile, inter-subject and inter-species variation, problematic formulation, toxicity of vehicles, prodrug approach, expensive and prolonged development, burden on patients in the case of multiple doses daily). Another critical issue is that low solubility might lead to erratic assay results in vitro, including erroneous SAR, discrepancies between biochemical and cell-based assays, artificially low potency, low HTS hit rate, underestimated toxicity (CYP450 inhibition, hERG blockage), or ultimately, inability to measure critical properties (membrane permeability, chemical and metabolic stability). Frequently, the correction of solubility issues is deferred during development by using novel formulations or delivery systems. However, this greatly increases the risk to project completion, because solubility issues might prove to be intractable. Early warning of the problem allows reacting and starting formulation efforts to prevent formulation from becoming a critical issue later on. Measurement of solubility from the early discovery level allows selection and optimization of compounds for improved solubility. This greatly enhances the prospects for success of a development candidate. This NIVA-CYPI-KS enables 8 individual compounds to be assessed in dose response format with up to 8 concentrations each. Strategies such as single-concentration to IC_{50} projection [194] might be considered to increase throughput after an extensive validation study. The use of 384-wellplates was also evaluated. However, it did not yield homogeneous suspension of the incubation components. Further investigation into the use of alternative shakers, mixing speed, and other conditions is needed to achieve stable

suspensions of the incubation matrix in a 384-well plate comparable to those achieved in a 96-deep-well plate. For all of the above mentioned reasons, this NIVA-CYPI-KS not only represents an improvement in terms of saving of resources but also interpretation of final results since the ability to simultaneously review the readouts for solubility and CYP3A4 inhibition through the GUI of GeneData Screener® enables identifiying those compound concentrations displaying solubility issues and then rejecting the corresponding data points for IC_{50} calculation since, especially in the case of moderate and strong inhibitors, those data points might affect dose response curve fitting and consequently the calculated IC_{50} value calculated.

5.4.3.1 Application of NIVA-CYPI-KS to lead compounds

To illustrate this situation, 5 drug discovery compounds from different FUNDACIÓN MEDINA research programs, which had been previously tested for the evaluation of CYP3A4 inhibition using the CSIVM-CYPI, were selected due to the partial inhibition profile observed from their respective dose response curves. The results obtained from the re-evaluation of these selected compounds using NIVA-CYPI-KS revealed that all the data points showing a partial inhibition profile displayed absorbance values above the organic solvent / buffer control and, consequently, they could be identified as presenting solubility issues (Figure 34). These data points were masked in the absorbance solubility layer in the GeneData Screener® GUI and afterwards synchronized with the corresponding CYP3A4 inhibition layer. As a result, these activity data points coming from compound concentrations in buffer solution showing absorbance values higher than
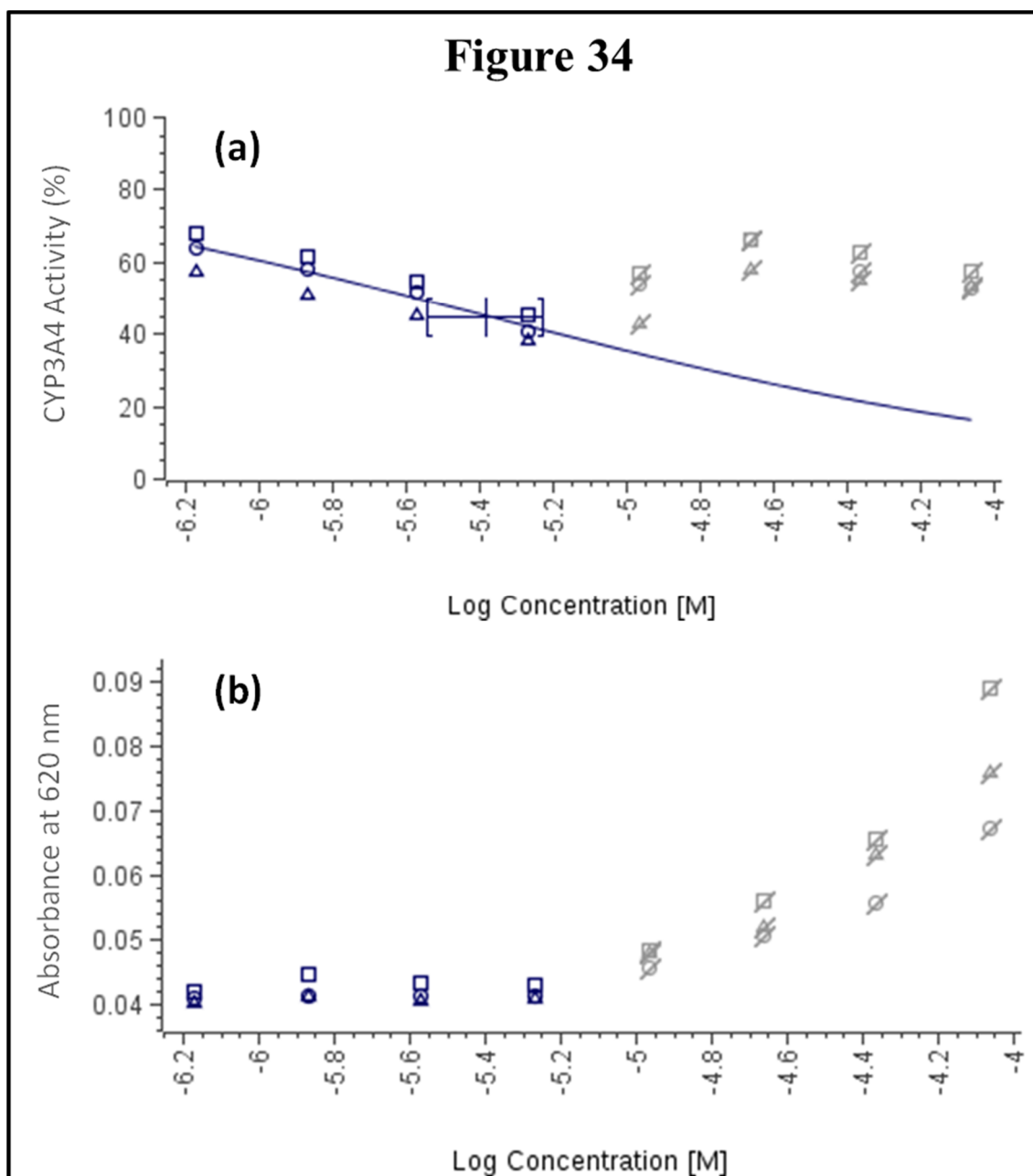
Figure 34

Figure 34. Dose response curves for lead compound 4 using NIVA-CYPI-KS.
(data are triplicates for each concentration point) (a) CYP3A4 Inhibition evaluation. (b) KS
evaluation.

buffer DMSO controls were not taken into account by the GeneData Screener® fitting

engine. After masking concentration points displaying solubility issues, the IC$_{50}$ value

was calculated by extrapolation from curve fitting using the Hill equation and assuming

the plateau values to be 0% and 100% at infinite concentration of test compound and at

zero concentration, respectively. This way the IC$_{50}$ rendered lower values (at least 17

fold) than those obtained from full dose response curves, considering all activity data points (Table 8).

Table 8. Summary of results for drug discovery compounds using NIVA-CYPI-KS

| | CYP3A4 IC$_{50}$ (µM) | | | Solubility range (µM) | | |
Compound ID	From full titration curve (a)	From corrected titration curve (b)	# of masked data points (c)	Lower bound	Upper bound	Solubility category
Compound 1	>86	4.27	4	5.39	10.78	Unacceptable
Compound 2	>86	5.01	4	5.39	10.78	Unacceptable
Compound 3	>86	2.86	4	5.39	10.78	Unacceptable
Compound 4	>86	4.12	4	5.39	10.78	Unacceptable
Compound 5	>86	5.76	4	5.39	10.78	Unacceptable

NIVA-CYPI-KS= Novel in vitro approach for simultaneous CYP450-inhibition and turbidimetric solubility evaluation. (a) The IC$_{50}$ is derived from a titration curve of 8 concentration levels without masking any data points. (b) The IC$_{50}$ is derived from the previous titration curve but masking the data points displaying solubility issues by turbidimetric evaluation. (c) Number of masked data points for IC$_{50}$ calculation due to solubility issues by turbidimetric evaluation.

Interestingly, the five drug discovery compounds considered for this study displayed turbidimetric solubility limits lower than 50 µM (Table 8), which represents a higher risk of developing artificially low inhibition of CYP450, as we have described in a previous section of the present work, undertaken to assess how compound aqueous solubility contributes to the lack of correlation observed in different in vitro models commonly used in CYP450 inhibition assessment. In that section, we demonstrated that this novel approach is really a very useful procedure for identifying drug candidates with artificially low CYP3A4 inhibition potential due to solubility issues.

6 CONCLUSIONS

NOS & CYP450 relationship

- This study suggests that the metabolites of RXT might be responsible for some of the observed pharmacological activity of RXT, highlighting the role of CYP450 activity in the development of pharmacological immunomodulation, especially for compounds undergoing time-dependent biotransformations through this enzymatic system.

Immunomodulatory activity

- It has been developed and validated an HTS platform which has been proven to be a robust, reliable, and comprehensive methodology in the 96-well format for the discovery of natural product–based drugs with immunomodulatory properties meeting the demanding requirements of HTS drug discovery. This allows large screening campaigns in a shorter time frame than typically required in natural product discovery.

- This HTS system also enabled to pick up on active extracts containing already known compounds for which the immunomodulatory activity had not been previously reported (TAN-2483A and TAN-2483B).

Solubility & CYP450 inhibition relationship

- It can be conclude that the distribution of KS clearly differs between commercial compounds and drug discovery compounds, with a clear bias towards low water solubility molecules in the latter set. Drug discovery compounds with low KS values largely contribute to the lack of correlation between testing methods for CYP450 inhibition. This means that these compounds are prone to being

categorized differently in terms of CYP450 inhibitory potency depending on the in vitro model used.

In summary these conclusions highlight the role of CYP450 enzyme system in the development of NO production and the importance of compound aqueous solubility for the correct interpretation of the in vitro results. Additionally, this work also demonstrates the feasibility to develop HTS platforms to evaluate key compound properties such us CYP450 inhibition, aqueous solubility and immunomodulatory activity

A novel in vitro approach for ADME

- A high-throughput ADME profiling system has been implemented using this NIVA-CYPI-KS which provides the throughput required to analyze a large number of early ADME samples while maintaining high data quality. Its ability to integrate and synchronize CYP3A4 inhibition and solubility data in a single result reviewing session speeds up the candidate selection process and provides a more correct compound classification in terms of potential to inhibit CYP3A4 activity.

7 REFERENCES

1. Boucher J-L, Genet A, Vadon S, Delaforge M, Henry Y, Mansuy D: **Cytochrome P450 catalyzes the oxidation of Nω-hydroxy-L-arginine by NADPH and O2 to nitric oxide and citrulline**. *Biochem Biophys Res Commun* 1992, **187**:880–886.

2. Gorren AC, Mayer B: **Nitric-oxide synthase: a cytochrome P450 family foster child**. *Biochim Biophys Acta* 2007, **1770**:432–445.

3. Masters BS: **The journey from NADPH-cytochrome P450 oxidoreductase to nitric oxide synthases**. *Biochem Biophys Res Commun* 2005, **338**:507–519.

4. Bredt DS, Hwang PM, Glatt CE, Lowenstein C, Reed RR, Snyder SH: **Cloned and expressed nitric oxide synthase structurally resembles cytochrome P-450 reductase**. *Nature* 1991, **351**:714–718.

5. Sono M, Roach MP, Coulter ED, Dawson JH: **Heme-Containing Oxygenases**. *Chem Rev* 1996, **96**:2841–2888.

6. Meunier B, de Visser SP, Shaik S: **Mechanism of oxidation reactions catalyzed by cytochrome p450 enzymes**. *Chem Rev* 2004, **104**:3947–3980.

7. Martin J, Fay M: **Cytochrome P450 drug interactions: are they clinically relevant?** *Aust Prescr* 2001, **24**:10–12.

8. Smith HS: **Opioid metabolism.** *Mayo Clin Proc* 2009, **84**:613–24.

9. Page RL, Miller GG, Lindenfeld J: **Drug Therapy in the Heart Transplant Recipient**. *Circulation* 2005, **111**.

10. Joubert J, Malan SF: **Novel nitric oxide synthase inhibitors: a patent review**. *Expert Opin Ther Pat* , **21**:537–560.

11. Niwa T, Shiraga T, Takagi A: **Effect of antifungal drugs on cytochrome P450 (CYP) 2C9, CYP2C19, and CYP3A4 activities in human liver microsomes**. *Biol Pharm Bull* 2005, **28**:1805–1808.

12. Wolff DJ, Datto GA, Samatovicz RA: **The dual mode of inhibition of calmodulin-dependent nitric-oxide synthase by antifungal imidazole agents**. *J Biol Chem* 1993, **268**:9430–9436.

13. Hutzler JM, Melton RJ, Rumsey JM, Schnute ME, Locuson CW, Wienkers LC: **Inhibition of Cytochrome P450 3A4 by a Pyrimidineimidazole: Evidence for Complex Heme Interactions**. *Chem Res Toxicol* 2006, **19**:1650–1659.

14. Hutzler JM, Melton RJ, Rumsey JM, Schnute ME, Locuson CW, Wienkers LC: **Inhibition of Cytochrome P450 3A4 by a Pyrimidineimidazole: Evidence for Complex Heme Interactions**. *Chem Res Toxicol* 2006, **19**:1650–1659.

15. Jones JP, Joswig-Jones CA, Hebner M, Chu Y, Koop DR: **The effects of nitrogen-heme-iron coordination on substrate affinities for cytochrome P450 2E1**. *Chem Biol*

Interact 2011, **193**:50–6.

16. Gao X, Ray R, Xiao Y, Ray P: **Suppression of inducible nitric oxide synthase expression and nitric oxide production by macrolide antibiotics in sulfur mustard-exposed airway epithelial cells.** *Basic Clin Pharmacol Toxicol* 2008, **103**:255–61.

17. Buret AG: **Immuno-modulation and anti-inflammatory benefits of antibiotics: the example of tilmicosin.** *Can J Vet Res = Rev Can Rech vétérinaire* 2010, **74**:1–10.

18. Yamazaki H, Shimada T: **Comparative studies of in vitro inhibition of cytochrome P450 3A4-dependent testosterone 6beta-hydroxylation by roxithromycin and its metabolites, troleandomycin, and erythromycin.** *Drug Metab Dispos* 1998, **26**:1053–1057.

19. Zweers-Zeilmaker WM, Van Miert ASJPAM, Horbach GJ, Witkamp RF: **In vitro complex formation and inhibition of hepatic cytochrome P450 activity by different macrolides and tiamulin in goats and cattle.** *Res Vet Sci* 1999, **66**:51–55.

20. Soldatow VY, Lecluyse EL, Griffith LG, Rusyn I: **In vitro models for liver toxicity testing.** *Toxicol Res (Camb)* 2013, **2**:23–39.

21. Periti P, Mazzei T, Mini E, Novelli A: **Pharmacokinetic Drug Interactions of Macrolides.** *Clin Pharmacokinet* 1992, **23**:106–131.

22. Chawla A: **Control of Macrophage Activation and Function by PPARs.** *Circ Res* 2010, **106**.

23. Gayathri B, Manjula N, Vinaykumar KS, Lakshmi BS, Balakrishnan A: **Pure compound from Boswellia serrata extract exhibits anti-inflammatory property in human PBMCs and mouse macrophages through inhibition of TNFα, IL-1β, NO and MAP kinases.** *Int Immunopharmacol* 2007, **7**:473–482.

24. Kim GS, Kang SR, Han DY, Park K Il, Park HS, Cho YB, Lee HJ, Lee WS, Ryu CH, Ha YL, Lee DH, Kim JA: **Suppressive effect on lipopolysaccharide-induced proinflammatory mediators by Citrus aurantium L. in macrophage RAW 264.7 cells via NF-κB signal pathway.** *Evidence-based Complement Altern Med* 2011, **2011**.

25. MacMicking J, Xie QW, Nathan C: **Nitric oxide and macrophage function.** *Annu Rev Immunol* 1997, **15**:323–350.

26. Ghonime M, Emara M, Shawky R, Soliman H, El-Domany R, Abdelaziz A: **Immunomodulation of RAW 264.7 murine macrophage functions and antioxidant activities of 11 plant extracts.** *Immunol Invest* 2015, **44**:237–52.

27. Ahn KS, Noh EJ, Zhao HL, Jung SH, Kang SS, Kim YS: **Inhibition of inducible nitric oxide synthase and cyclooxygenase II by Platycodon grandiflorum saponins via suppression of nuclear factor-κB activation in RAW 264.7 cells.** *Life Sci* 2005, **76**:2315–2328.

28. Lyu S-Y, Park W-B: **Production of Cytokine and NO by RAW 264.7 Macrophages and PBMC In Vitro Incubation with Flavonoids.** *Arch Pharm Res* 2005, **28**:573–581.

29. Collin-Osdoby P, Osdoby P: **RANKL-mediated osteoclast formation from murine RAW 264.7 cells.** *Methods Mol Biol* 2012, **816**:187–202.

30. Rodríguez-Antona C, Donato MT, Boobis A, Edwards RJ, Watts PS, Castell JV, Gómez-Lechón M-J: **Cytochrome P450 expression in human hepatocytes and hepatoma cell lines: molecular mechanisms that determine lower expression in cultured cells**. *Xenobiotica* 2002, **32**:505–520.

31. Hill JR, Hill, R. J: **In Vitro Drug Metabolism Using Liver Microsomes**. In *Current Protocols in Pharmacology*. Hoboken, NJ, USA: John Wiley & Sons, Inc.; 2004:7.8.1-7.8.11.

32. Cederbaum AI: **Molecular mechanisms of the microsomal mixed function oxidases and biological and pathological implications.** *Redox Biol* 2015, **4**:60–73.

33. Wienkers LC, Heath TG: **Predicting in vivo drug interactions from in vitro drug discovery data**. *Nat Rev Drug Discov* 2005, **4**:825–833.

34. Hollenberg PF: **Characteristics and common properties of inhibitors, inducers, and activators of CYP enzymes**. *Drug Metab Rev* 2002, **34**:17–35.

35. Silverman R.: *Mechanism-Based Enzyme Inactivation: Chemistry and Biology*. Boca Raton: Boca Raton; 1988.

36. Ator, M.A.; Ortiz de Montellano PR: **Mechanism-Based (Suicide) Enzyme Inactivation.** In *In The Enzymes: Mechanisms of Catalysis*. 3rd Ed. Edited by Segman DS, Boyer, P.D. E. New York: Academic Press; 1990:214–282.

37. Kent UM, Juschyshyn MI, Hollenberg PF: **Mechanism-based inactivators as probes of cytochrome P450 structure and function.** *Curr Drug Metab* 2001, **2**:215–43.

38. Krippendorff BF, Neuhaus R, Lienau P, Reichel A, Huisinga W: **Mechanism-based inhibition: deriving K(I) and k(inact) directly from time-dependent IC(50) values**. *J Biomol Screen* 2009, **14**:913–923.

39. De Montellano PRO: *Cytochrome P450: Structure, Mechanism, and Biochemistry: Third Edition*. 2005.

40. Ackley DC, Rockich KT, Baker TR: **Metabolic Stability Assessed by Liver Microsomes and Hepatocytes**. In *Optimization in Drug Discovery*. Totowa, NJ: Humana Press; 2004:151–162.

41. Masimirembwa CM, Bredberg U, Andersson TB: **Metabolic stability for drug discovery and development: pharmacokinetic and biochemical challenges.** *Clin Pharmacokinet* 2003, **42**:515–28.

42. Nassar AF: **Approaches to Performing Metabolite Elucidation: One Key to Success in Drug Discovery and Development**. In *Drug Metabolism Handbook*. Hoboken, NJ, USA: John Wiley & Sons, Inc.; :229–251.

43. Zhu M, Zhang H, Humphreys WG: **Drug metabolite profiling and identification by high-resolution mass spectrometry.** *J Biol Chem* 2011, **286**:25419–25.

44. Reichman M: **Automated Drug Screening for ADMET Properties**. In *Drug Metabolism handbook: Conceps and Applications*. Edited by Nassar AF. Hoboken, New Jersey: John Wiley & Sons, Inc.; 2009:129–166.

45. Popa-Burke IG, Issakova O, Arroway JD, Bernasconi P, Chen M, Coudurier L, Galasinski S, Jadhav AP, Janzen WP, Lagasca D, Liu D, Lewis RS, Mohney RP, Sepetov N, Sparkman DA, Hodge CN: **Streamlined system for purifying and quantifying a diverse library of compounds and the effect of compound concentration measurements on the accurate interpretation of biological assay results**. *Anal Chem* 2004, **76**:7278–7287.

46. Ghonime M, Emara M, Shawky R, Soliman H, El-Domany R, Abdelaziz A: **Immunomodulation of RAW 264.7 Murine Macrophage Functions and Antioxidant Activities of 11 Plant Extracts**. *Immunol Invest* 2015, **44**:237–252.

47. Duary RK, Batish VK, Grover S: **Immunomodulatory activity of two potential probiotic strains in LPS-stimulated HT-29 cells.** *Genes Nutr* 2014, **9**:398.

48. Astashkina A, Mann B, Grainger DW: **A critical evaluation of in vitro cell culture models for high-throughput drug screening and toxicity**. *Pharmacol Ther* 2012, **134**:82–106.

49. Amor S, Puentes F, Baker D, van der Valk P: **Inflammation in neurodegenerative diseases.** *Immunology* 2010, **129**:154–69.

50. Rubio-Perez JM, Morillas-Ruiz JM: **A review: inflammatory process in Alzheimer's disease, role of cytokines.** *ScientificWorldJournal* 2012, **2012**:756357.

51. Brunetti J, Roscia G, Lampronti I, Gambari R, Quercini L, Falciani C, Bracci L, Pini A: **Immunomodulatory and Anti-inflammatory Activity in Vitro and in Vivo of a Novel Antimicrobial Candidate.** *J Biol Chem* 2016, **291**:25742–25748.

52. Jantan I, Ahmad W, Bukhari SNA: **Plant-derived immunomodulators: an insight on their preclinical evaluation and clinical trials.** *Front Plant Sci* 2015, **6**:655.

53. Vezza T, Rodríguez-Nogales A, Algieri F, Utrilla MP, Rodriguez-Cabezas ME, Galvez J: **Flavonoids in Inflammatory Bowel Disease: A Review.** *Nutrients* 2016, **8**:211.

54. Kanwar JR, Kanwar RK: **Gut health immunomodulatory and anti-inflammatory functions of gut enzyme digested high protein micro-nutrient dietary supplement-Enprocal.** *BMC Immunol* 2009, **10**:7.

55. Bahrami B, Child MW, Macfarlane S, Macfarlane GT: **Adherence and cytokine induction in Caco-2 cells by bacterial populations from a three-stage continuous-culture model of the large intestine.** *Appl Environ Microbiol* 2011, **77**:2934–42.

56. Schuerer-Maly CC, Eckmann L, Kagnoff MF, Falco MT, Maly FE: **Colonic epithelial cell lines as a source of interleukin-8: stimulation by inflammatory cytokines and bacterial lipopolysaccharide.** *Immunology* 1994, **81**:85–91.

57. Nishitani Y, Zhang L, Yoshida M, Azuma T, Kanazawa K, Hashimoto T, Mizuno M:

Intestinal anti-inflammatory activity of lentinan: influence on IL-8 and TNFR1 expression in intestinal epithelial cells. *PLoS One* 2013, **8**:e62441.

58. Seo JY, Yu J-H, Lim JW, Mukaida N, Kim H: **Nitric oxide-induced IL-8 expression is mediated by NF-kappaB and AP-1 in gastric epithelial AGS cells.** *J Physiol Pharmacol* 2009, **60 Suppl 7**:101–6.

59. Schuerer-Maly C-C, Eckmann L, Kagnoff MF, Falco MT, Malyt F-E: **Colonic epithelial cell lines as a source of interleukin-8: stimulation by inflammatory cytokines and bacterial lipopolysaccharide**. *Immunology* 1994, **81**:85–91.

60. Feher M, Schmidt JM: **Property Distributions: Differences between Drugs, Natural Products, and Molecules from Combinatorial Chemistry**. *J Chem Inf Comput Sci* 2003, **43**:218–227.

61. Lipinski CA, Lombardo F, Dominy BW, Feeney PJ: **Experimental and computational approaches to estimate solubility and permeability in drug discovery and development settings.** *Adv Drug Deliv Rev* 2001, **46**:3–26.

62. Lee ML, Schneider G: **Scaffold architecture and pharmacophoric properties of natural products and trade drugs: Application in the design of natural product-based combinatorial libraries**. *J Comb Chem* 2001, **3**:284–289.

63. Stahura FL, Godden JW, Xue L: **Distinguishing Between Natural Products and Synthetic Molecules by Descriptor Shannon Entropy Analysis and Binary QSAR Calculations**. *J Chem Inf Comput Sci* 2000, **40**:1245–1252.

64. Schmid II, Sattler II, Grabley S, Thiericke R: **Natural Products in High Throughput Screening: Automated High-Quality Sample Preparation**. *J Biomol Screen* 1999, **4**:15–25.

65. Annang F, Perez-Moreno G, Garcia-Hernandez R, Cordon-Obras C, Martin J, Tormo JR, Rodriguez L, de Pedro N, Gomez-Perez V, Valente M, Reyes F, Genilloud O, Vicente F, Castanys S, Ruiz-Perez LM, Navarro M, Gamarro F, Gonzalez-Pacanowska D: **High-throughput screening platform for natural product-based drug discovery against 3 neglected tropical diseases: human African trypanosomiasis, leishmaniasis, and Chagas disease.** *J Biomol Screen* 2015, **20**:82–91.

66. Genilloud O, González I, Salazar O, Martín J, Tormo JR, Vicente F: **Current approaches to exploit actinomycetes as a source of novel natural products**. *J Ind Microbiol Biotechnol* 2011, **38**:375–389.

67. Monciardini P, Iorio M, Maffioli S, Sosio M, Donadio S: **Discovering new bioactive molecules from microbial sources**. *Microb Biotechnol* 2014, **7**:209–220.

68. D'Arena G, Simeon V, De Martino L, Statuto T, D'Auria F, Volpe S, Deaglio S, Maidecchi A, Mattoli L, Mercati V, Musto P, De Feo V: **Regulatory T-cell modulation by green tea in chronic lymphocytic leukemia**. *Int J Immunopathol Pharmacol* 2013, **26**:117–125.

69. Skinner MA, Bentley-Hewitt K, Rosendale D, Naoko S, Pernthaner A: **Effects of**

Kiwifruit on Innate and Adaptive Immunity and Symptoms of Upper Respiratory Tract Infections. *Adv Food Nutr Res* 2013, **68**:301–320.

70. Kayser O, Masihi KN, Kiderlen AF: **Natural products and synthetic compounds as immunomodulators**. *Expert Rev Anti Infect Ther* 2003, **1**:319–335.

71. Atanasov AG, Waltenberger B, Pferschy-Wenzig E-M, Linder T, Wawrosch C, Uhrin P, Temml V, Wang L, Schwaiger S, Heiss EH, Rollinger JM, Schuster D, Breuss JM, Bochkov V, Mihovilovic MD, Kopp B, Bauer R, Dirsch VM, Stuppner H: **Discovery and resupply of pharmacologically active plant-derived natural products: A review.** *Biotechnol Adv* 2015, **33**:1582–614.

72. Gautam R, Jachak SM: **Recent developments in anti-inflammatory natural products**. *Medicinal Research Reviews* 2009:767–820.

73. E. A. Elsayed, H. El Enshasy MAMW and RA: **Mushrooms: A Potential Natural Source of Anti-Inflammatory Compounds for Medical Applications**. *Mediators Inflamm* 2014, **2014**:15.

74. Webb S: **Leveraging the Promise of Chemical Genomics**. *Biotechniques* 2012, **52**:17–9.

75. Koehn FE, Carter GT: **The evolving role of natural products in drug discovery**. *Nat Rev Drug Discov* 2005, **4**:206–220.

76. Singh SB, Pelaez F: **Biodiversity, chemical diversity and drug discovery**. In *Natural Compounds as Drugs Volume I*. Basel: Birkhäuser Basel; 2008:141–174.

77. Clardy J, Walsh C: **Lessons from natural molecules**. *Nature* 2004, **432**:829–837.

78. Wang J, Soisson SM, Young K, Shoop W, Kodali S, Galgoci A, Painter R, Parthasarathy G, Tang YS, Cummings R, Ha S, Dorso K, Motyl M, Jayasuriya H, Ondeyka J, Herath K, Zhang C, Hernandez L, Allocco J, Basilio N, Tormo JR, Genilloud O, Vicente F, Pelaez F, Colwell L, Lee SH, Michael B, Felcetto T, Gill C, Silver LL, et al.: **Platensimycin is a selective FabF inhibitor with potent antibiotic properties**. *Nature* 2006, **441**(May):358–361.

79. Zlokarnik G, Grootenhuis PD, Watson JB: **High throughput P450 inhibition screens in early drug discovery**. *Drug Discov Today* 2005, **10**:1443–1450.

80. Krippendorff BF, Lienau P, Reichel A, Huisinga W: **Optimizing classification of drug-drug interaction potential for CYP450 isoenzyme inhibition assays in early drug discovery**. *J Biomol Screen* 2007, **12**:92–99.

81. Yao M, Cai H, Zhu M: **Fast and Reliable CYP Inhibition Assays**. In *ADME-Enabling Technologies in Drug Design and Development*. Hoboken, NJ, USA: John Wiley & Sons, Inc.; 2012:213–232.

82. Moody GC, Griffin SJ, Mather AN, McGinnity DF, Riley RJ: **Fully automated analysis of activities catalysed by the major human liver cytochrome P450 (CYP) enzymes: assessment of human CYP inhibition potential**. *Xenobiotica* 1999, **29**:53–75.

83. Rodrigues AD, Lin JH: **Screening of drug candidates for their drug--drug interaction potential**. *Curr Opin Chem Biol* 2001, **5**:396–401.

84. Stresser DM, Turner SD, Blanchard AP, Miller VP, Crespi CL: **Cytochrome P450 fluorometric substrates: identification of isoform-selective probes for rat CYP2D2 and human CYP3A4.** *Drug Metab Dispos* 2002, **30**:845–52.

85. Bell L, Bickford S, Nguyen PH, Wang J, He T, Zhang B, Friche Y, Zimmerlin A, Urban L, Bojanic D: **Evaluation of fluorescence- and mass spectrometry-based CYP inhibition assays for use in drug discovery**. *J Biomol Screen* 2008, **13**:343–353.

86. Fowler S, Zhang H: **In vitro evaluation of reversible and irreversible cytochrome P450 inhibition: current status on methodologies and their utility for predicting drug-drug interactions**. *AAPS J* 2008, **10**:410–424.

87. Jenkins KM, Angeles R, Quintos MT, Xu R, Kassel DB, Rourick RA: **Automated high throughput ADME assays for metabolic stability and cytochrome P450 inhibition profiling of combinatorial libraries**. *J Pharm Biomed Anal* 2004, **34**:989–1004.

88. Walsky RL, Obach RS: **Validated assays for human cytochrome P450 activities**. *Drug Metab Dispos* 2004, **32**:647–660.

89. Yao M, Zhu M, Sinz MW, Zhang H, Humphreys WG, Rodrigues AD, Dai R: **Development and full validation of six inhibition assays for five major cytochrome P450 enzymes in human liver microsomes using an automated 96-well microplate incubation format and LC–MS/MS analysis**. *J Pharm Biomed Anal* 2007, **44**:211–223.

90. Li C, Kalyanaraman N: **Reaction Phenotyping**. In *ADME-Enabling Technologies in Drug Design and Development*. Hoboken, NJ, USA: John Wiley & Sons, Inc.; 2012:189–212.

91. Miller VP, Stresser DM, Blanchard AP, Turner S, Crespi CL: **Fluorometric high-throughput screening for inhibitors of cytochrome P450**. *Ann N Y Acad Sci* 2000, **919**:26–32.

92. Guengerich FP, Parikh A, Johnson EF, Richardson TH, von Wachenfeldt C, Cosme J, Jung F, Strassburg CP, Manns MP, Tukey RH, Pritchard M, Fournel-Gigleux S, Burchell B: **Heterologous expression of human drug-metabolizing enzymes.** *Drug Metab Dispos* 1997, **25**:1234–41.

93. FRIEDBERG T, PRITCHARD MP, BANDERA M, HANLON SP, YAO D, McLAUGHLIN LA, DING S, BURCHELL B, WOLF CR: **MERITS AND LIMITATIONS OF RECOMBINANT MODELS FOR THE STUDY OF HUMAN P450-MEDIATED DRUG METABOLISM AND TOXICITY: AN INTRALABORATORY COMPARISON**. *Drug Metab Rev* 1999, **31**:523–544.

94. Brandon EFA, Raap CD, Meijerman I, Beijnen JH, Schellens JHM: **An update on in vitro test methods in human hepatic drug biotransformation research: pros and cons**. .

95. McMasters DR, Torres RA, Crathern SJ, Dooney DL, Nachbar RB, Sheridan RP, Korzekwa KR: **Inhibition of recombinant cytochrome P450 isoforms 2D6 and 2C9 by diverse drug-like molecules**. *J Med Chem* 2007, **50**:3205–3213.

96. Saal C, Petereit AC: **Optimizing solubility: kinetic versus thermodynamic solubility temptations and risks**. *Eur J Pharm Sci* , **47**:589–595.

97. Hoelke B, Gieringer S, Arlt M, Saal C: **Comparison of nephelometric, UV-spectroscopic, and HPLC methods for high-throughput determination of aqueous drug solubility in microtiter plates**. *Anal Chem* 2009, **81**:3165–3172.

98. Bevan CD, Lloyd RS: **A high-throughput screening method for the determination of aqueous drug solubility using laser nephelometry in microtiter plates.** *Anal Chem* 2000, **72**:1781–7.

99. Kerns EH: **High throughput physicochemical profiling for drug discovery**. *Journal of Pharmaceutical Sciences* 2001:1838–1858.

100. Ishiguro K, Ihara Y, Uchida T, Imahori K: **A novel tubulin-dependent protein kinase forming a paired helical filament epitope on tau.** *J Biochem* 1988, **104**:319–21.

101. Manoukian AS, Woodgett JR: **Role of glycogen synthase kinase-3 in cancer: regulation by Wnts and other signaling pathways.** *Adv Cancer Res* 2002, **84**:203–29.

102. Hardt SE, Sadoshima J: **Glycogen synthase kinase-3beta: a novel regulator of cardiac hypertrophy and development.** *Circ Res* 2002, **90**:1055–63.

103. AVILA J, Lucas JJ, Perez M, Hernandez F: **Role of Tau Protein in Both Physiological and Pathological Conditions**. *Physiol Rev* 2004, **84**:361–384.

104. Wang Z, Smith KS, Murphy M, Piloto O, Somervaille TCP, Cleary ML: **Glycogen synthase kinase 3 in MLL leukaemia maintenance and targeted therapy**. *Nature* 2008, **455**:1205–1209.

105. Hernandez F, Nido J, Avila J, Villanueva N: **GSK3 Inhibitors and Disease**. *Mini-Reviews Med Chem* 2009, **9**:1024–1029.

106. Kerns EH, Di L: *Drug-like Properties: Concepts, Structure Design and Methods from ADME to Toxicity Optimization. Volume 53*; 2013.

107. Martins P, Jesus J, Santos S, Raposo L, Roma-Rodrigues C, Baptista P, Fernandes A: **Heterocyclic Anticancer Compounds: Recent Advances and the Paradigm Shift towards the Use of Nanomedicine's Tool Box**. *Molecules* 2015, **20**:16852–16891.

108. Wang B, Siahaan T, Soltero R: *Drug Delivery : Principles and Applications*. Hoboken ; [Chichester]: Wiley-Interscience; 2005.

109. Crespi CL, Miller VP, Stresser DM: **Design and Application of Fluorogenic Assays for Human Cytochrome P450 Inhibition**. In *Cytochrome P450. Volume Vol 357*. Edited by Johnson EF, Waterman MR. Amsterdam ; London: Academic Press; 2002.

110. Hann MM: **Molecular obesity, potency and other addictions in drug discovery**.

Medchemcomm 2011, **2**:349–355.

111. Petereit A, Saal C: **What is the Solubility of My Compound? Assessing Solubility for Pharmaceutical Research and Development Compounds**. *Am Pharm Rev* 2011, **14**.

112. Dressman J, Butler J, Hempenstall J: **The BCS: Where Do We Go from Here?** *Pharm Technol* 2001, **25**:68–76.

113. Rodríguez-Antona C, Donato MT, Boobis A, Edwards RJ, Watts PS, Castell JV, Gómez-Lechón M-J: **Cytochrome P450 expression in human hepatocytes and hepatoma cell lines: molecular mechanisms that determine lower expression in cultured cells**. *Xenobiotica* 2002, **32**:505–520.

114. Garrido-Mesa N, Camuesco D, Arribas B, Comalada M, Bailon E, Cueto-Sola M, Utrilla P, Nieto A, Zarzuelo A, Rodriguez-Cabezas ME, Galvez J: **The intestinal anti-inflammatory effect of minocycline in experimental colitis involves both its immunomodulatory and antimicrobial properties**. *Pharmacol Res* 2010, **63**:308–319.

115. Hukkanen J, Pelkonen O, Hakkola J, Raunio H: **Expression and regulation of xenobiotic-metabolizing cytochrome P450 (CYP) enzymes in human lung.** *Crit Rev Toxicol* 2002, **32**:391–411.

116. Hukkanen J: **Xenobiotic-metabolizing cytochrome P450 enzymes in human lung**. 2000.

117. Perez J, Diaz C, Asensio F, Palafox A, Genilloud O, Vicente F: **A novel in vitro approach for simultaneous evaluation of CYP3A4 inhibition and kinetic aqueous solubility**. *J Biomol Screen* 2015, **20**:254–264.

118. Obach RS: **Prediction of human clearance of twenty-nine drugs from hepatic microsomal intrinsic clearance data: An examination of in vitro half-life approach and nonspecific binding to microsomes**. *Drug Metab Dispos* 1999, **27**:1350–1359.

119. Obach RS, Walsky RL, Venkatakrishnan K, Gaman EA, Houston JB, Tremaine LM: **The utility of in vitro cytochrome P450 inhibition data in the prediction of drug-drug interactions**. *J Pharmacol Exp Ther* 2006, **316**:336–348.

120. Yang S, Shi W, Hu D, Zhang S, Zhang H, Wang Z, Cheng L, Sun F, Shen J, Cao X: **In Vitro and in Vivo Metabolite Profiling of Valnemulin Using Ultraperformance Liquid Chromatography–Quadrupole/Time-of-Flight Hybrid Mass Spectrometry**. *J Agric Food Chem* 2014, **62**:9201–9210.

121. Burt HJ, Galetin A, Houston JB: **IC50-based approaches as an alternative method for assessment of time-dependent inhibition of CYP3A4**. *Xenobiotica* 2010, **40**:331–343.

122. Barsoumian H, El-Rami F, Abdelnoor AM: **The effect of five antibacterial agents on the physiological levels of serum nitric oxide in mice**. *Immunopharmacol Immunotoxicol* , **33**:652–655.

123. Mosmann T: **Rapid colorimetric assay for cellular growth and survival:**

application to proliferation and cytotoxicity assays. *J Immunol Methods* 1983, **65**:55–63.

124. Polasek TM, Miners JO: **Quantitative prediction of macrolide drug-drug interaction potential from in vitro studies using testosterone as the human cytochrome P4503A substrate**. *Eur J Clin Pharmacol* 2006, **62**:203–208.

125. Silverman RB: **Mechanism-based enzyme inactivators**. *Methods Enzym* 1995, **249**:240–283.

126. Zhong D, Li X, Wang A, Xu Y, Wu S: **Identification of the metabolites of roxithromycin in humans**. *Drug Metab Dispos* 2000, **28**:552–559.

127. Pérez-Victoria I, Martín J, Reyes F: **Combined LC/UV/MS and NMR Strategies for the Dereplication of Marine Natural Products**. *Planta Med* 2016, **82**(09/10):857–871.

128. Bills GF, Menéndez VG, Platas G: **Kabatiella bupleuri sp. nov. (Dothideales), a pleomorphic epiphyte and endophyte of the Mediterranean plant Bupleurum gibraltarium (Apiaceae)**. *Mycologia* 2012, **104**:962–73.

129. Gao X, Snider BB: **Syntheses of (-)-TAN-2483A, (-)-massarilactone B, and the fusidilactone B ring system. Revision of the structures of and syntheses of (+/-)-Waol A (FD-211) and (+/-)-Waol B (FD-212)**. *J Org Chem* 2004, **69**:5517–27.

130. Audoin C, Bonhomme D, Ivanisevic J, de la Cruz M, Cautain B, Monteiro MC, Reyes F, Rios L, Perez T, Thomas OP: **Balibalosides, an original family of glucosylated sesterterpenes produced by the mediterranean sponge Oscarella balibaloi.** *Mar Drugs* 2013, **11**:1477–89.

131. Rodrigues AD: **Integrated cytochrome P450 reaction phenotyping. Attempting to bridge the gap between cDNA-expressed cytochromes P450 and native human liver microsomes**. *Biochemical Pharmacology* 1999:465–480.

132. Stresser DM, Turner SD, Blanchard AP, Miller VP, Crespi CL: **Cytochrome P450 fluorometric substrates: identification of isoform-selective probes for rat CYP2D2 and human CYP3A4**. *Drug Metab Dispos* 2002, **30**:845–852.

133. Zhang JH, Chung TD, Oldenburg KR: **A Simple Statistical Parameter for Use in Evaluation and Validation of High Throughput Screening Assays**. *J Biomol Screen* 1999, **4**:67–73.

134. Rogge MC, Taft DR: **Preclinical Drug Development**. 2010.

135. Pérez J, Díaz C, Asensio F, Palafox A, Genilloud O, Vicente F: **A Novel In Vitro Approach for Simultaneous Evaluation of CYP3A4 Inhibition and Kinetic Aqueous Solubility**. *J Biomol Screen* 2015, **20**:254–264.

136. Bogle RG, Whitley GS, Soo SC, Johnstone AP, Vallance P: **Effect of anti-fungal imidazoles on mRNA levels and enzyme activity of inducible nitric oxide synthase**. *Br J Pharmacol* 1994, **111**:1257–1261.

137. Vermuyten K, Laurijssens L, Vanden Bossche H: **Azole antifungals: weak inhibitors of inducible nitric oxide synthase in mouse and human cells**. *Mycoses* 1997, **40**:119–125.

138. Zarogoulidis P, Papanas N, Kioumis I, Chatzaki E, Maltezos E, Zarogoulidis K: **Macrolides: from in vitro anti-inflammatory and immunomodulatory properties to clinical practice in respiratory diseases**. *Eur J Clin Pharmacol* , **68**:479–503.

139. LeCluyse EL: **Human hepatocyte culture systems for the in vitro evaluation of cytochrome P450 expression and regulation**. *Eur J Pharm Sci* 2001, **13**:343–368.

140. Bogle RG, Vallance P: **Functional effects of econazole on inducible nitric oxide synthase: production of a calmodulin-dependent enzyme**. *Br J Pharmacol* 1996, **117**:1053–1058.

141. Dercho RA: **Novel azole-based heme oxygenase inhibitors: in vivo characterization and therapeutic application in cancer**. Queen's University; 2015.

142. Savjani KT, Gajjar AK, Savjani JK: **Drug solubility: importance and enhancement techniques.** *ISRN Pharm* 2012, **2012**:195727.

143. Pérez J, Díaz C, Salado IG, Pérez DI, Peláez F, Genilloud O, Vicente F: **Evaluation of the effect of compound aqueous solubility in cytochrome P450 inhibition assays**. *Adv Biosci Biotechnol* 2013, **4**:12.

144. Scheven M, Scheven C, Hahn K, Senf A: **Post-antibiotic effect and post-expositional polyene antagonism of azole antifungal agents in Candida albicans: dependence on substance lipophilia**. *Mycoses* 1995, **38**:435–442.

145. Moeller TA, Shukla SJ, Xia M: **Assessment of compound hepatotoxicity using human plateable cryopreserved hepatocytes in a 1536-well-plate format.** *Assay Drug Dev Technol* 2012, **10**:78–87.

146. Galetin A, Burt H, Gibbons L, Houston JB: **Prediction of time-dependent cyp3a4 drug-drug interactions: impact of enzyme degradation, parallel elimination pathways, and intestinal inhibition**. *Drug Metab Dispos* 2006, **34**:166–175.

147. Walker GS, Ryder TF, Sharma R, Smith EB, Freund A: **Validation of Isolated Metabolites from Drug Metabolism Studies as Analytical Standards by Quantitative NMR**. *Drug Metab Dispos* 2011, **39**:433–440.

148. Espina R, Yu L, Wang J, Tong Z, Vashishtha S, Talaat R, Scatina J, Mutlib A: **Nuclear magnetic resonance spectroscopy as a quantitative tool to determine the concentrations of biologically produced metabolites: implications in metabolites in safety testing**. *Chem Res Toxicol* 2009, **22**:299–310.

149. Kassel DB: **The Expanding Role of HPLC in Drug Discovery**. In *HPLC for Pharmaceutical Scientists*. John Wiley & Sons, Inc.; 2006:533–575.

150. Kohri K, Tamaoki J, Kondo M, Aoshiba K, Tagaya E, Nagai A: **Macrolide antibiotics inhibit nitric oxide generation by rat pulmonary alveolar macrophages**. *Eur Respir J* 2000, **15**:62–67.

151. Tamaoki J, Kondo M, Kohri K, Aoshiba K, Tagaya E, Nagai A: **Macrolide antibiotics protect against immune complex-induced lung injury in rats: role of nitric oxide from alveolar macrophages**. *J Immunol* 1999, **163**:2909–2915.

152. Ahmad N, Chen LC, Gordon MA, Laskin JD, Laskin DL: **Regulation of cyclooxygenase-2 by nitric oxide in activated hepatic macrophages during acute endotoxemia.** *J Leukoc Biol* 2002, **71**:1005–11.

153. Krovat BC: **Fingerprinting of Cytochrome P450 and Microsomal Epoxide Hydrolase Gene Expression in Human Blood Cells**. *Toxicol Sci* 2000, **55**:352–360.

154. Korhonen R: **Dexamethasone Inhibits Inducible Nitric-Oxide Synthase Expression and Nitric Oxide Production by Destabilizing mRNA in Lipopolysaccharide-Treated Macrophages**. *Mol Pharmacol* 2002, **62**:698–704.

155. Wang R, Belosevic M: **The in vitro effects of estradiol and cortisol on the function of a long-term goldfish macrophage cell line.** *Dev Comp Immunol* 1995, **19**:327–336.

156. Dusting GJ, Akita K, Hickey H, Smith M, Gurevich V: **Cyclosporin A and tacrolimus (FK506) suppress expression of inducible nitric oxide synthase in vitro by different mechanisms.** *Br J Pharmacol* 1999, **128**:337–44.

157. Hughes JP, Rees S, Kalindjian SB, Philpott KL: **Principles of early drug discovery.** *Br J Pharmacol* 2011, **162**:1239–49.

158. Falconer M, Smith F, Surah-Narwal S, Congrave G, Liu Z, Hayter P, Ciaramella G, Keighley W, Haddock P, Waldron G, Sewing A: **High-throughput screening for ion channel modulators.** *J Biomol Screen Off J Soc Biomol Screen* 2002, **7**:460–465.

159. Ogasawara Y, Yoshida J, Shiono Y, Miyakawa T, Kimura K: **New eremophilane sesquiterpenoid compounds, eremoxylarins A and B directly inhibit calcineurin in a manner independent of immunophilin.** *J Antibiot (Tokyo)* 2008, **61**:496–502.

160. Hayashi, Kozo, Takizawa, Masayuki, Noguchi K: **Tan-2483-Related Compound, Its Production And Use**. 1998.

161. Gao X, Nakadai M, Snider BB: **Synthesis of (-)-TAN-2483A. Revision of the structures and syntheses of (+/-)-FD-211 (waol A) and (+/-)-FD-212 (waol B).** *Org Lett* 2003, **5**:451–4.

162. Demain AL, Sanchez S: **Microbial drug discovery: 80 years of progress.** *J Antibiot (Tokyo)* 2009, **62**:5–16.

163. Gibson GE, Zhang H: **Interactions of oxidative stress with thiamine homeostasis promote neurodegeneration.** *Neurochem Int* 2002, **40**:493–504.

164. Lee JA, Kim JH, Woo SY, Son HJ, Han SH, Jang BK, Choi JW, Kim DJ, Park KD, Hwang O: **A novel compound VSC2 has anti-inflammatory and antioxidant properties in microglia and in Parkinson's disease animal model**. *Br J Pharmacol* 2014.

165. Stewart AM, Meier K, Schulz B, Steinert M, Snider BB: **Synthesis and biological evaluation of (+/-)-dinemasone C and analogues.** *J Org Chem* 2010, **75**:6057–60.

166. Tan J, Town T, Mullan M: **CD45 inhibits CD40L-induced microglial activation via negative regulation of the Src/p44/42 MAPK pathway**. *J Biol Chem* 2000, **275**:37224–37231.

167. Byeon SE, Yi Y-S, Oh J, Yoo BC, Hong S, Cho JY: **The role of Src kinase in macrophage-mediated inflammatory responses.** *Mediators Inflamm* 2012, **2012**:512926.

168. Miller TM, Cleveland DW: **Medicine. Treating neurodegenerative diseases with antibiotics.** *Science* 2005, **307**:361–2.

169. Perry VH, Newman TA, Cunningham C: **The impact of systemic infection on the progression of neurodegenerative disease.** *Nat Rev Neurosci* 2003, **4**:103–12.

170. Crespi CL, Miller VP, Penman BW: **Microtiter plate assays for inhibition of human, drug-metabolizing cytochromes P450**. *Anal Biochem* 1997, **248**:188–190.

171. Di L, Kerns EH, Li SQ, Carter GT: **Comparison of cytochrome P450 inhibition assays for drug discovery using human liver microsomes with LC-MS, rhCYP450 isozymes with fluorescence, and double cocktail with LC-MS**. *Int J Pharm* 2007, **335**:1–11.

172. Cohen LH, Remley MJ, Raunig D, Vaz AD: **In vitro drug interactions of cytochrome p450: an evaluation of fluorogenic to conventional substrates**. *Drug Metab Dispos* 2003, **31**:1005–1015.

173. Di L, Kerns EH: **Profiling drug-like properties in discovery research**. *Curr Opin Chem Biol* 2003, **7**:402–408.

174. Gibbs MA, Thummel KE, Shen DD, Kunze KL: **Inhibition of cytochrome P-450 3A (CYP3A) in human intestinal and liver microsomes: comparison of Ki values and impact of CYP3A5 expression**. *Drug Metab Dispos* 1999, **27**:180–187.

175. Lipinski CA, Lombardo F, Dominy BW, Feeney PJ: **Experimental and computational approaches to estimate solubility and permeability in drug discovery and development settings**. *Adv Drug Deliv Rev* 2001, **46**:3–26.

176. Bergstrom CA, Norinder U, Luthman K, Artursson P: **Experimental and computational screening models for prediction of aqueous drug solubility**. *Pharm Res* 2002, **19**:182–188.

177. Lipinski CA: **Drug-like properties and the causes of poor solubility and poor permeability**. *J Pharmacol Toxicol Methods* 2000, **44**:235–249.

178. Tran TH, Von Moltke LL, Venkatakrishnan K, Granda BW, Gibbs MA, Obach RS, Harmatz JS, Greenblatt DJ: **Microsomal protein concentration modifies the apparent inhibitory potency of CYP3A inhibitors**. *Drug Metab Dispos* 2002, **30**:1441–1445.

179. Fowler SM, Taylor JM, Friedberg T, Wolf CR, Riley RJ: **CYP3A4 active site**

volume modification by mutagenesis of leucine 211. *Drug Metab Dispos* 2002, **30**:452–456.

180. Kroemer HK, Gautier JC, Beaune P, Henderson C, Wolf CR, Eichelbaum M: **Identification of P450 enzymes involved in metabolism of verapamil in humans**. *Naunyn Schmiedebergs Arch Pharmacol* 1993, **348**:332–337.

181. Busse D, Cosme J, Beaune P, Kroemer HK, Eichelbaum M: **Cytochromes of the P450 2C subfamily are the major enzymes involved in the O-demethylation of verapamil in humans**. *Naunyn Schmiedebergs Arch Pharmacol* 1995, **353**:116–121.

182. Venkatakrishnan K, von Moltke LL, Greenblatt DJ: **CYP2C9 is a principal low-affinity phenacetin O-deethylase: fluvoxamine is not a specific CYP1A2 inhibitor**. *Drug Metab Dispos* 1999, **27**:1519–1522.

183. Tracy TS, Korzekwa KR, Gonzalez FJ, Wainer IW: **Cytochrome P450 isoforms involved in metabolism of the enantiomers of verapamil and norverapamil**. *Br J Clin Pharmacol* 1999, **47**:545–552.

184. Wang YH, Jones DR, Hall SD: **Prediction of cytochrome P450 3A inhibition by verapamil enantiomers and their metabolites**. *Drug Metab Dispos* 2004, **32**:259–266.

185. Racha JK, Zhao ZS, Olejnik N, Warner N, Chan R, Moore D, Satoh H: **Substrate dependent inhibition profiles of fourteen drugs on CYP3A4 activity measured by a high throughput LCMS/MS method with four probe drugs, midazolam, testosterone, nifedipine and terfenadine**. *Drug Metab Pharmacokinet* 2003, **18**:128–138.

186. Hellum BH, Nilsen OG: **In vitro inhibition of CYP3A4 metabolism and P-glycoprotein-mediated transport by trade herbal products**. *Basic Clin Pharmacol Toxicol* 2008, **102**:466–475.

187. Kalliokoski T, Kramer C, Vulpetti A, Gedeck P: **Comparability of mixed IC(5)(0) data - a statistical analysis**. *PLoS One* , **8**:e61007.

188. Stresser DM, Blanchard AP, Turner SD, Erve JC, Dandeneau AA, Miller VP, Crespi CL: **Substrate-dependent modulation of CYP3A4 catalytic activity: analysis of 27 test compounds with four fluorometric substrates**. *Drug Metab Dispos* 2000, **28**:1440–1448.

189. Martel S, Castella ME, Bajot F, Ottaviani G, Bard B, Henchoz Y, Valloton BG, Reist M, Carrupt P-A: **Experimental and virtual physicochemical and pharmacokinetic profiling of new chemical entities**. *Chimia (Aarau)* 2005, **59**:308–314.

190. Taub ME, Kristensen L, Frokjaer S: **Optimized conditions for MDCK permeability and turbidimetric solubility studies using compounds representative of BCS classes I-IV**. *Eur J Pharm Sci* 2002, **15**:331–340.

191. Tanaka S, Oba K, Fukushima M, Nakayasu K, Hasebe K: **Water solubility enhancement of pyrene in the presence of humic substances**. *Anal Chim Acta* 1997, **337**:351–357.

192. Florence AT, Attwood D: **Using LogP**. In *Physicochemical principles of pharmacy.* 4th ed. London: Pharmaceutical Press; 2006:175.

193. O'Neil MJ: **The Merck index an encyclopedia of chemicals, drugs, and biologicals**. 2006:1 online resource.

194. Gao F, Johnson DL, Ekins S, Janiszewski J, Kelly KG, Meyer RD, West M: **Optimizing Higher Throughput Methods to Assess Drug-Drug Interactions for CYP1A2, CYP2C9, CYP2C19, CYP2D6, rCYP2D6, and CYP3A4 In Vitro Using a Single Point IC50**. *J Biomol Screen* 2002, **7**:373–382.